

DRIFT CHARACTERISTICS OF THE NORTHEASTERN BERING
SEA ICE DURING 1982



Frontispiece. A PMEL ice station. The GOES data collection package on the left collects wind, current, and temperature data hourly and transmits every six hours. The ARGOS position platform on the right transmits to NOAA polar orbiting satellites.

NOAA Technical Memorandum ERL PMEL-55

DRIFT CHARACTERISTICS OF NORTHEASTERN BERING SEA ICE DURING 1982

Michael Reynolds
Carol H. Pease

Pacific Marine Environmental Laboratory
Seattle, Washington
April 1984



**UNITED STATES
DEPARTMENT OF COMMERCE**

**Malcolm Baldrige,
Secretary**

**NATIONAL OCEANIC AND
ATMOSPHERIC ADMINISTRATION**

**John V. Byrne,
Administrator**

**Environmental Research
Laboratories**

**Vernon E. Derr
Director**

NOTICE

Mention of a commercial company or product does not constitute an endorsement by NOAA Environmental Research Laboratories. Use for publicity or advertising purposes of information from this publication concerning proprietary products or the tests of such products is not authorized.

Table of Contents

	<u>Page</u>
Abstract	1
1. Introduction	2
2. Methods	7
2.1 Geographic Position	7
2.2 Meteorological - Oceanographic Measurements	8
2.3 ARGOS Data Processing	13
2.4 GOES Data Processing	13
2.5 Aircraft Observations	14
3. Results	23
3.1 Lagrangian Drift	23
3.2 Meteorological Data	29
3.3 Oceanographic Data	33
4. Discussion	38
5. Summary	42
6. Acknowledgements	44
7. References	45
Appendix A - ARGOS tracklines	48
A1. Platform 2320	49
A2. Platform 2321B	59
A3. Platform 2322B	66
A4. Platform 2323	76
A5. Platform 2324	79
A6. Platform 2325	90
Appendix B. Meteorological Data	102
B1. Station 010C (ARGOS 2322B)	103
B2. Station 5170 (ARGOS 2320)	110
Appendix C. Oceanographic Data	119
C1. Station 010C (ARGOS 2322B)	120
C2. Station 5170 (ARGOS 2320)	127

TABLES

	<u>Page</u>
1. Summary of ARGOS Platforms 2320-2325	6
2. Summary of AXBT launches from the NOAA aircraft	17

FIGURES

FRONTISPIECE. PMEL ice station	ii
1. Place names for vicinity of Bering and Chukchi Seas	3
2. Bathymetry of northeastern Bering and Chukchi Seas	4
3. Locations and dates of station deployments	5
4. Schematic of PMEL GOES ice station	9
5. Current meter developed for under-ice measurements	11
6. Battery voltage for the two GOES stations	12
7. Sea-level pressure analysis for 00 GMT 12 February 1982	15
8. Sea-level pressure analysis for 00 GMT 15 February 1982	18
9. Sea-level pressure analysis for 00 GMT 16 February 1982	20
10. Aircraft flight track over the Bering Sea on 16 February 1982	21
11. Satellite images of the Bering and Chukchi Seas on 16 February 1982	22
12. Drift of ARGOS platform 2320 with GOES Station 5170	24
13. Drift of ARGOS platform 2321B	26
14. Drift of ARGOS platform 2322B with GOES Station 010C	27
15. Drift of ARGOS platform 2323	28
16. Drift of ARGOS platform 2324	30
17. Drift of ARGOS platform 2325	31
18. Summary of meteorological data collected at Station 010C	32
19. Summary of meteorological data collected at Station 5170	34
20. Windrose of data collected at Station 5170	35
21. Summary of oceanographic data collected at Station 010C	36
22. Summary of oceanographic data collected at Station 5170	37

DRIFT CHARACTERISTICS OF THE NORTHEASTERN BERING

SEA ICE DURING 1982

Michael Reynolds and Carol H. Pease
Pacific Marine Environmental Laboratory
7600 Sand Point Way NE, Bin C15700
Seattle, Washington 98115-0070

ABSTRACT. From 26 January to 10 February 1982, scientists from NOAA/PMEL deployed an array of 6 ARGOS drifting ice platforms in the vicinity of Nome, Alaska in the northeastern Bering Sea. Two of the platforms had meteorological and oceanographic stations which measured surface winds and currents and telemetered the data to the GOES-West satellite. During this time the NOAA WP-3D instrumented airplane made three flights over this area and out to the ice edge.

The ARGOS platforms were allowed to drift freely and terminated in the ice pack due to ice deformation or to melt out. The last platform ceased transmitting on 30 June 1982 at 2300 GMT. Rather than a net drift southward toward the ice edge, the four platforms drifted northward into the Chukchi Sea, while two which were deployed later in Norton Sound remained in the vicinity of Norton Sound. Activity among the former was striking; in response to alternating wind and current directions, the floes oscillated through the Straits three or more times, and typical north-south excursions were 350 km. The floes accelerated to speeds of greater than 1 m/s as they passed through the Strait in either direction. The two platforms in Norton Sound oscillated north and south on the same time scales as the others but were restricted to the spatial scales of western Norton Sound.

* Contribution No. 649 from Pacific Marine Environmental Laboratory

1. Introduction

In the last few years, experimental studies of ice motion in the eastern Bering Sea (Fig. 1) indicated that an ice floe is typically created along the coastlines of Alaska or St. Lawrence Island and drifts southwestward, primarily under the influence of net northeasterly winds, until it melts at the ice edge (Muench and Ahlnäs, 1976; Pease, 1980; McNutt, 1981). Measurements taken by PMEL in February 1981 of ice drift near the ice edge indicated a southerly drift of the floes and a seaward acceleration in the marginal ice zone (Macklin, et al., 1983). Ice drift measurements taken in the late winter and spring of 1982, and described in this memorandum, do not directly confirm this simple picture. Instead, they indicate that ice floes in the northern Bering Sea move in a complicated fashion, dependent on the winds and barotropic ocean circulation and restricted by the bathymetry (Fig. 2).

Scientists from NOAA and Flow Research, Inc., were in Nome, Alaska, from 22 January to about 13 February, 1982, to study ice properties and motion in the Bering Sea. NOAA scientists deployed a total of six ARGOS Data Acquisition Platforms (ADAP's) capable of providing geographic position. At two of the sites, meteorological and oceanographic data were collected. Flow's scientists deployed additional stations in the area. All platforms were left on the ice to drift freely until they stopped transmitting due to sinking during melt or being crushed during ice deformation. The last PMEL platform ceased transmitting on 30 June, 1982.

Figure 3 shows the deployment sites and times for the PMEL instruments. This report will summarize only the data collected from these instruments. Weather delays and rapid ice movement precluded any attempts to deploy a

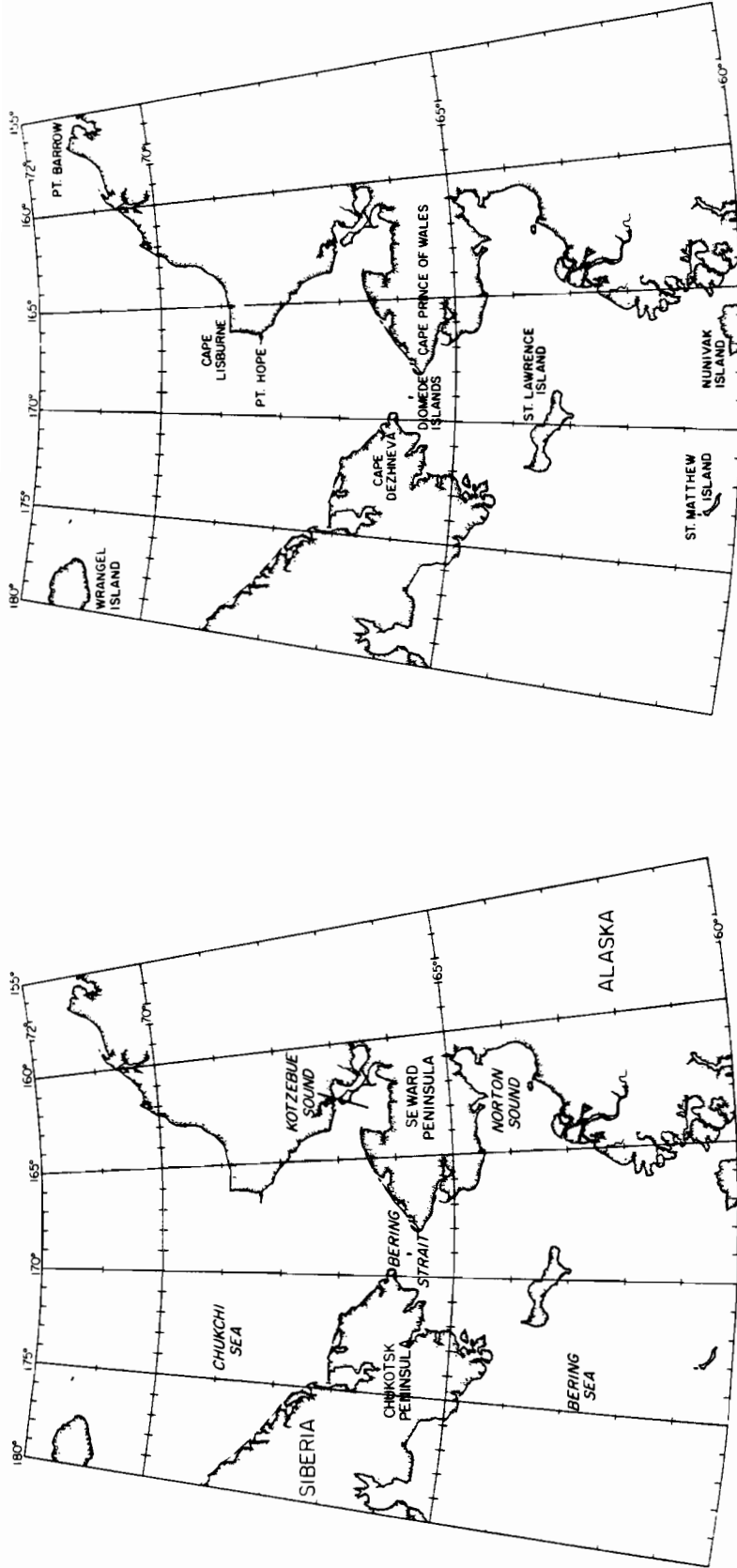


Figure 1. Place names for vicinity of Bering and Chukchi Seas. Seas, sounds, and land masses are on the left and capes, points, and islands are on the right. The projection is Lambert conic.

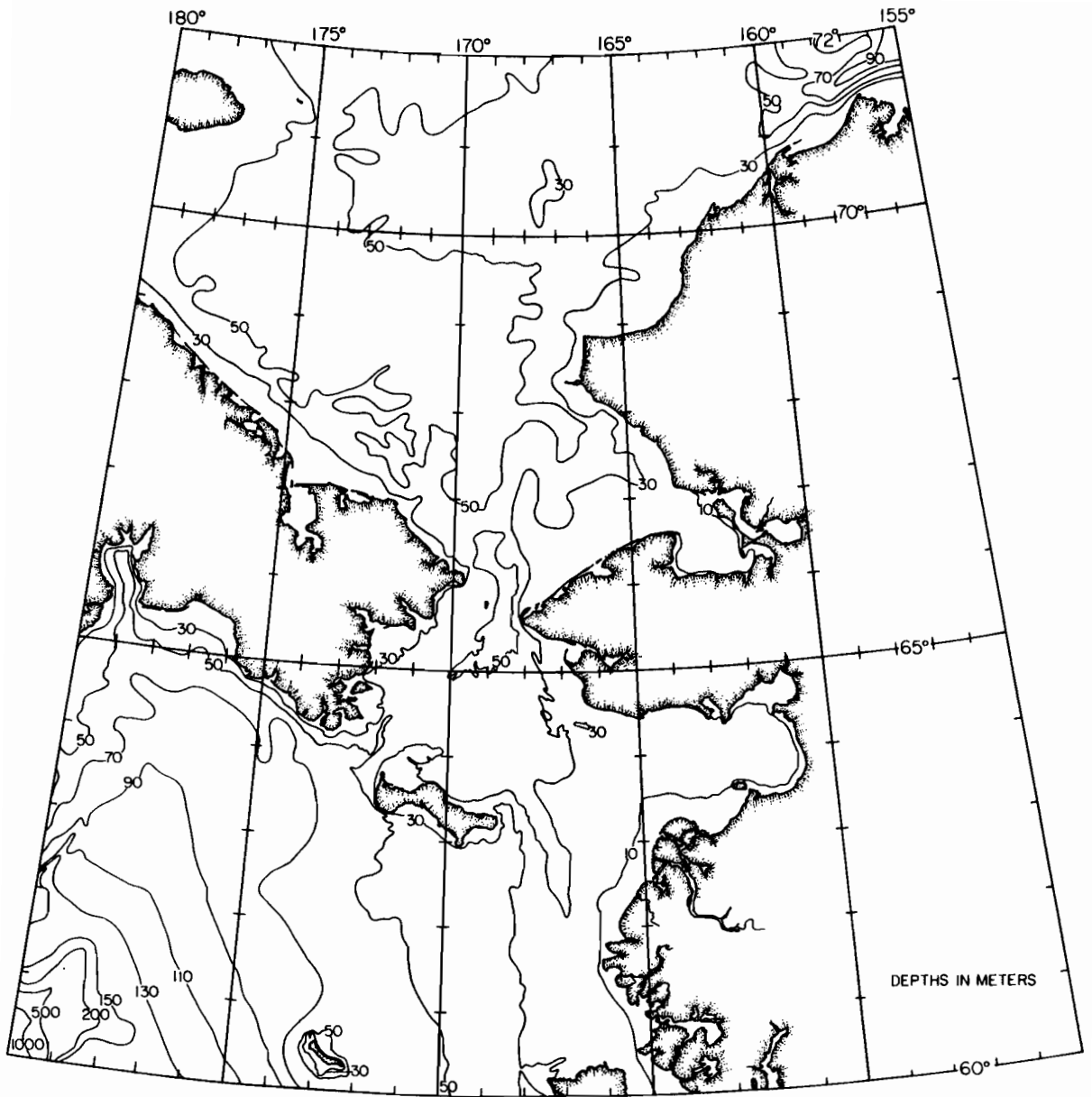


Figure 2. Bathymetry of the northeastern Bering and Chukchi Seas. South of Bering Strait is adapted from Pratt and Walton (1974) and north is adapted from NOS chart 16003 (1983).

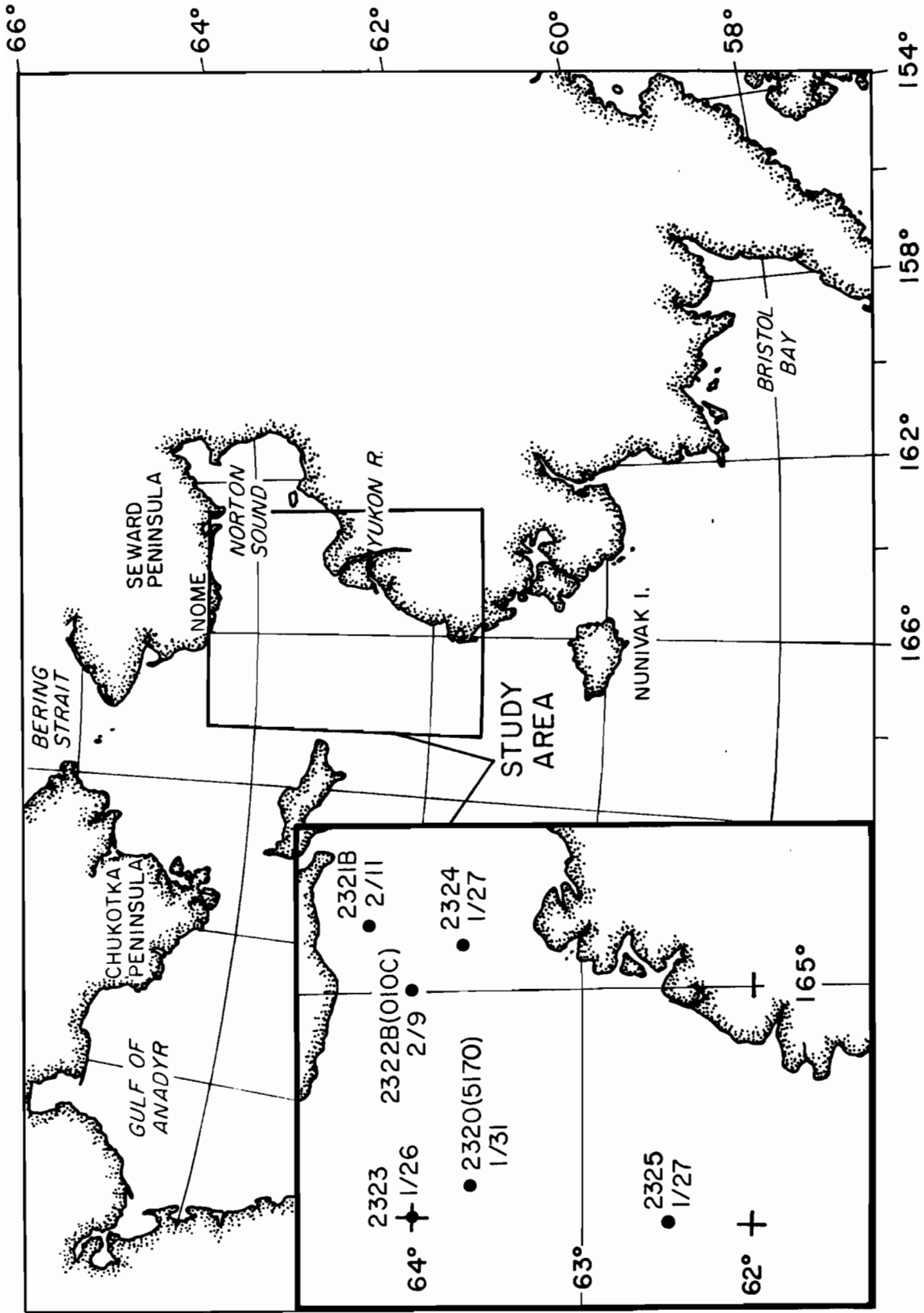


Figure 3. Locations and dates of deployments during January and February, 1982. Locations of meteorological stations are designated with parentheses.

neat geometric grid, and the final pattern was rather irregular. Deployment operations originated in Nome, AK. A helicopter (UH-1H N57RF), provided by the NOAA Research Flight Center, carried scientists and equipment to selected sites. Several of the stations were moving rapidly north under the influence of the currents and winds at the time, and this rapid motion, coupled with periods of bad weather during which there were no flights, caused problems in achieving our desired array configuration. Two stations, 2321A and 2322A, had to be completely recovered and redeployed in an attempt at maintaining a reasonably compact initial array. Weather during the deployment period was highly unseasonable with strong consistent southerly winds, warm temperatures, and rain. The final 6 stations provided excellent coverage of the area with platforms in Norton Sound and in the northeastern Bering Sea. Table 1 summarizes the performance of all PMEL platforms and stations, identified by the ARGOS platform numbers 2320-2325 and GOES Station numbers 5170 and 010C.

Table 1. Summary of ARGOS Platforms 2320-2325 during 1982

ARGOS ID	Start Date (GMT)	Stop Date (GMT)	Initial Position		GOES ID
			LAT. (N)	LONG. (W)	
2320	1/31	6/7	63°39.6'	167°33.0'	5170
2321A	2/11	2/11	63°29.9'	164°25.2'	
2321B	2/12	4/28	64°12.1'	164°05.3'	
2322A	2/4	2/5	64°28.9'	167°02.8'	010C
2322B	2/9	6/6	63°58.9'	164°59.5'	010C
2323	1/26	2/15	63°59.2'	168°01.1'	
2324	1/27	6/13	63°42.6'	164°31.6'	
2325	1/28	6/30	62°27.3'	168°30.1'	

The NOAA WP-3D instrumented aircraft made three overflights of the study area and south to the ice edge. These observations and their interpretations will not be covered in detail in this report. However, for completeness, a summary of aircraft operations will be given in Section 2.5. Additional descriptions of the aircraft observations can be obtained from Walter and Overland (1984), and Walter *et al.* (1984).

2. Methods

2.1 Geographic Position

The location of each station was determined by satellite with a position-only transponder called an ARGOS Data Acquisition Platform (ADAP) Model 901, made by Polar Research Laboratories. ARGOS is a cooperative project between Centre National d'Etudes Spatiales (CNES) of France, the U.S. National Aeronautics and Space Administration (NASA), and NOAA. The ARGOS receiving system is carried by NOAA polar orbiting satellites. Each ADAP transmitted independently at 401.650 Hz at regular intervals (typically 60 s). Ten fixed platforms around the world are used to calculate the exact orbit of each satellite. This information is sufficient for Service ARGOS to calculate the position of any other platform to within 200 m in longitude and 100 m in latitude.

When the satellite's orbit places it in view of the platforms, the transmissions are received by the satellite and stored on a tape recorder. Within minutes the orbit takes the satellite over one of three ground receiving stations at which time the data are transmitted down, processed, and disseminated to the user. The number of satellite passes over any

ADAP varies from seven per day at the equator to 28 per day at the poles. In our experience, the number of successful fixes varies from 8 to 12 per day. The length of time from satellite overpass until the corresponding fix was available was typically 6-8 hours, a delay which created some problems in recovering one of the stations.

Three ADAPs were packaged in rugged, waterproof polyethylene cases and three were packaged in wooden boxes. All were powered by lithium batteries which were suitable for six-months operation with virtually no low-temperature derating. There was no observable difference in performance between the two different packaging types.

2.2 Meteorological-Oceanographic Measurements

Two meteorological and oceanographic measurement systems (see Frontispiece and Fig. 4) were deployed at ADAP sites 2320 and 2322. The sites, respectively designated by their GOES addresses 010C and 5170, collected data hourly and transmitted every six hours to GOES-West (Geosynchronous Orbiting Environmental Satellite).

The meteorological instrumentation, described in detail by Reynolds (1983), included a cup anemometer, vane, and air temperature sensor. Wind measurements were taken at a height of 3 m. Vector averages of wind components were computed in the following way: the orientation of the flow was measured with an Aanderaa compass at the beginning of each sample period. Wind components relative to the station were updated at a 50 Hz rate and summed over a 20 minute sample period for a relative vector average. During analysis, the wind components were rotated according to the compass direction for a true wind direction.

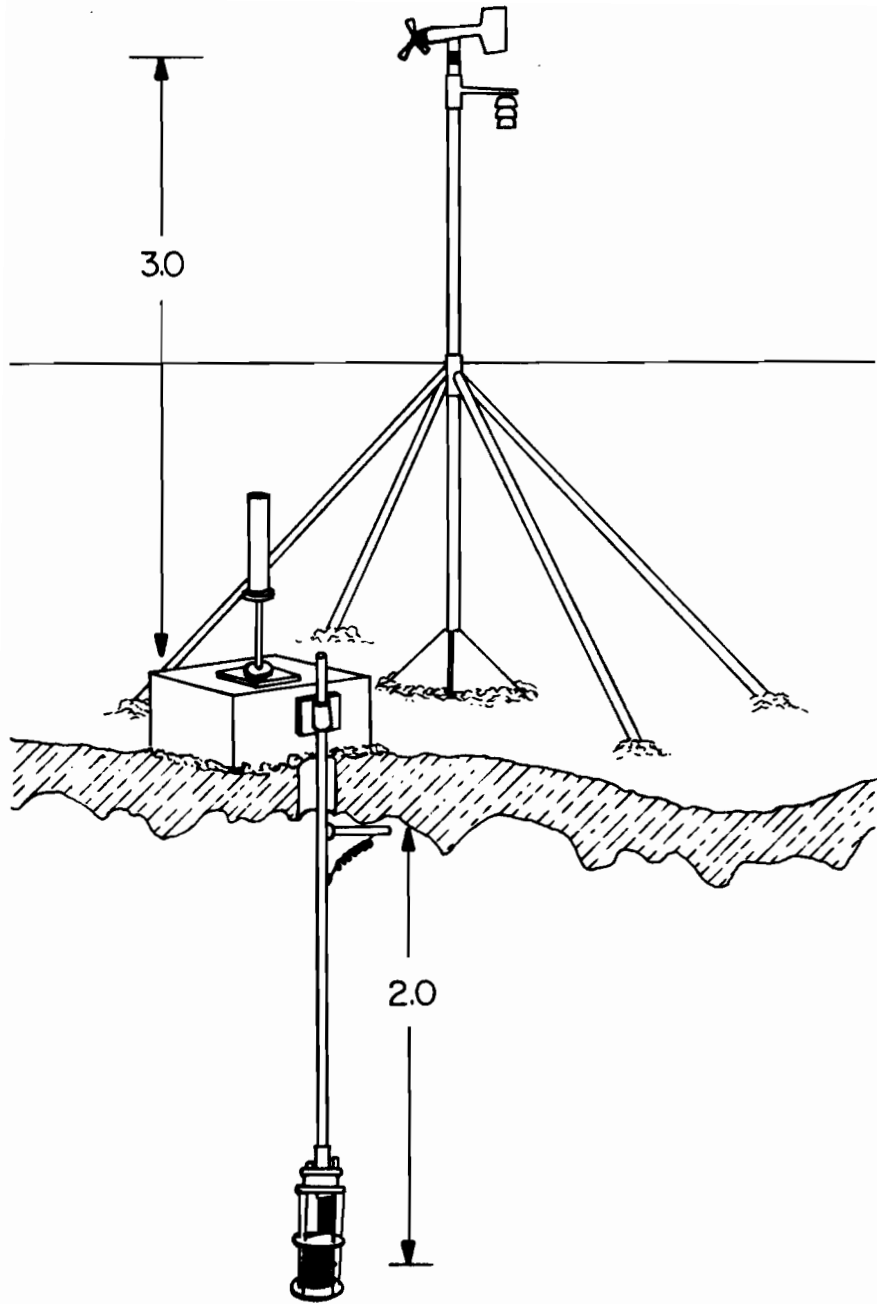


Figure 4. Schematic of PMEL GOES ice station.

Temperature was measured by coupling a thermistor with a voltage-controlled oscillator into a single, molded package. The number of cycles counted in a sample period is an excellent measure of mean temperature. Additionally Station 010C carried a Paroscientific pressure sensor which provided 1-min average surface pressures to an accuracy of ± 0.5 mbar.

Ocean current speed and direction were measured at each station with a Savonius-rotor current meter which was patterned after the EG&G vector-averaging meter and developed at PMEL (Fig. 5). Eight magnets were placed in the rotor, and rotation was sensed with a magnetically sensitive diode. Also, magnets coupled the vane position to a compass mounted in the current-meter housing. The current was estimated by counting the number of rotor rotations over a 20-minute period for an average speed. Tests have shown this number to agree with the vector averaged speed with less than 5% error. Direction was estimated by adding a single instantaneous measurement of the vane to the system compass reading. Such an estimate is noticeably noisy but useable. The current meter was held approximately 2 m below the ice with an aluminum pole. The floe with ARGOS platform 2320 was 0.3 m thick, with ARGOS 2322A was 0.9 m thick, and with ARGOS 2322B was 0.2 m thick at the time of station deployment.

Data from all the sensors were collected in the data collection package (DCP), Model 525A, manufactured by Handar, Inc. Samples were taken hourly, then every six hours six samples were transmitted at 40 Watts RF power to GOES-West. Power for the GOES equipment was provided by automobile batteries. Each camp had two, 80 amp-hour batteries which provided adequate power over the length of the experiment and in relatively cold (-20°C) temperatures (Fig. 6).

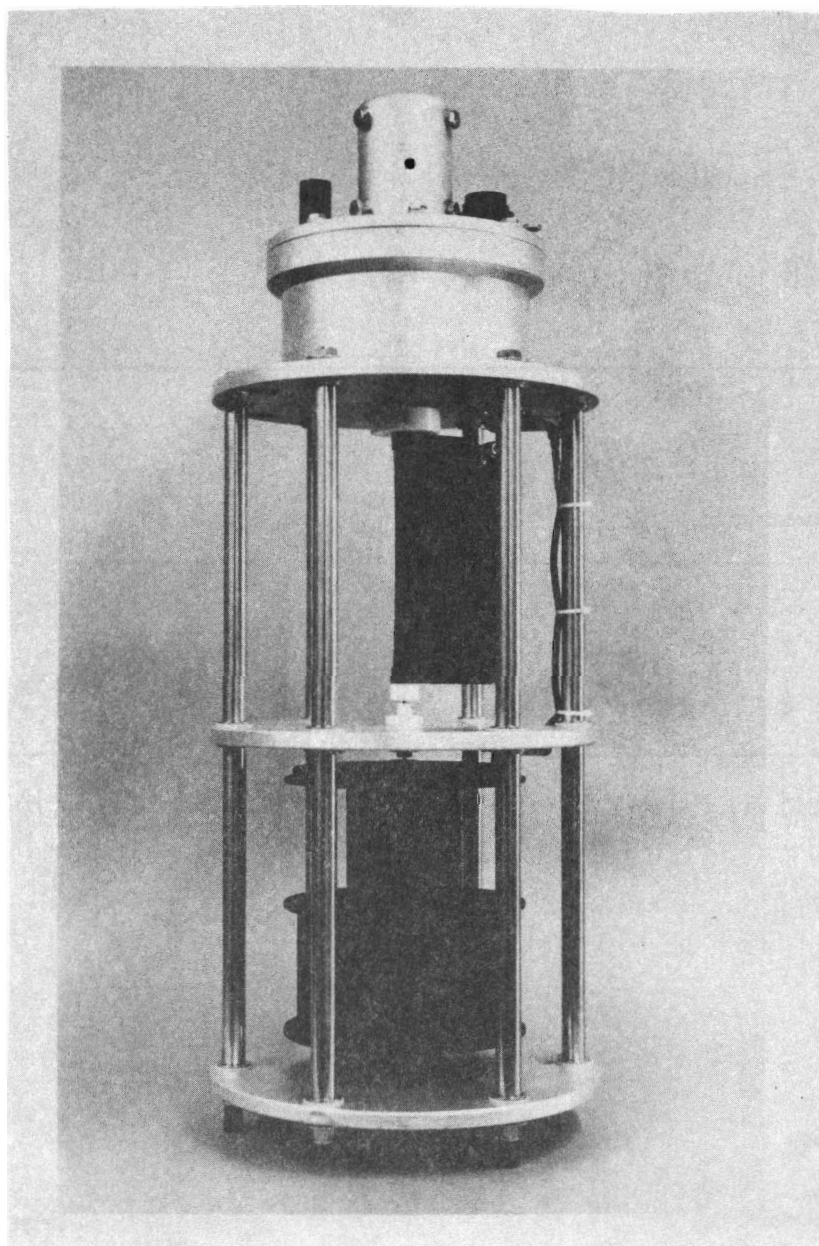


Figure 5. Current meter developed by PMEL for under-ice measurements.

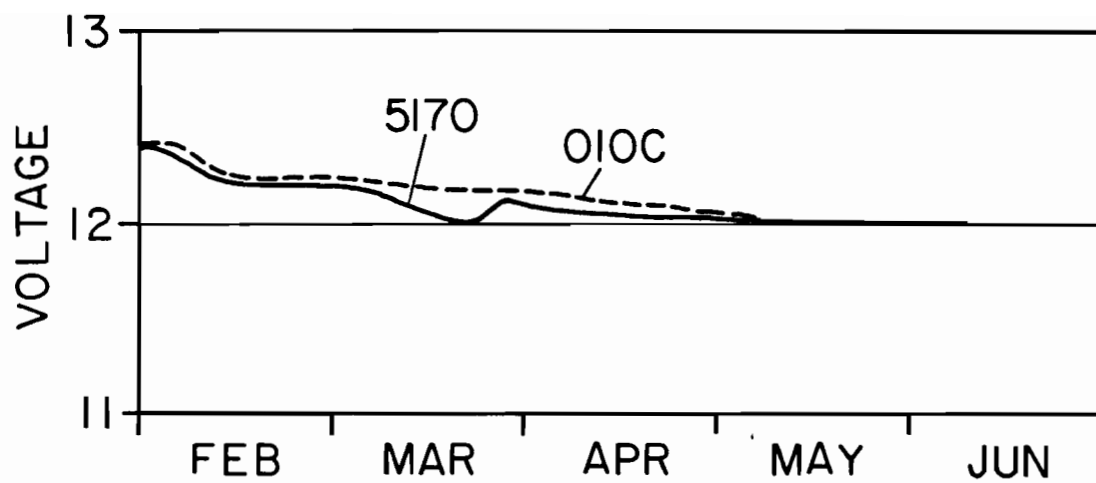


Figure 6. Plot of the battery voltage with time for the two GOES stations.

The GOES satellite retransmitted the samples at a higher frequency to a receiving station at Wallops Island, VA, where the signal was demodulated and data were sent to the Central Data Distribution Facility in Camp Springs, MD. There the data were stored for dial-up dissemination to the user. Since the GOES is an equatorial satellite, reception was questionable in the higher latitudes. However, even though Station 5170 reached 68°N latitude in the Chukchi Sea, no signal strength problems occurred. Coverage may extend to approximately 75° latitude.

2.3 ARGOS Data Processing

Data were received from Service ARGOS in the form of computer print-outs and digital tapes every two weeks during the experiment. Each position was graded according to quality; the best fixes required two satellite passes while those of lesser quality had one. All single pass data were rejected during our processing. Spline curves were fit to the remaining fixes and time series with regular intervals of one hour were created. These estimates were used to compute floe velocity and acceleration. Additional discussion of processing of ARGOS data can be found at the beginning of Appendix A.

2.4 GOES Data Processing

GOES data were available by dial-up modem from the computer at Wallops Island. The data were loaded daily into a Tektronix Model 4051 computer with tape cartridge and then transferred into the NOAA CDC-6600 for processing. Any parity errors which occurred were easily edited by hand. Unless

specified, the data presented here are either raw 20 minute averages or, for summary plots, block averaged. All averaging of angles was done by averaging vector components.

2.5 Aircraft Observations

During and immediately following the deployment of equipment on the ice, the NOAA WP-3D made three flights over the Bering Sea. Measurements were taken by gust probe, laser altimeter, and air-deployable expendable bathythermometers (AXBT's). The gust probe measures vertical momentum and heat fluxes.

The dominant winter weather pattern over the Bering Sea is northeasterly winds with strong cold air advection and ice advance. At the beginning of the experiment, however, southerly winds and overcast conditions associated with a ridge of high pressure over Alaska and severe weather over the central continental U.S. were established. The positive feedback of the warm southerly winds maintained the ridge over Alaska for two weeks until major storm activity near Japan shifted the storm track pattern over Siberia and reestablished northerly winds over the Bering Sea. White and Clark (1975) state that for the 21 years, 1950 to 1970, 10 Januaries, 6 Februaries, and 9 Marches had similar sustained ridging activity. For this reason flights were concentrated in the last week of the experiment.

On 11 February a reconnaissance flight was made along the ice edge from Bristol Bay westward at an altitude of 1000 to 1500 m. A surface weather map for 12 February 00 GMT (Fig. 7) shows that the winds were northeasterly at this time although temperatures of -11°C at Bristol Bay and -1°C at St. Paul I. indicate significant warming in the boundary

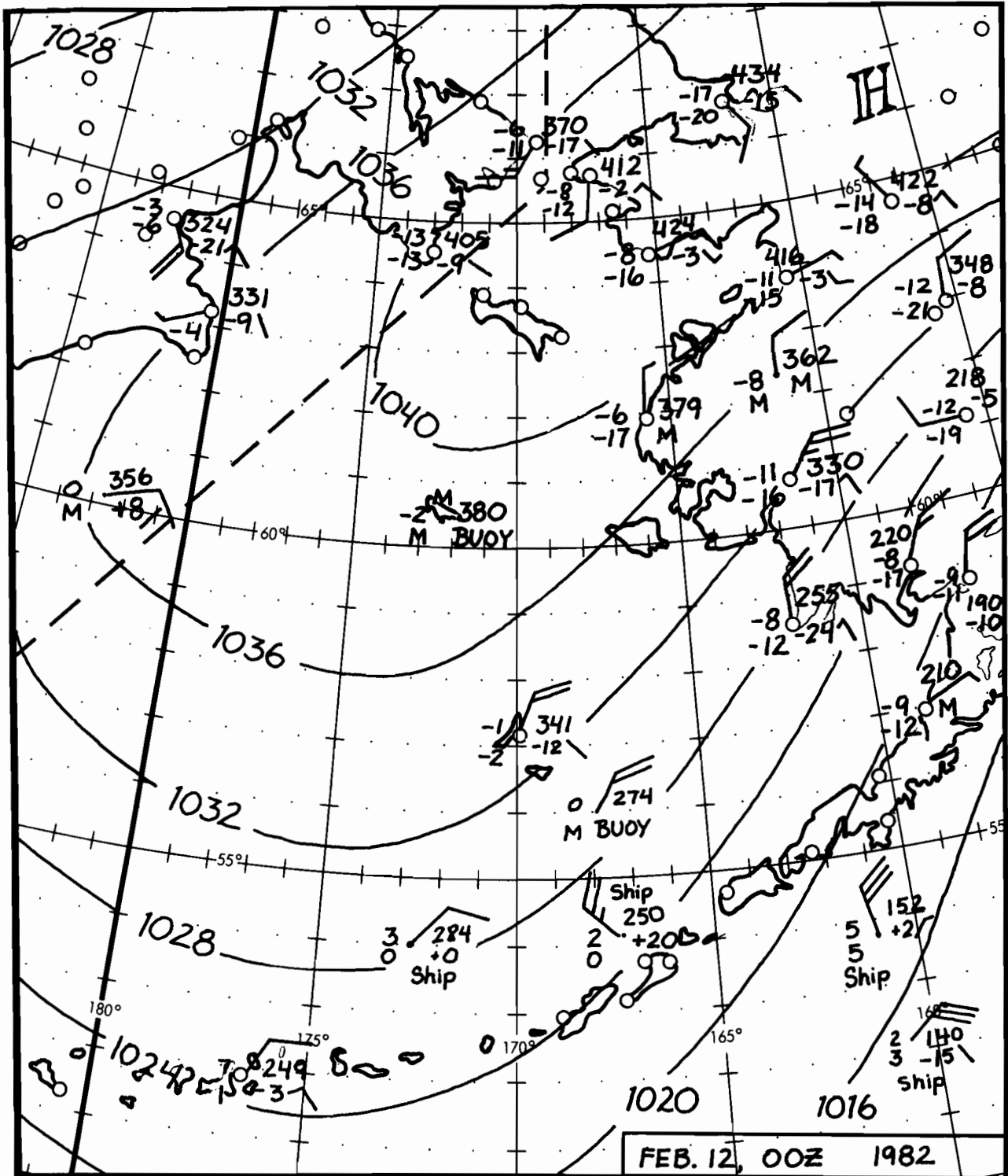


Figure 7. Sea-level pressure analysis for 00 GMT 12 February 1982.

layer. Near 171°W a run was made south of the edge with AXBT's dropped at the points in Table 2, and a set of stacked crosswind flux measurements were made at the levels 40, 90, 150 and 225 m near 61.5°N, 169°W.

On 14 February a drag coefficient study flight was made with the gust probe, laser altimeter, dropsondes, and AXBT's. A weather map for 15 February 00 GMT (Fig. 8) indicates northerly flow under the influence of a high pressure region at the surface over Siberia. A series of stacked crosswind gust probe runs were made near 63.4°N, 167.5°W at levels: 90, 200 and 340 m. In the area where these flux measurements were made, the boundary layer was nearly neutral with a surface air temperature of about -24°C. The presence of a large number of leads in the ice led to a relatively large moisture flux from the open water to the cold dry air, and the formation of patches of ground fog. Surface winds were on the order of 20 m s^{-1} and thus secondary roll circulations due to dynamic instability were present in the boundary layer. These longitudinal rolls swept the patches of ground fog into lineal features aligned along the convergent areas of the rolls. The lineal features had separations on the order of 4.8-6 km (Walter and Overland, 1984). The momentum drag coefficient measured was 3.0×10^{-3} (Walter *et al.*, 1984). AXBT's were dropped at three locations and are summarized in Table 2.

The following day, 15 February (late GMT 15th and early 16th), a flight was made which studied the polynya south of St. Lawrence Island and the Marginal Ice Zone. Instruments used in this flight were the gust probe, laser altimeter, dropsondes, and AXBT's. Gust probe stacks and laser measurements were made over the St. Lawrence polynya, halfway to the ice edge, and over water beyond the edge. Flux measurements were made crosswind at 90 m, 150 m and 190 m near the polynya (63.15°N, 170.5°W).

Table 2. Summary of AXBT launches from the NOAA WP-3D Aircraft on 11, 14, and 15 February 1982.

DATE/AXBT #	TIME (GMT) OF FIRST REPORT (HR,MN,SC)	LAT (°N)	LONG (°W)	SST (°C) (±0.2)
11 FEB 82				
#1	212859	60.34	170.95	-1.1
#2	213347	60.12	171.21	-1.0
#3	214150(?)	60.50	171.41	(bad record)
#4	221239	60.20	171.12	-0.6
#5	221703	59.96	171.30	-0.5
#6	222330	59.60	171.57	-0.5
#7	223027	59.21	171.85	0.0
#8	223900	58.73	172.19	+1.4
#9	233500	60.53	169.69	-1.7
14 FEB 82				
#1	221303	63.63	166.62	-1.7
#2	221654	63.47	166.88	-1.8
#3	235920	63.27	167.64	-1.6
15 FEB 82				
#1	223001	63.34	171.11	-3.2 (ICE)
(16 FEB 82)				
#2	002940	59.86	171.00	-1.3
#3	003129	59.74	171.00	-1.0
#4	003805	59.40	170.83	-0.4
#5	004816	59.39	170.06	-1.7

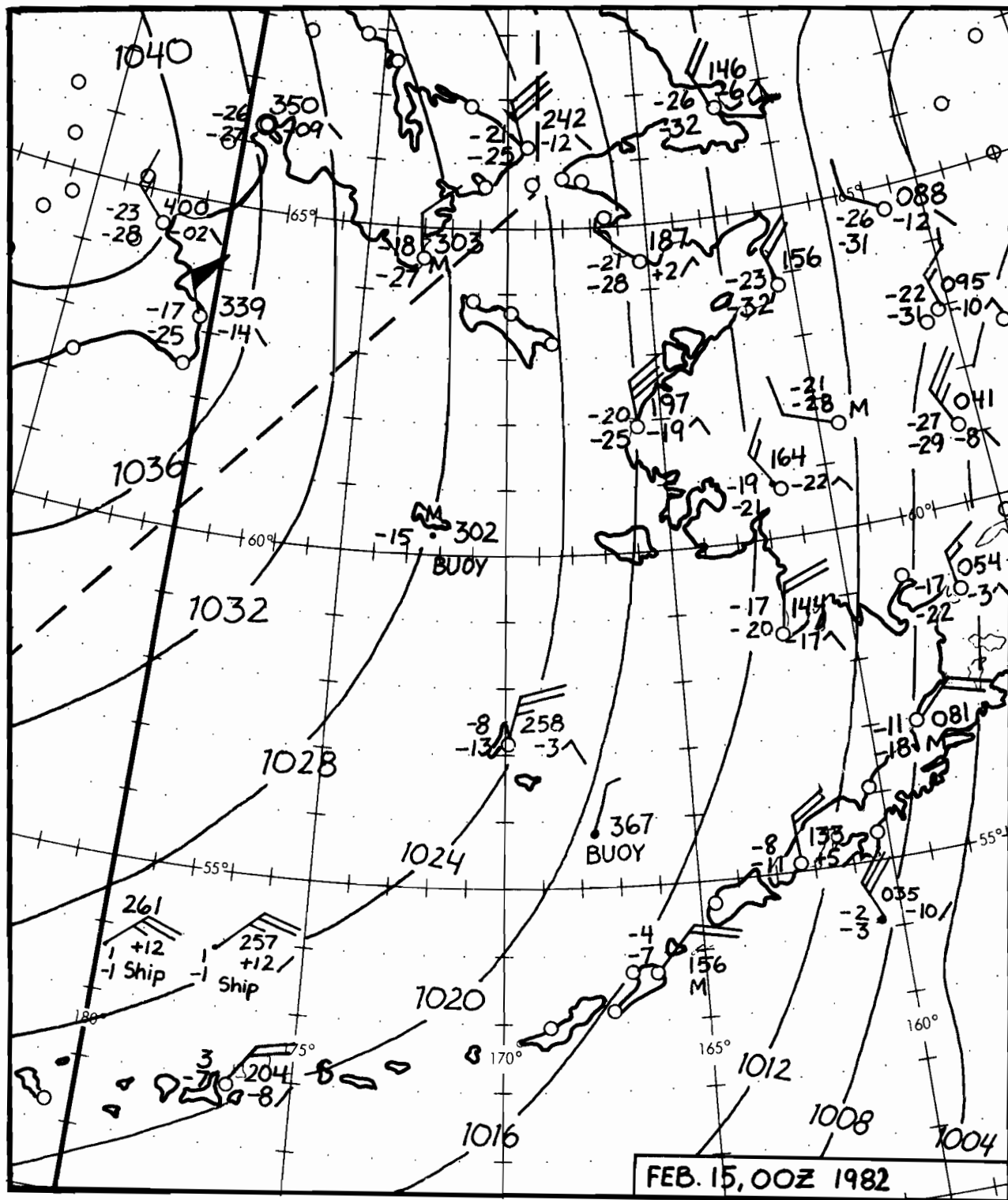


Figure 8. Sea-level pressure analysis for 00 GMT 15 February 1982.

Crosswind stacks were flown at 90, 190 and 340 m at 61.5°N, 170.3°W and at 90, 195, 350 m at 59.4°N, 170.5°W. Gust probe and laser measurements were made on the southbound legs from the polynya to the ice edge at 90-m altitude. A series of AXBT's were dropped south of the ice edge (Table 2).

For the 16 February 00 GMT flight, the weather map shows a tightened gradient between the Siberian high and a low pressure system in the Gulf of Alaska (Fig. 9). Temperatures were much colder due to the direct northerly trajectories of the air. The ferry to the observation area (Fig. 10) passed at altitude (≥ 3000 m) from Anchorage to Cape Romanzof to a region near 63°50'N, 169°30'W. After an airsonde drop, the plane descended to 300 m for a laser run across the compact, broken first-year ice north of St. Lawrence Island, it crossed the island and made a series of crosswind gust probe runs at 90, 150, 190 m over the polynya (Fig. 11). Some 10's of meters in extent of fast ice along the south shore of St. Lawrence was observed, although it was somewhat difficult to distinguish fast ice from the beach and lagoon ice. The polynya was largely covered with grease ice organized into rows parallel to the wind. From 10 to 20 km from the beach there was a transition from grease ice to nilas with holes. The nilas-to-grey-ice zone extended south along 171°W about another 50 km with the holes more filled in toward the south. The transition from nilas and grey ice to first-year ice occurred abruptly at about 62°53'N along 171°W (Figs. 10, 11). The ice in the next 200 km along 171°W was characterized as first-year with rectangular floes of small size (20-100 m) and some small leads. In some areas it was obvious that the floes were refreezing into km-sized aggregates. At 61°30'N the plane made crosswind gust probe runs at 90, 190, 340 m over first year floes. As the flight continued toward the ice edge some large leads and more small floes forming aggregates

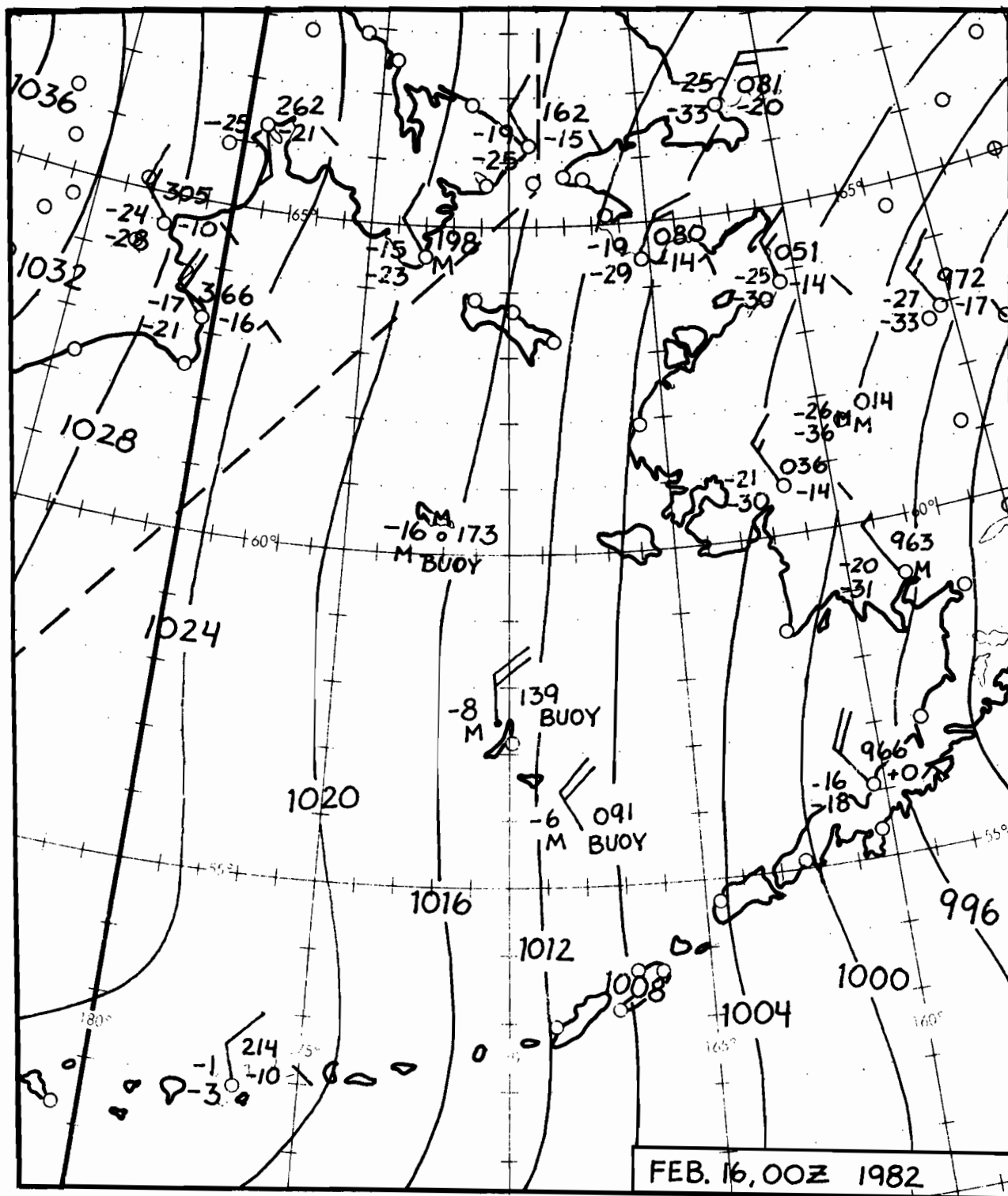


Figure 9. Sea-level pressure analysis for 00 GMT 16 February 1982.

P3-FLIGHT 15 FEBRUARY 1982

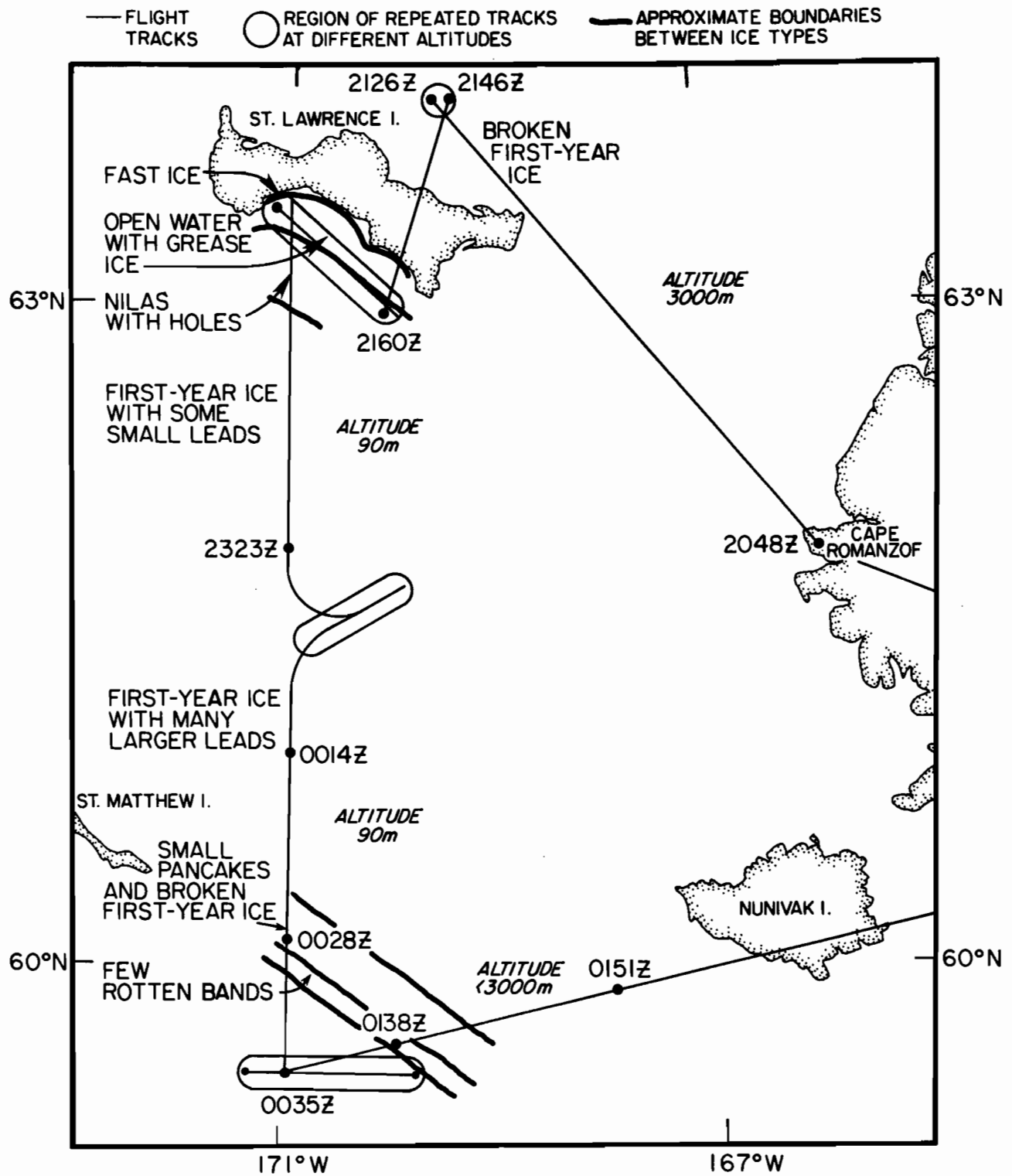


Figure 10. Map of NOAA WP-3D aircraft flight track over the Bering Sea on 16 February 1982.



Figure 11. Composite NOAA VHRR infra-red satellite images of the Bering and Chukchi Seas at about 2000 GMT 16 February 1982.

were observed. At about 60°18'N along 171°W there was a relatively sharp transition from first-year floes to a random mixture of pancakes, brash, and very broken first-year ice (Figs. 10, 11). This region was also reforming into aggregates or breccia north of about 60°5'N. South of 60°5'N, the cakes were individual and appeared to be melting. There were only a few bands and the plane was over open water by 59°50'N along 171°W. The plane made crosswind gust probe runs at 90, 195, 350 m over open water along 59°25'N. At the east end of the runs, however, the plane passed over a very rotten band at about 59°25'N and 169°55'W.

3. Results

3.1 Lagrangian Drift

Appendix A summarizes the hourly drift for each platform. Of the six ARGOS platforms considered, four floes travelled first westward then northward. Under the influence of currents and winds they passed through the Bering Strait into the Chukchi Sea. As currents and regional winds changed, these stations made several passes through the Strait. Each time this occurred, floes were accelerated to velocities of greater than 1 m s^{-1} in the Strait.

The other two platforms were deployed later in northern Norton Sound. They travelled with the same north/south oscillation but were constrained by boundaries of Norton Sound.

Platform 2320 (with GOES Station 5170) first moved northward (Fig. 12) under the influence of southerly winds and northward currents (wind arrows

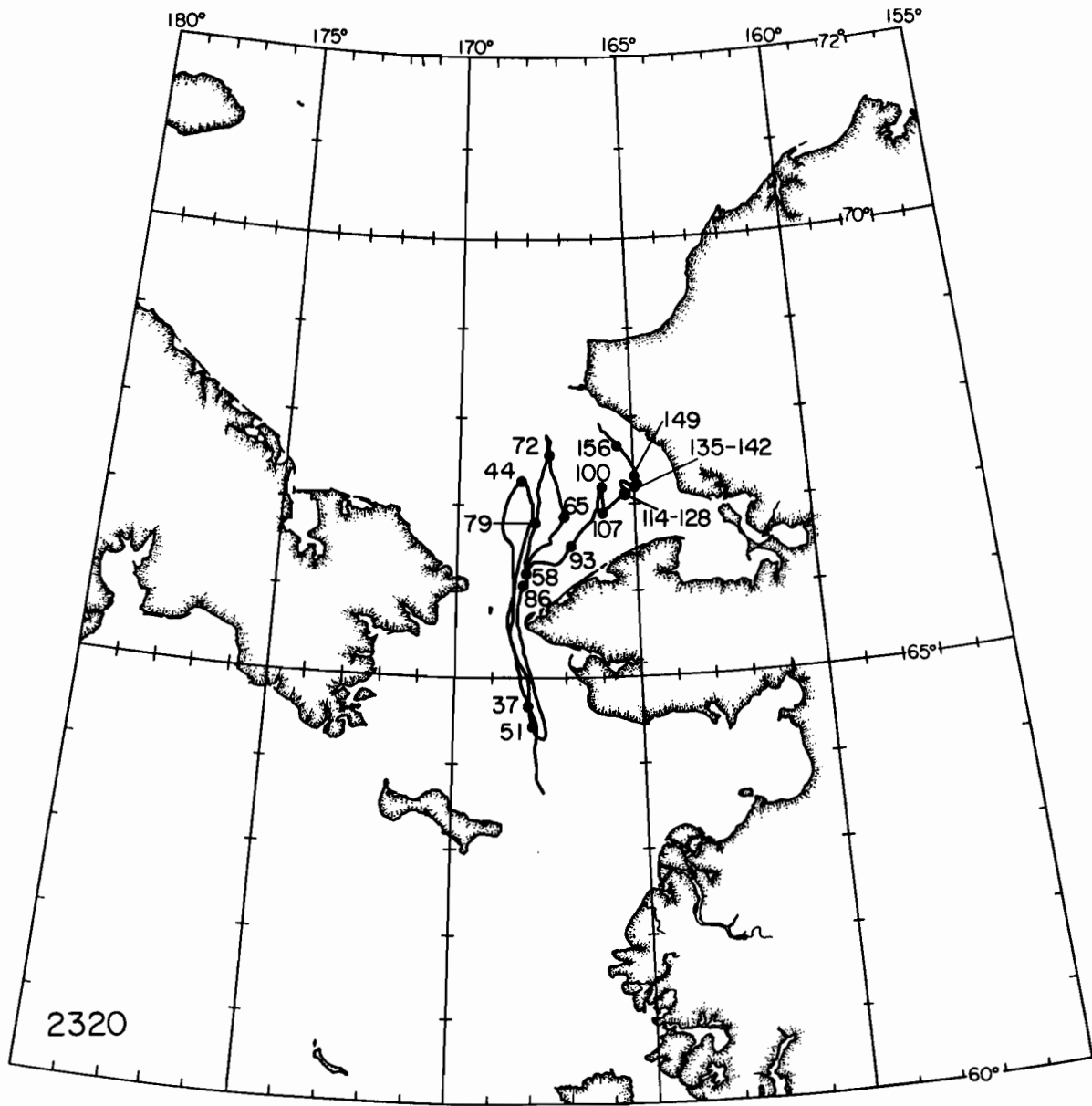


Figure 12. Summary plot of drift of ARGOS platform 2320 (with GOES Station 5170). 00Z of the Julian day is labelled weekly beginning with 6 February 1982 (JD 37).

are plotted on the trackline shown in Appendix A). It accelerated to a velocity of approximately 1 m s^{-1} as it passed through the Bering Strait (Julian Days (JD) 32-44). Then under the influence of northerly winds and southward currents, the station returned almost as far south as it was released (JD 44-52). Again reversing direction, the floe moved northward and passed through the Bering Strait for a third time. For the remainder of its operating life, the station remained in the vicinity of the Alaskan coast in the Chukchi Sea. Winds were generally weak, and any easterly winds did not persist long enough to move the floe into a region of stronger oceanic current until late spring. The floe thickness was about 0.3 m.

Platform 2321B was placed inside Norton Sound near the north shore (Fig. 13). The floe motion was relatively weak indicating weak currents and possible interaction with the coast. Tidal influences are also apparent.

Platform 2322B (with GOES Station 010C) was also placed in Norton Sound, nearer the mouth and moved somewhat more than 2321B. Motion was primarily north-south in response to currents, but had a net westward component. A summary plot (Fig. 14) shows a pattern which suggests the floe was strongly dependent on currents, with both current and ice drift responding to meteorological forcing. This floe was about 0.2 m thick at the time of station deployment.

Platform 2323 was relatively short lived (Fig. 15). However, it traveled initially NW then northward through the Bering Strait, similar to the path of 2320, 2324 and 2325. It was lost in a zone of intense shearing on the western side of Bering Strait on 15 February 1982 (JD 46).

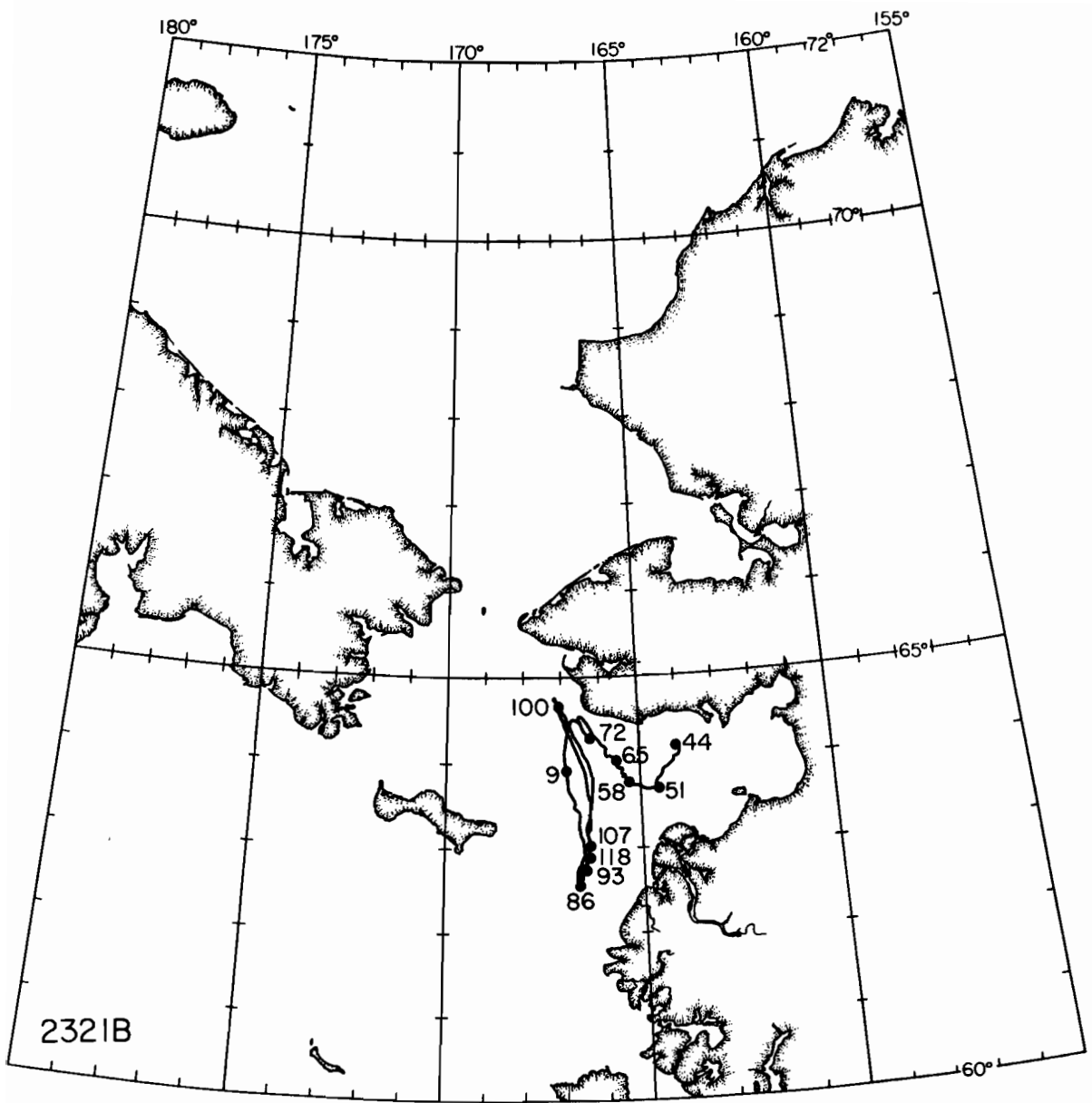


Figure 13. Summary plot of drift of ARGOS platform 2321B. 00Z of the Julian day is labelled weekly beginning with 13 February 1982 (JD 44).

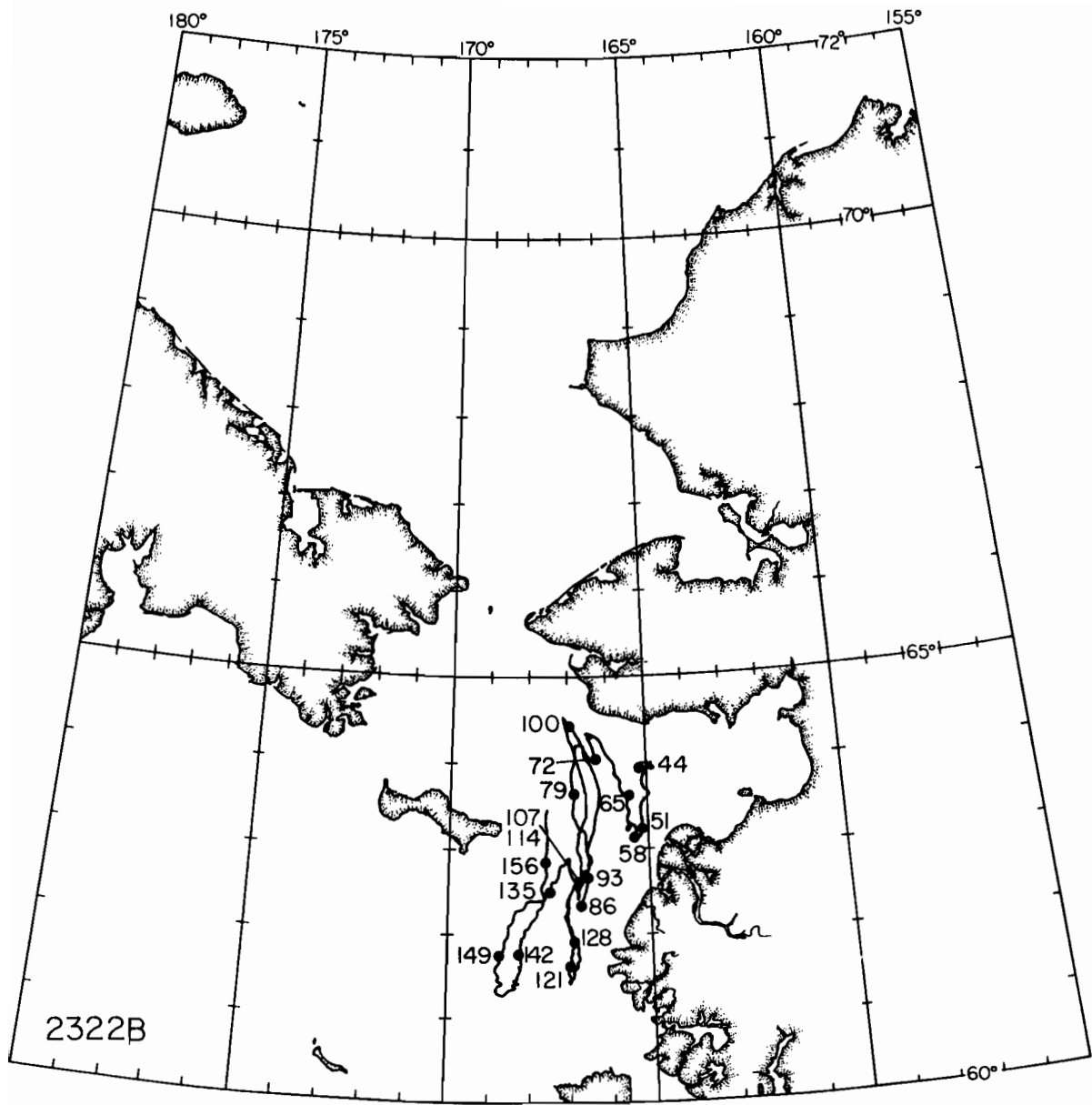


Figure 14. Summary plot of ARGOS platform 2322B (with GOES Station 010C). 00Z of the Julian day is labelled weekly beginning with 13 February 1982 (JD 44).

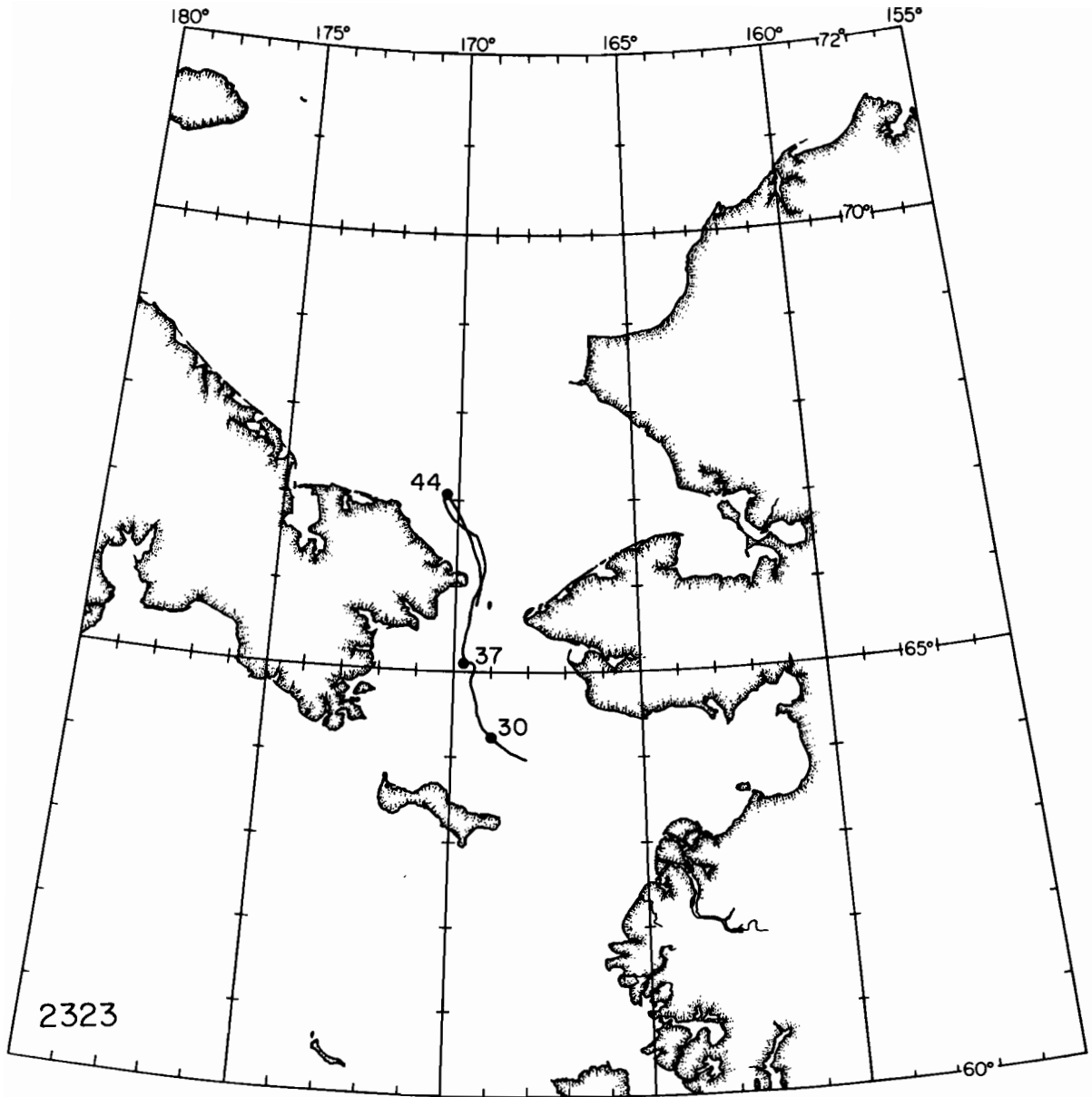


Figure 15. Summary plot of ARGOS platform 2323. 00Z of the Julian day is labelled weekly beginning with 30 January 1982 (JD 30).

Platform 2324 was deployed inside Norton Sound, earlier than and south of 2321B and 2322B which both stayed in the vicinity of the mouth of the Sound. Instead, 2324 first moved westward, then southward, then made three passes through the Bering Strait before it settled in the Chukchi Sea (Fig. 16) during the spring. Platform 2324 moved very slowly in the mouth of Kotzebue Sound for most of March and April. After that time, the floe followed the Alaskan coastal current on the eastern side past Point Hope and Cape Lisburne.

Finally, Platform 2325 was deployed in an extreme southern position almost midway between Nunivak I. and St. Lawrence I. (Fig. 17). This floe acted in a similar fashion as 2320, 2323, and 2324 in that it first moved westward, then made (in this case) five passes through the Bering Strait. Generally this floe hugged the western shore and followed the current through the trough (Fig. 2) north of the Chuotka Peninsula.

3.2 Meteorological Data

Meteorological Station 010C (the GOES address) was co-located with ARGOS Platform 2322. It was deployed at site 2322A (Fig. 3) for two days but was re-located at 2322B because of the northward drift. A summary meteorological time-series plot of the data for 010C is given in Figure 18. This data is representative of winds in the vicinity of Norton Sound since 2322B remained in that area without extensive migration. Winds remained surprisingly light during March and April and directions were primarily northerly or southeasterly. The compass reading, given by the dashed line in the middle plot, indicates rotation of the floe. The floe haltingly

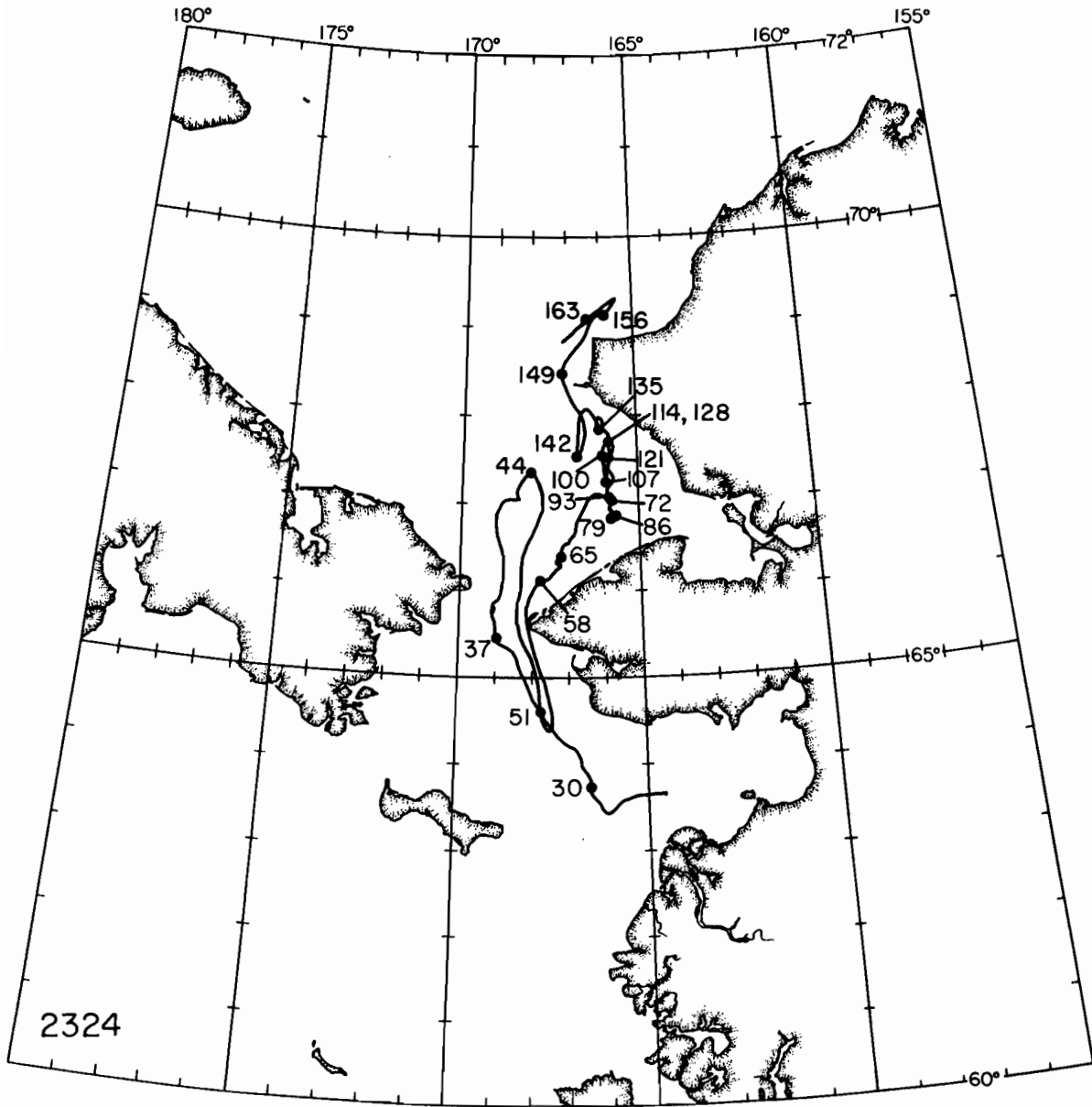


Figure 16. Summary plot of ARGOS platform 2324. 00Z of the Julian day is labelled weekly beginning with 30 January 1982 (JD 30).

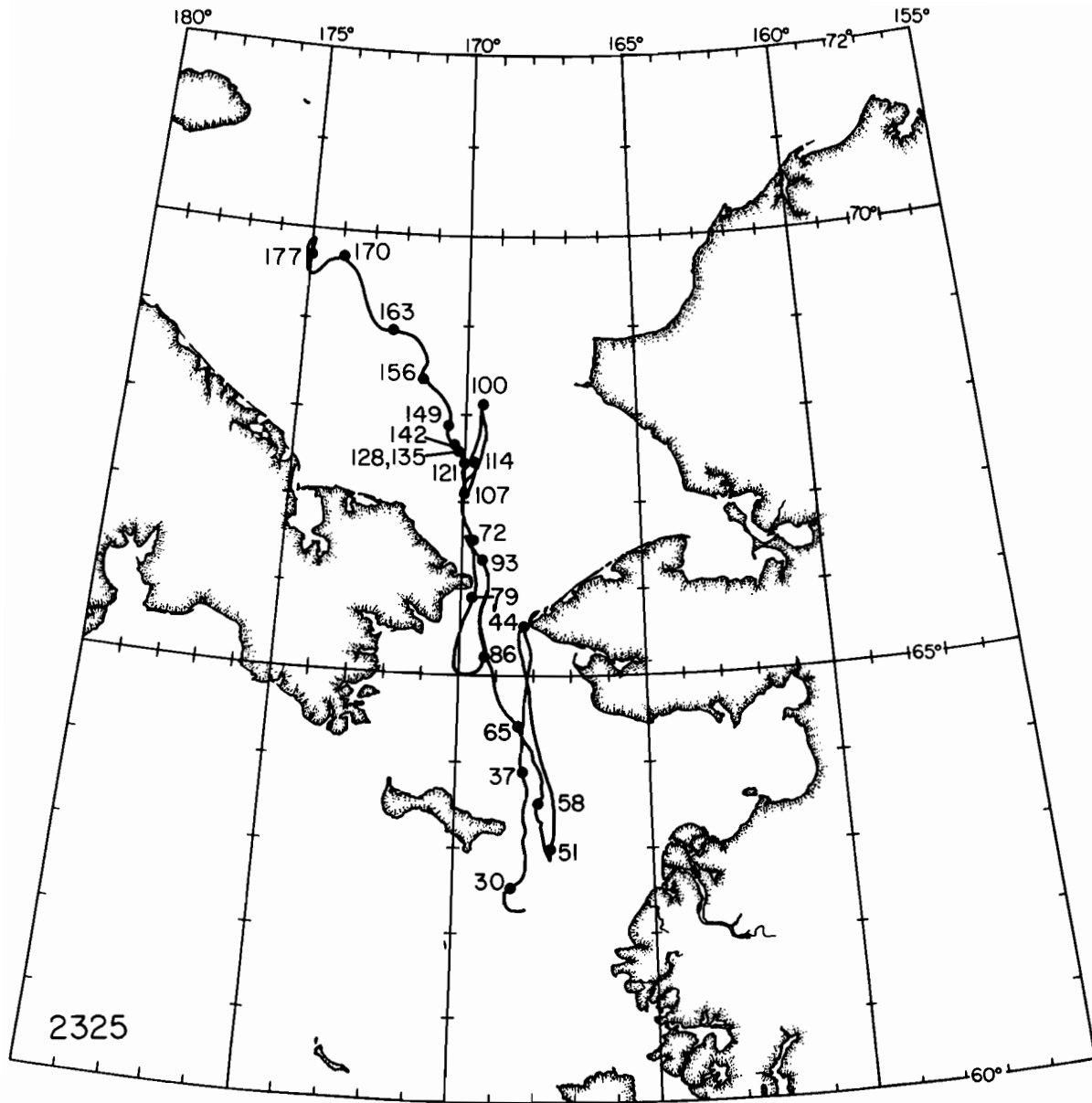


Figure 17. Summary plot of ARGOS platform 2325. 00Z of the Julian day is labelled weekly beginning with 30 January 1982 (JD 30).

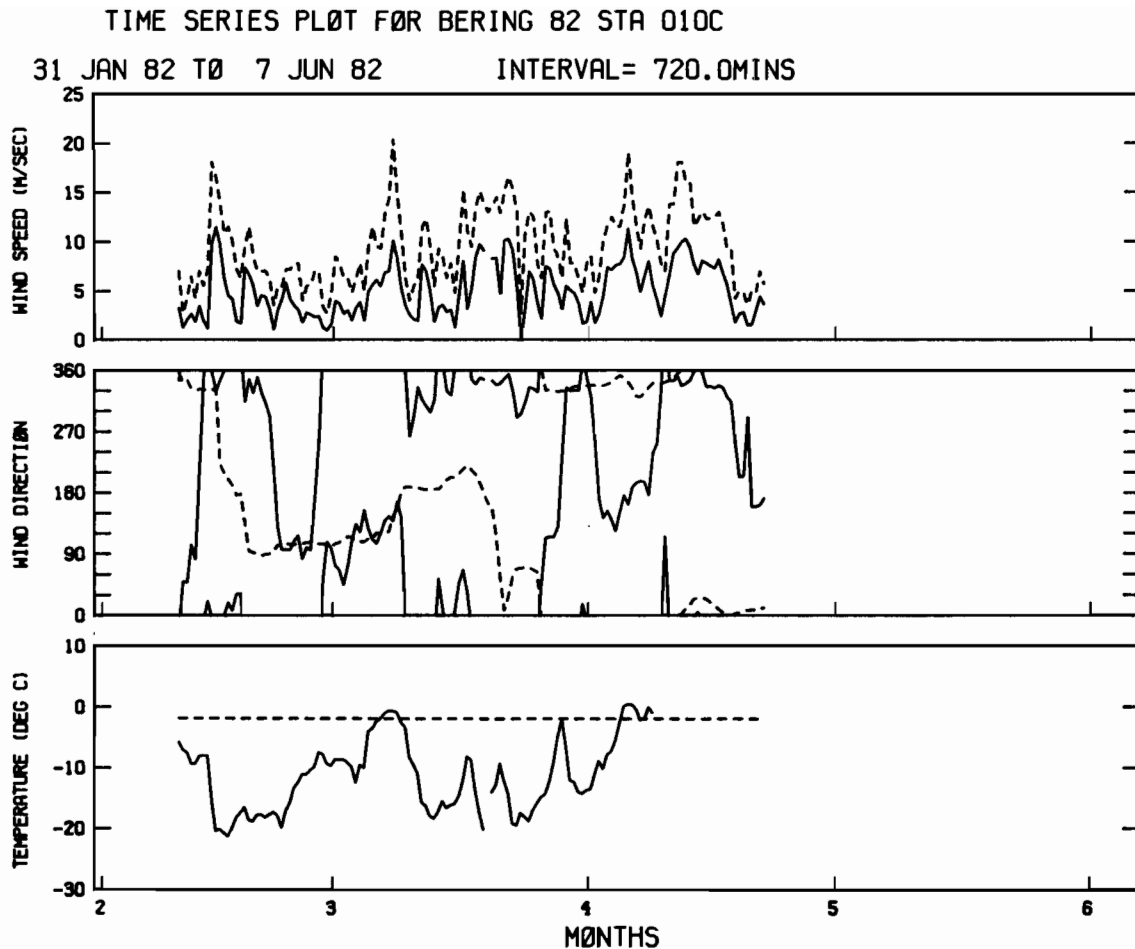


Figure 18. Summary plot of meteorological data collected at Station 010C. Data were collected hourly and block averaged over six hours. Winds are relative to the ice floe. In the speed plot, the solid line is the vector-average speed (20-min average) and the dashed line is the maximum gust observed in the sample period. In the direction plot, the solid line is vector-average direction (meteorological sense), and the dashed line is the compass reading. In the temperature plot, the solid line is the air temperature and the dashed line is water temperature.

rotated clockwise one complete circle during the two-month lifetime of this station with one large shift in mid-February and another in mid-March.

Meteorological Station 5170, co-located with ARGOS platform 2320, made three full trips through the Bering Strait and finally stopped transmitting after $4\frac{1}{2}$ months. Winds at 5170 were slightly stronger than those at 010C (Fig. 19). The gust circuit was faulty for this station and those data are not plotted. Good visual correlation between wind speeds and directions at the two locations gives confidence that both stations were functioning properly. A tendency for northwesterly and southeasterly wind directions, evident in the wind rose (Fig. 20), suggests the dominant synoptic pressure patterns for the northern Bering Sea. When a low moves in the southern or western Bering Sea, southeasterly wind directions prevail, and when the high over the Siberian plateau and Aleutian low prevail, northeasterlies are observed.

The floe heading was surprisingly stable during the entire experiment (Fig. 19). After a full counterclockwise rotation during mid-February, the heading remained much the same for the next $3\frac{1}{2}$ months during extensive migration. The rotation of the two stations during the mid-February event were in the opposite senses, implying local current responses to the same change in conditions were different.

3.3 Oceanographic Data

Oceanographic measurements at Stations 010C and 5170 are shown in Figures 21 and 22. Directions in these plots are in the oceanographic sense and refer to the direction toward which the relative current flows. The data are relative to the ice drift.

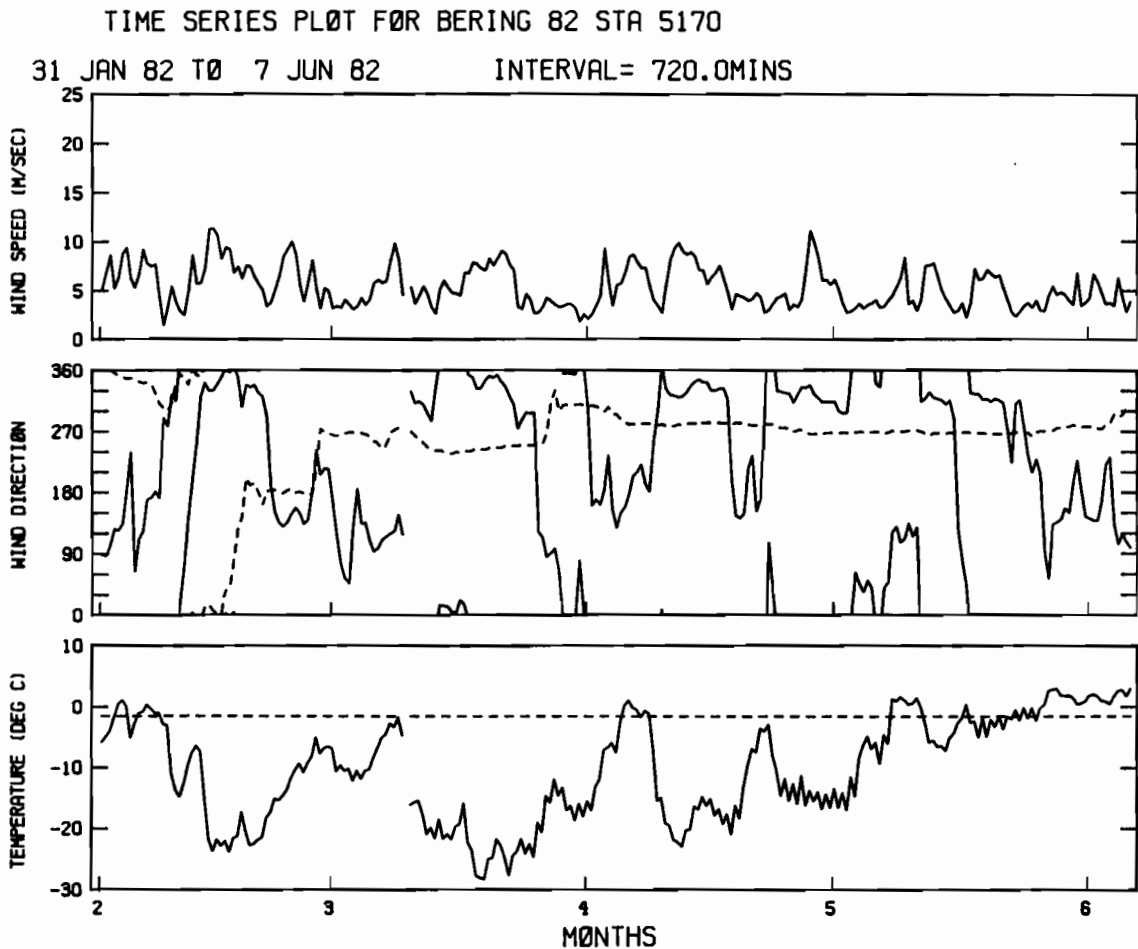


Figure 19. Summary plot of meteorological data collected at Station 5170. Data were collected hourly and block averaged over six hours. Winds are relative to the ice floe. In the speed plot, the solid line is the vector-average speed (20-min average) and the dashed line is the maximum gust observed in the sample period. In the direction plot, the solid line is vector-average direction (meteorological sense), and the dashed line is the compass reading. In the temperature plot, the solid line is the air temperature and the dashed line is water temperature.

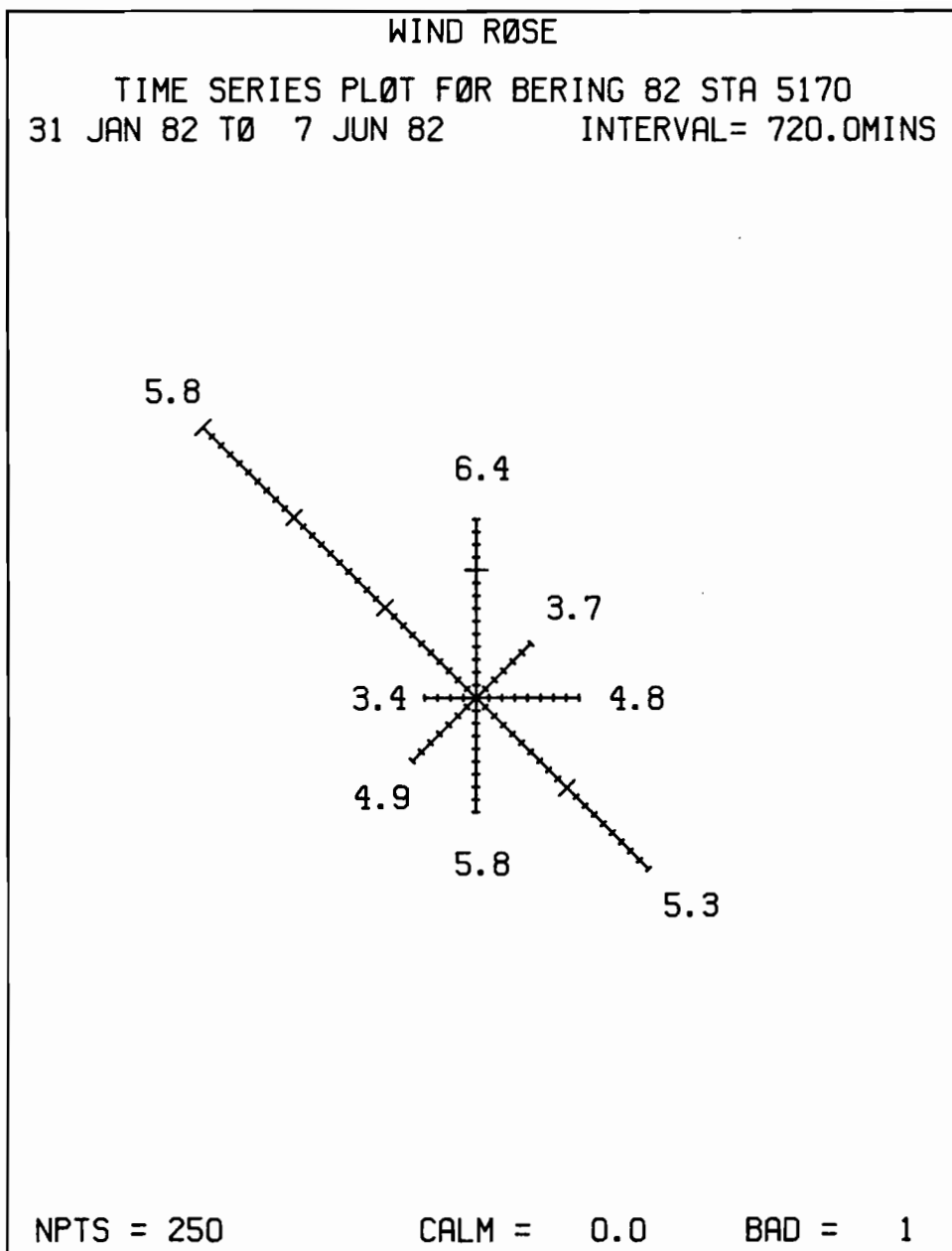


Figure 20. A wind rose of data collected from meteorological Station 5170. Percentage of occurrences are shown by the tic marks for each sector, and the mean wind in each sector is shown at the end of each radius.

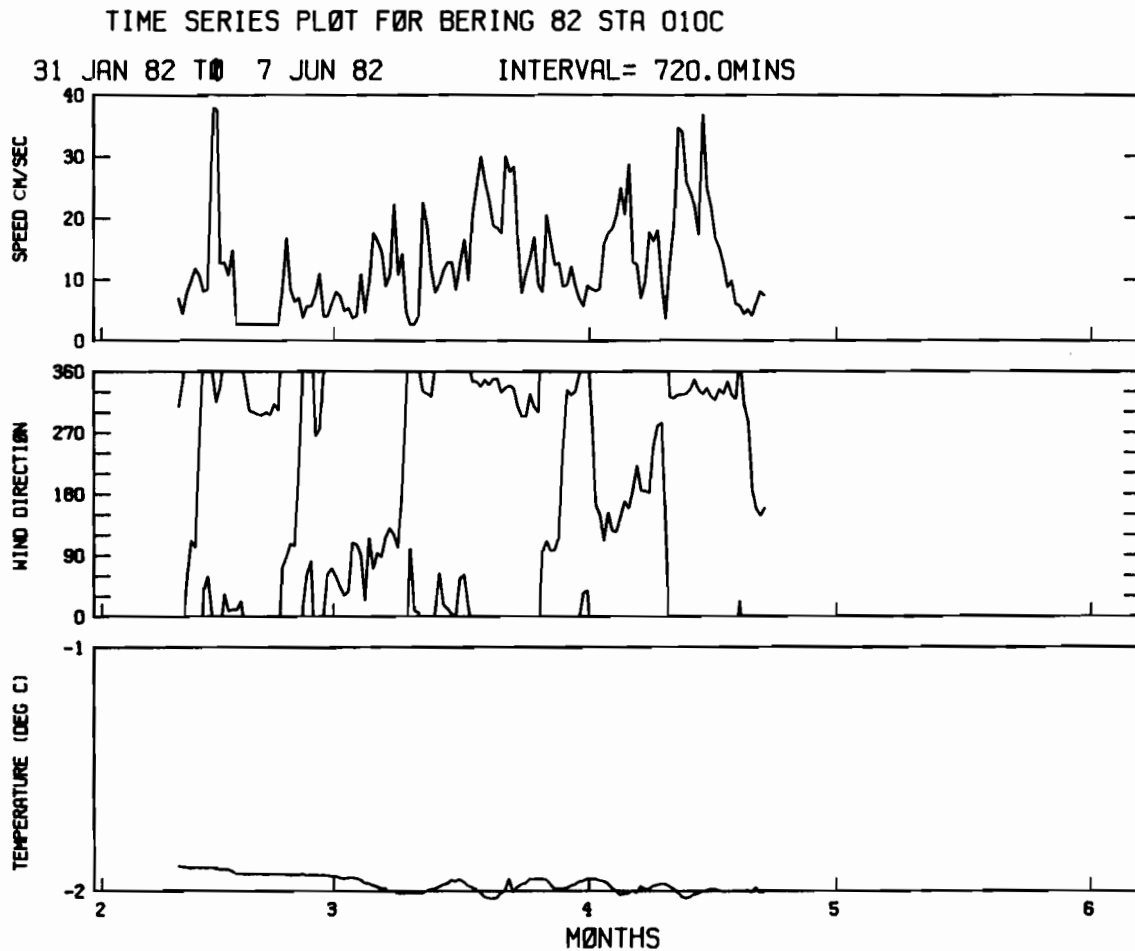


Figure 21. Summary plot of oceanographic data collected at Station 010C. Data was collected hourly and block averaged over six hours. Speed is an average speed in cm s^{-1} derived from total number of rotor turns over a 20-minute period. Direction is derived by adding instantaneous measurements of vane heading and compass every hour. Directions are in the oceanographic sense.

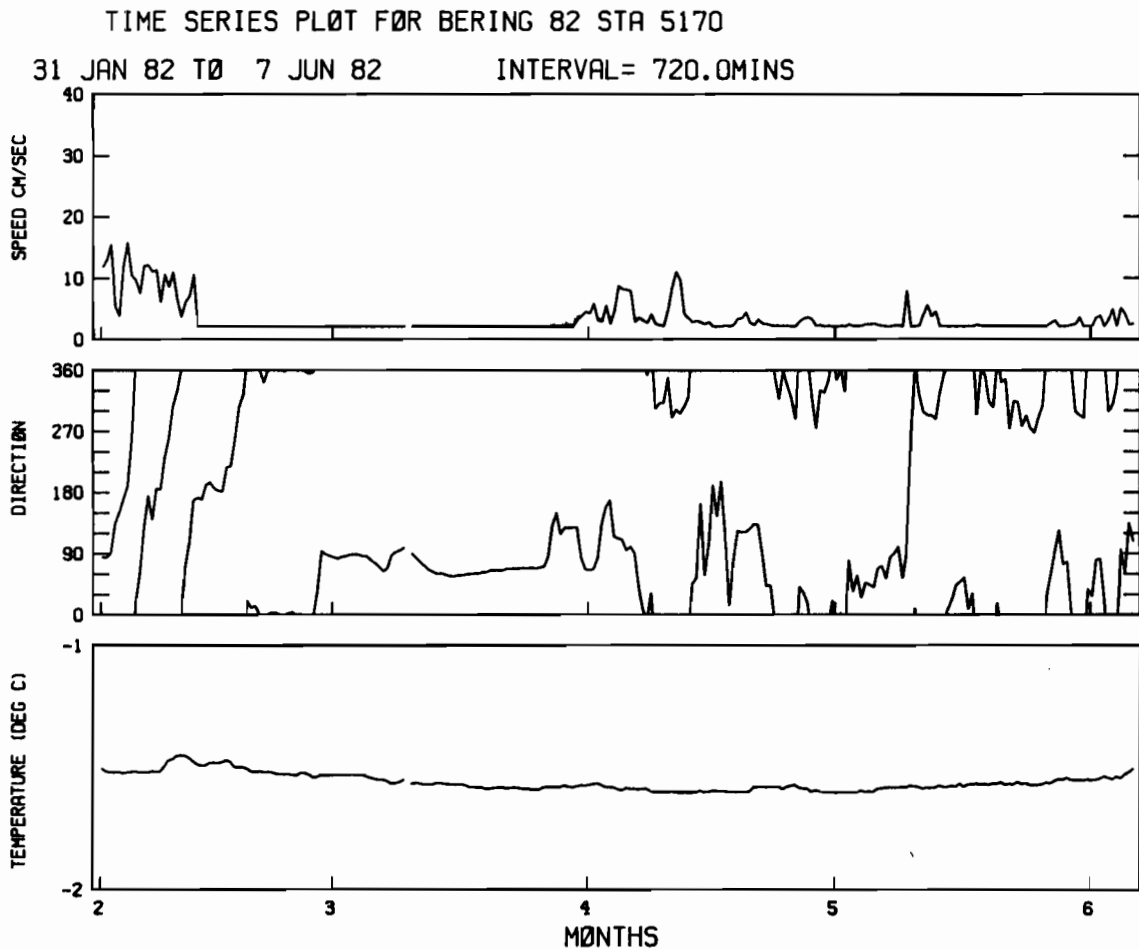


Figure 22. Summary plot of oceanographic data collected at Station 5170. Data was collected hourly and block averaged over six hours. Speed is an average speed in cm s^{-1} derived from total number of rotor turns over a 20-minute period. Direction is derived by adding instantaneous measurements of vane heading and compass every hour. Directions are in the oceanographic sense.

Over a short period in February (17th-22nd), the rotor at Station 010C was blocked and the value given is the stall speed of 2 cm s^{-1} . The vane direction appears good, and it is possible a fragment of ice blocked the rotor without affecting the vane. From mid-February (12th) until the end of March (31st), the current meter at Station 5170 was probably blocked by ice. Current directions during this stalled period are perfectly correlated with the compass. Since the current angle is given as the sum of the vane and compass, it is evident that the vane was constant. After this period, the vane worked properly. The small relative current from the end of March onward appears to be real since this floe exhibited very small drift velocities from the end of March on.

Another reasonable criterion of direction quality is to compare the wind and current directions. The ice tends to move down wind, and it can be shown that under ideal conditions the wind direction (meteorological sense) and current direction (oceanographic sense) will be nearly equal. One can overlay the wind and current plots and see good agreement in direction at all times except the period from mid-February to late March when the rotor was blocked.

4. Discussion

The general northward flow of water through the Bering Strait is accompanied by a general northward drift of ice. The incidence and duration of southward flow reversals in the vicinity of the Bering Strait show the drift of ice corresponds with the surface current and that both are driven by the overall wind pattern (Coachman et al., 1975; Coachman and Aagaard,

1981; Roach *et al.*, 1983). The ice drift direction is highly correlated over the same spatial scales as the current in the northern Bering Sea (Salo *et al.*, 1983). The ice-cover does not stop reversals in the Strait, only tracks them.

The ice moving from north to south through the Bering Strait during midwinter, in what have come to be called "break-out events" (Sodhi, 1977; Reimer *et al.*, 1979; Kovacs *et al.*, 1982), mostly likely is ice which has formed in Norton Sound and other areas in the northern Bering Sea and drifted north through the Bering Strait. Norton Sound and adjacent Bering Sea coastal waters may prove to be at least as an important source of ice for the Chukchi Sea as for the shelf south of St. Lawrence Island toward the Bering Sea ice edge (Muench and Alnäs, 1976; Pease, 1980; McNutt, 1981).

The alternate role of Norton Sound and adjacent waters as a source of ice can be seen clearly in both our data and similar data for the previous ice season (Thomas and Pritchard, 1981). Both years are characterized as having maximum ice extents in the average range for the Bering Sea. In the late fall and winter and in heavy ice years Norton Sound and vicinity contribute a larger percentage of ice production toward the south due to the persistent northeasterly winds characteristic of those times (Overland and Pease, 1981; Pease *et al.*, 1982), while in spring and in lighter ice years contribute toward the north due to the mean northward current and reduced wind persistence. Further indirect historical evidence includes the water transports along a section across the Chukchi Sea from Cape Lisburne from 1976-77 (Coachman and Aagaard, 1981). Maximum ice extent in the Bering was heavier than normal that winter and Coachman and Aagaard observed a net long-term water transport toward the north of only about 20% of that previously estimated (Coachman *et al.*, 1975). These results

suggest that the interannual variability of ice transport through the Bering Strait is extreme and tracks the surface water transport (Kovacs *et al.*, 1982).

Ice does not track water parcels exactly, even though the ice and water are highly coupled. The ice moves faster than the water when the wind and barotropic current are in the same direction. When the wind and barotropic current are in opposite directions, the ice moves more slowly than the water. This opposing situation occurs during the changes from one regime to another and can be seen in the detailed time series for ARGOS Platform 2320 in Appendix A. At the time of reversal, however, the ice moves in the same direction as the current. This suggests that the apparent arching north of the Strait during break-out events (Sodhi *et al.*, 1977; Reimer *et al.*, 1979; Kovacs *et al.*, 1982) (Fig. 11) are rather maps of the extent of current reversal and that the ice has no strength in failure when changes in direction are due to water stress.

There is a diurnal tidal signal in the ice movement in the vicinity of Norton Sound (Pearson *et al.*, 1981) and a semi-diurnal tidal signal near Kotzebue Sound (Kinder *et al.*, 1977). The magnitude of the tidal excursion in Norton Sound is larger than that in Kotzebue Sound, but a numerical comparison is left for a later study. The semi-diurnal excursion is less important in Norton Sound than on the open shelf in the central and southern Bering Sea (Pearson *et al.*, 1981; Salo *et al.*, 1983). The tidal signal is not discernable in the Strait itself. This is due to the extreme ice velocities resulting from the coupled contributions of wind stress and the barotropic current and possibly a weak tidal signal.

In the spring (and possibly at other times) there is a noticeable bifurcation in the northward flow of ice out of Bering Strait which tracks

a bifurcation in the surface current. Ice which passes through the Bering Strait close to Cape Dezhneva tracks parallel to the Chukotsk coast along the center line of the broad trough (deeper than 50 m) which heads toward Wrangel Island. Ice which passes through the Bering Strait between Little Diomedede Island and Cape Prince of Wales follows the 30-m isobath along the Alaska coast past Point Hope and Cape Lisburne toward Barrow Canyon. These divisions of ice flow field through the Strait are only approximate since the contributions from one side or the other vary in time with changes in the wind regime and the thermohaline conditions. For instance one of the ARGOS platforms from the Thomas and Pritchard study (1981) passed close to Cape Prince of Wales yet joined the broad stream along the Chukotsk coast because of a major and prolonged wind event. Water intrusion patterns from the eastern Bering Strait during summer 1974 (Garrison and Becker, 1975) show that bifurcation can occur as far north as Point Hope, but other sources (Coachman *et al.*, 1975; Garrison and Becker, 1976; Paquette and Bourke, 1981) point to the semi-permanent nature of the Alaskan coastal current across the mouth of Kotzebue Sound, around Point Hope and Cape Lisburne, and exiting through Barrow Canyon.

The net transport of ice in Norton Sound during winter and spring was toward the west, but the spring transports were an order of magnitude smaller than winter. The north-south oscillations increased for any given floe as it moved westward into deeper water which appears to be more directly coupled to the reversals in the Strait. This increase in excursion length was greatest along the 20-m isobath. A shear zone in the flow field across the mouth of Norton Sound at approximately the 20-m isobath was observed on 15 and 16 February 1982 (Walter and Overland, 1984) and has been observed previously (Pease and Salo, 1981). The Yukon River

plume, a surface feature in Norton Sound in summer has a net westward and northward transport (Muench *et al.*, 1981) also, except for infrequent pulses.

Melting in the late spring was rapid and relatively uniform over large areas. Platforms in the mouths of Norton and Kotzebue Sound stopped transmitting during the first week of June, followed a week later by the platform near Cape Lisburne, followed in another two weeks by the platform on the Siberian side. There were some latitudinal differences and some differences probably attributable to thickness variations, but generally all the ice produced during mid-winter in Norton Sound melted by 1 July, whether that ice had been exported to the Chukchi Sea or not. A more careful analysis using available satellite imagery to corroborate these details would be helpful.

5. Summary

In general, Norton Sound supplied ice northward through the Bering Strait into the Chukchi Sea during the winter of 1982. Ice floes typically made several oscillations of the scale of 350 km through the Strait during the winter. Southward ice movements were coupled with barotropic current reversals which lasted about a week. Ice break-out events from the Chukchi to the Bering were observed during these reversals, although the ice was previously formed in Norton Sound. The apparent arching of the ice across the northern end of the Strait more accurately portrayed the pattern of current reversal and had little to do with arching due to ice strength.

This work is a preliminary analysis and data summary. Further analysis will include detailed studies of the energy at tidal frequencies in Norton and Kotzebue Sounds, stress and strain patterns related to the ice drift through the Bering Strait, and quantification of the net volume transport of ice northward during 1982.

6. Acknowledgements

This study is a contribution to the Marine Services Project of the Marine Services Research Division at the Pacific Marine Environmental Laboratory and was financed in part by the Office of Naval Research, Arctic Program Code 425 under project NR 307-473. Helicopter logistics were supported by the Bureau of Land Management through an interagency agreement with the National Oceanic and Atmospheric Administration under a multiyear program, responding to the needs of petroleum development of the Alaskan continental shelf and managed by the Outer Continental Shelf Environmental Assessment Program (OCSEAP) Office.

LCDR Ted Kaiser assisted with the buoy deployment and was responsible for the anemometer and current meter structures for the ice stations. J.E. Overland, B.A. Walter, and S.A. Macklin were the PMEL mission scientists on the NOAA WP-3D flights. S.A. Macklin and R.L. Brown analyzed the ARGOS buoy data.

The NWS Forecast Office in Nome, Alaska under MIC Grady Svoboda gave valuable assistance in forecasting and logistics. The Air National Guard in Nome provided space in their hanger to assemble the ice stations. Bruce Webster, ice forecaster from NWS Anchorage, gave ice and weather guidance, particularly related to the P3 flights.

Sigrid A. Salo handled all the ARGOS and GOES realtime data acquisition from Seattle during the deployment. Her daily phone briefings were both the alarm clock and the basis for planning every flight.

Lt. Bud Christman and Bob Neil were the NOAA helicopter pilot and mechanic. Both rode out the bad weather in good humor.

7. References

- Coachman, L.K., K. Aagaard and R.B. Tripp (1975): Bering Strait: The Regional Physical Oceanography, University of Washington Press, Seattle, WA, 172 pp.
- Coachman, L.K. and K. Aagaard (1981): Reevaluation of water transports in the vicinity of Bering Strait, Chapter 7 in The Eastern Bering Sea Shelf: Oceanography and Resources, 1, University of Washington Press, Seattle, WA, 95-110.
- Garrison, G.R. and P. Becker (1975): Marginal Sea Ice Zone Oceanographic Measurements - Bering and Chukchi Seas, 1973 and 1974, Applied Physics Laboratory, Univ. of Washington, Report APL-UW 7505, Seattle, WA, 144 pp.
- Garrison, G.R. (1976): Chukchi Sea Oceanography - 1975 Measurements and a Review of Coast Current Properties, Applied Physics Laboratory, Univ. of Washington, Report APL-UW 7614, Seattle, WA, 126 pp.
- Garrison, G.R. and P. Becker (1976): The Barrow Submarine Canyon: A drain for the Chukchi Sea, J. Geophys. Res., 81, 4445-4453.
- Kinder, T.H., J.D. Schumacher, R.B. Tripp and D.J. Pashinski (1977): The Physical Oceanography of Kotzebue Sound, Alaska, during Late Summer, 1976, University of Washington, Dept. of Oceanography Technical Report M77-99, Seattle, WA, 84 pp.
- Kovacs, A., D.S. Sodhi and G.F.N. Cox (1982): Bering Strait Sea Ice and the Fairway Rock Icefoot, Cold Regions Research and Engineering Laboratory Report 82-31, Hanover, NH, 40 pp.
- Macklin, S.A., C.H. Pease and R.M. Reynolds (1984): Bering Air-Sea-Ice Study (BASICS) - February and March 1981, NOAA Technical Memorandum ERL PMEL-52, 104 pp.

- McNutt, S.L. (1981): Remote sensing analysis of ice growth and distribution in the eastern Bering Sea, March 1979, Chapter 10 in The Eastern Bering Sea Shelf: Oceanography and Resources, 1, University of Washington Press, Seattle, WA, 141-166.
- Muench, R.D. and K. Ahlnäs (1976): Ice movement and distribution in the Bering Sea from March to June 1974, J. Geophys. Res., 81, 4467-4476.
- Muench, R.D., R.B. Tripp and J.D. Cline (1981): Circulation and hydrography of Norton Sound, Chapter 6 in The Eastern Bering Sea Shelf: Oceanography and Resources, 1, University of Washington Press, Seattle, WA, 77-93.
- Overland, J.E. and C.H. Pease (1982): Cyclone climatology of Bering Sea and its relation to sea ice extent, Mon. Wea. Rev., 110, 5-13.
- Paquette, R.G. and R.H. Bourke (1981): Ocean circulation and fronts as related to ice melt-back in the Chukchi Sea, J. Geophys. Res., 86, 4215-4230.
- Pease, C.H. (1980): Eastern Bering Sea ice processes, Monthly Weather Review, 108, 2015-2023.
- Pease, C.H. and S.A. Salo (1981): Drift Characteristics of Northeastern Bering Sea Ice during 1980, NOAA Technical Memorandum ERL PMEL-32, 78 pp.
- Pease, C.H., S.A. Schoenberg and J.E. Overland (1982): A Climatology of the Bering Sea and Its Relation to Sea Ice Extent, NOAA Technical Report ERL 419-PMEL 36, 29 pp.
- Pearson, C.A., H.O. Mofjeld and R.B. Tripp (1981): Tides of the eastern Bering Sea shelf, Chapter 8 in The Eastern Bering Sea Shelf: Oceanography and Resources, 1, University of Washington Press, Seattle, WA, 111-130.

- Pratt, R. and F. Walton (1974): Bathymetric Map of the Bering Shelf, Geological Society of America, Boulder, CO, 1 plate.
- Reimer, R.W., R.S. Pritchard and M.D. Coon (1979): Beaufort and Chukchi Sea Ice Motion, Part 2. Onset of Large Scale Chukchi Sea Ice Breakout, Flow Research Report No. 133, Kent, WA, 92 pp.
- Reynolds, M. (1983): A simple meteorological buoy with satellite telemetry, Ocean Engng., 10, 65-76.
- Roach, A.T., J.D. Schumacher, K. Aagaard and R.B. Tripp (1983): Inter-annual variations in transport through Bering Strait, EOS Transactions, 64, 1101.
- Salo, S.A., J.D. Schumacher and L.K. Coachman (1983): Winter Currents on the Eastern Bering Sea Shelf, NOAA Technical Memorandum ERL PMEL-45, 53 pp.
- Sodhi, D.S.(1977): Ice Arching and the Drift of Pack Ice through Restricted Channels, Cold Regions Research and Engineering Laboratory Report 77-18, Hanover, NH, 11 pp.
- Thomas, D.R. and R.S. Pritchard (1981): Norton Sound and Bering Sea Ice Motion: 1981, Flow Research Report No. 209, Kent, WA, 37 pp.
- Walter, B.A., Jr. and J.E. Overland (1984): Observations of longitudinal rolls in a near neutral atmosphere, Mon. Wea. Rev., 112, 200-208.
- Walter, B.A., J.E. Overland, and R. Gilmer (1984): Air-ice drag coefficients for first year sea ice derived from aircraft measurements, J. Geophys. Res., 89, (in press).
- White, W.B. and N.E. Clark (1975): On the development of blocking ridge activity over the central north Pacific, J. Atmos. Sci., 32, 489-502.

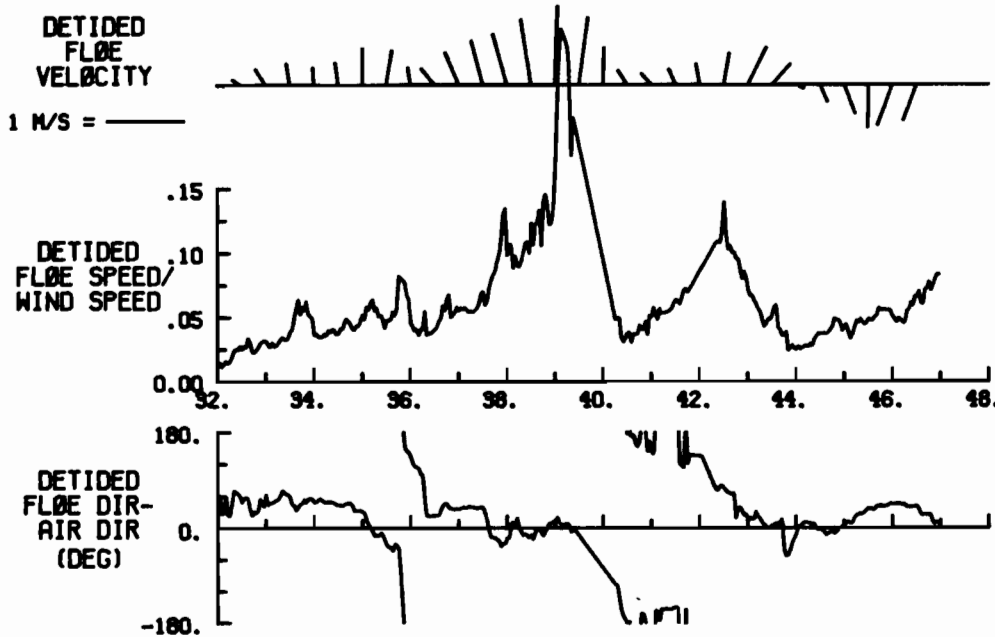
APPENDIX A

Lagrangian Drift Data

1. All floe and wind vectors in the diagrams are portrayed with respect to the oceanographic convention, i.e. they point in the direction that the floe or air is moving.
2. Wind vectors are from surface winds sampled hourly at the respective ice floes.
3. "FLOE SPEED/WIND SPEED" and "FLOE DIR - AIR DIR" diagrams exclude data from periods when the wind speed was less than 3 m s^{-1} .
4. Detided floe velocities are low-pass filtered at 35 hours. The floe tracks are plotted from unfiltered position data.
5. In the floe track plots, a \emptyset is plotted at the 00 GMT position and the Julian day is printed to the right of the \emptyset ; a * is plotted at the 12 GMT floe position.
6. Floe positions were telemetered by satellite at irregular intervals of several minutes to several hours. We fit curves to these data using the method of cubic splines and then resampled the tracks at hourly intervals.

A1. Station 2320

FLØE STATION 2320 FEB 01-15, 1982 (JD 32 - 46)



MEAN =
.23
TOWARD
352

MEAN =
.0597
SIGMA=
.0376

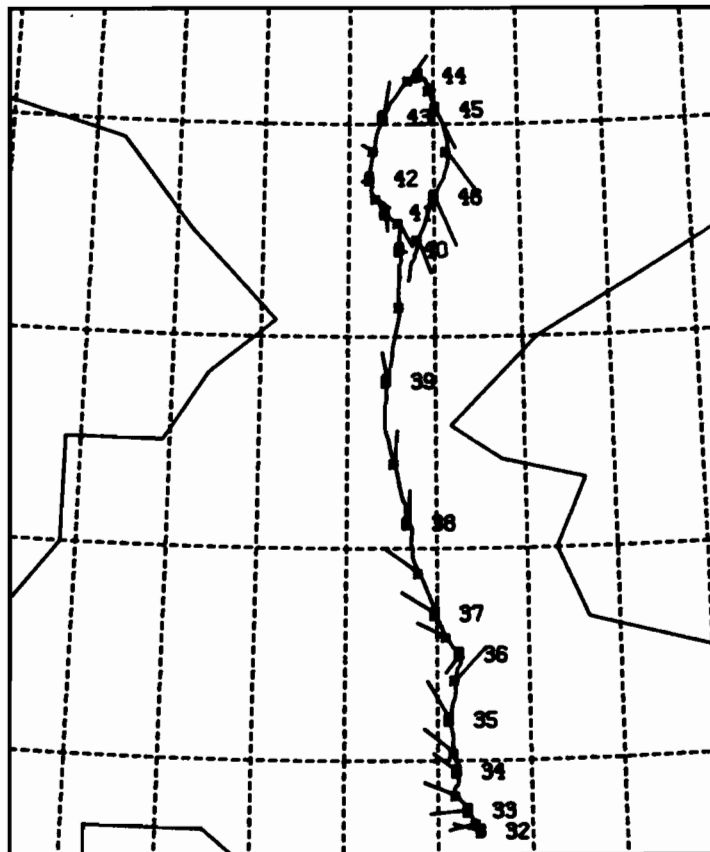
MEAN =
19.4
SIGMA=
63.1

(67.5 N,
164.5 W)

FLØE TRACK
WITH
SURFACE
WIND

10 M/S =
———

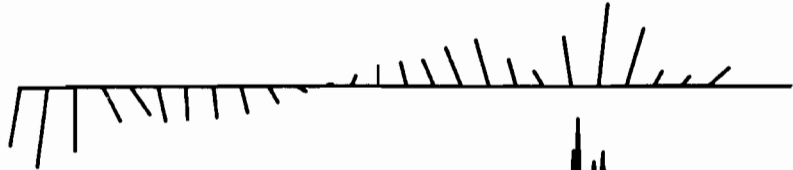
(63.5 N,
172.5 W)



FLØE STATION 2320 FEB 16-28, 1982 (JD 47 - 59)

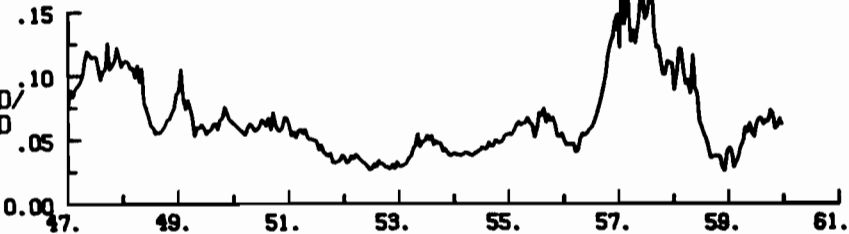
DETIDED
FLØE
VELØCITY

1 M/S = 



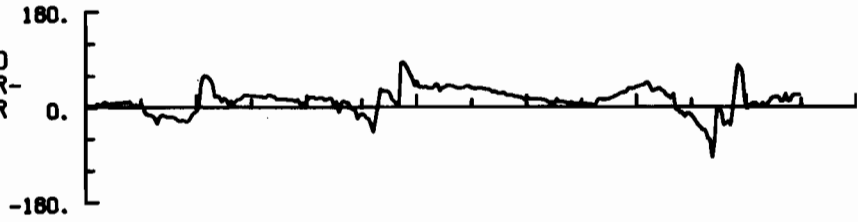
MEAN =
.04
TOWARD
52

DETIDED
FLØE SPEED/
WIND SPEED



MEAN =
.0680
SIGMA=
.0329

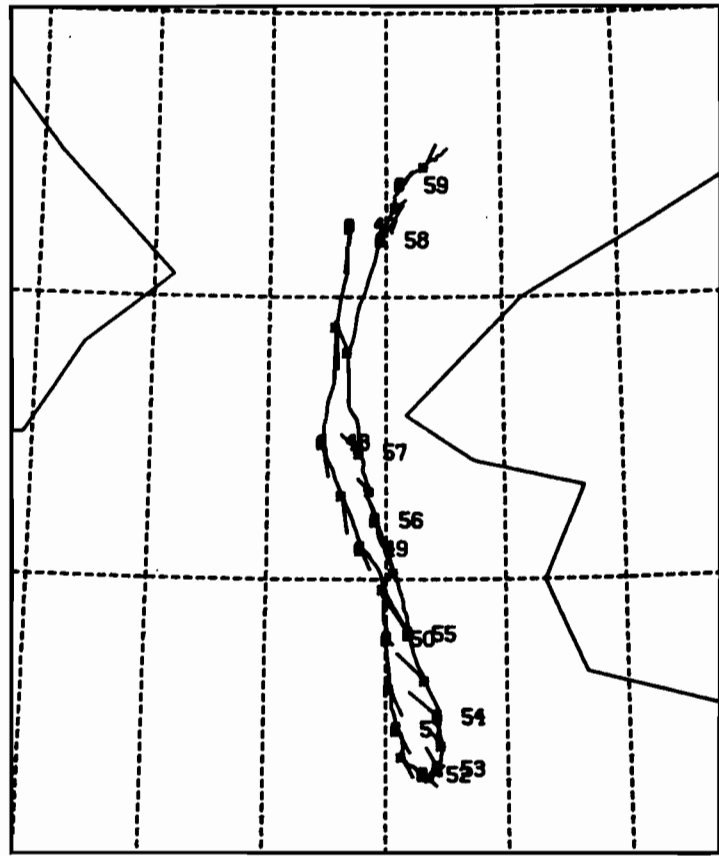
DETIDED
FLØE DIR-
AIR DIR
(DEG)



MEAN =
13.5
SIGMA=
24.5

FLØE
TRACK
WITH
SURFACE
WIND

10 M/S = 



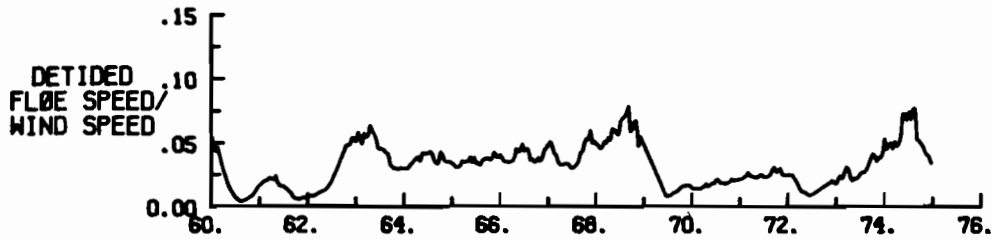
(67.0 N,
165.0 W)

(64.0 N,
171.0 W)

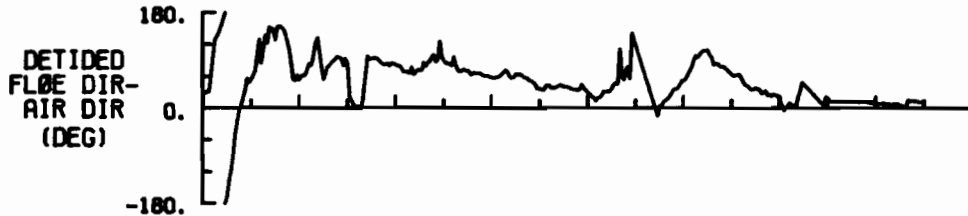
FLØE STATION 2320 MAR 01-15, 1982 (JD 60 - 74)



MEAN =
.06
TOWARD
353



MEAN =
.0325
SIGMA=
.0165



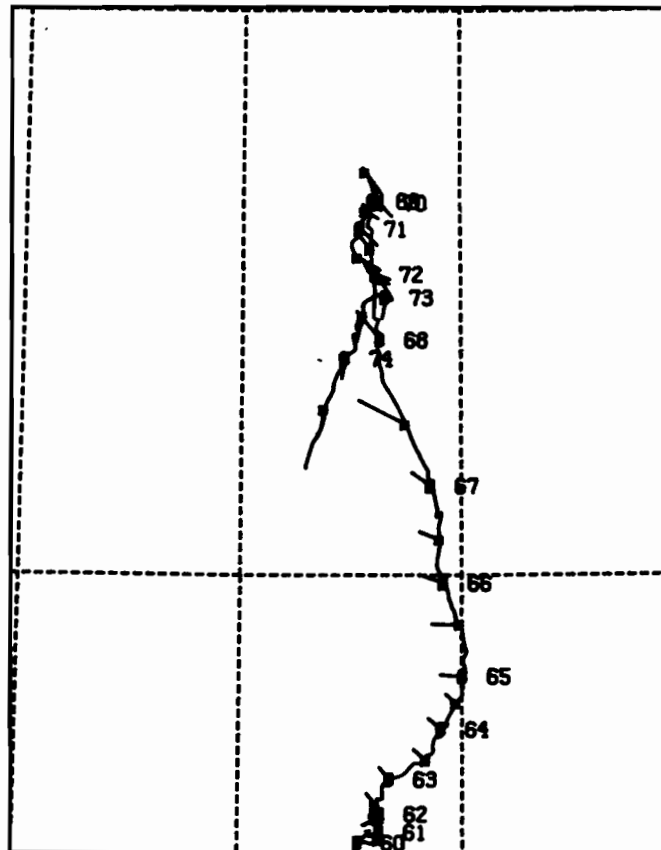
MEAN =
51.2
SIGMA=
44.7

(68.0 N,
166.0 W)

FLØE
TRACK
WITH
SURFACE
WIND

10 M/S =
———

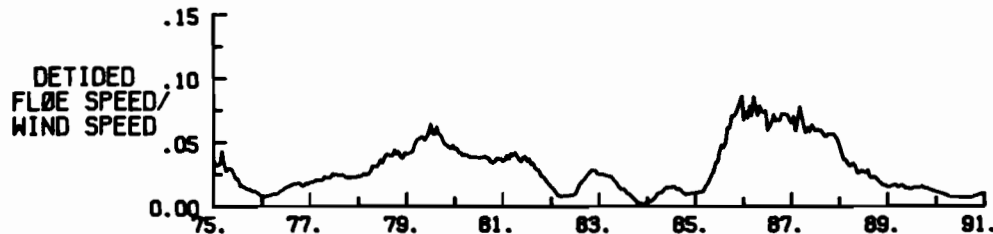
(66.5 N,
169.0 W)



FLØE STATION 2320 MAR 16-31, 1982 (JD 75 - 90)



MEAN =
.07
TOWARD
165



MEAN =
.0315
SIGMA=
.0196

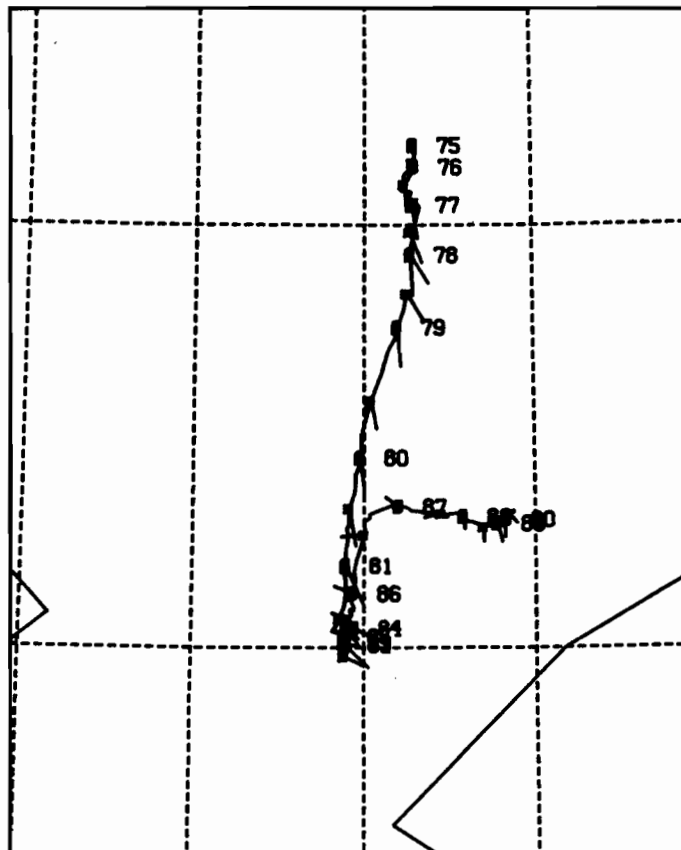


MEAN =
6.2
SIGMA=
74.3

(67.5 N,
166.0 W)

FLØE
TRACK
WITH
SURFACE
WIND

10 M/S =
—

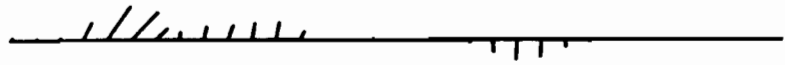


(65.5 N,
170.0 W)

FLØE STATION 2320 APR 01-15, 1982 (JD 91 -105)

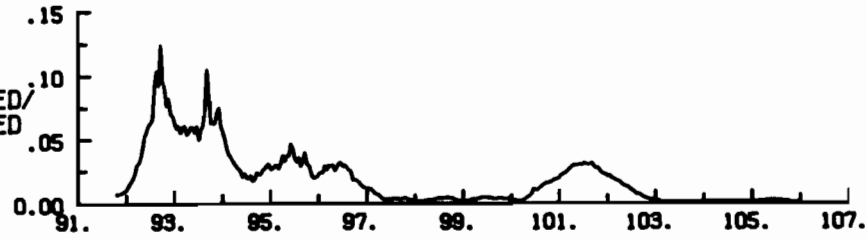
DETIDED
FLØE
VELOCITY

1 M/S = 



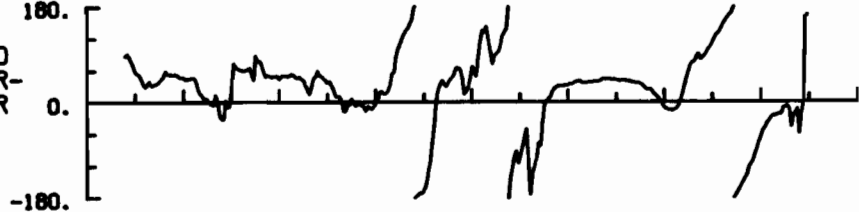
MEAN =
.06
TOWARD
43

DETIDED
FLØE SPEED/
WIND SPEED



MEAN =
.0198
SIGMA=
.0226

DETIDED
FLØE DIR-
AIR DIR
(DEG)

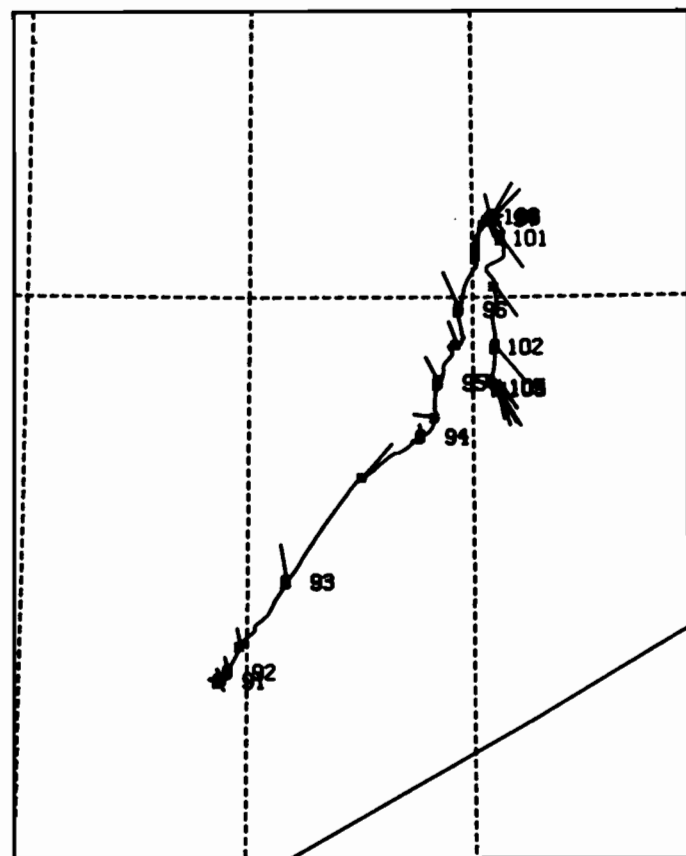


MEAN =
27.6
SIGMA=
63.1

(67.5 N,
165.0 W)

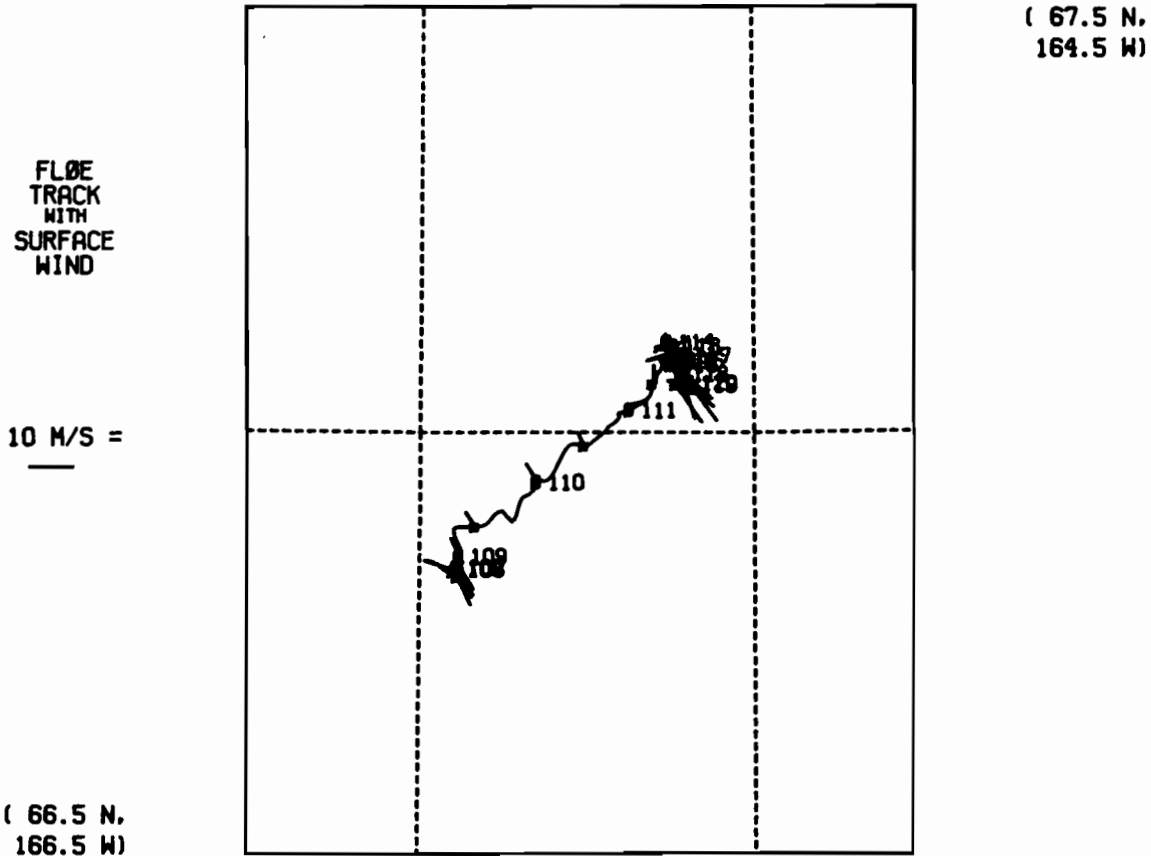
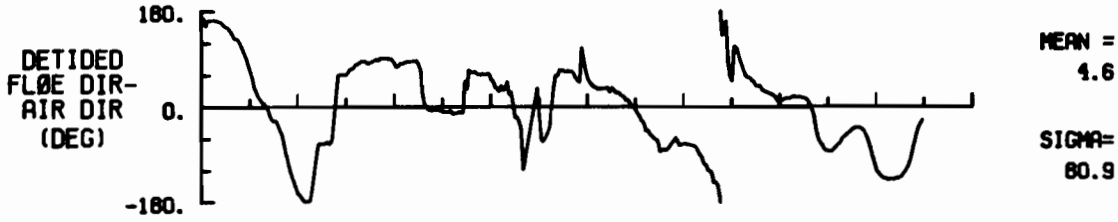
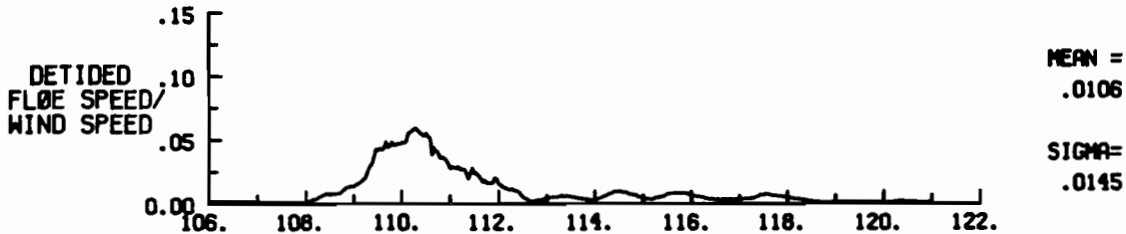
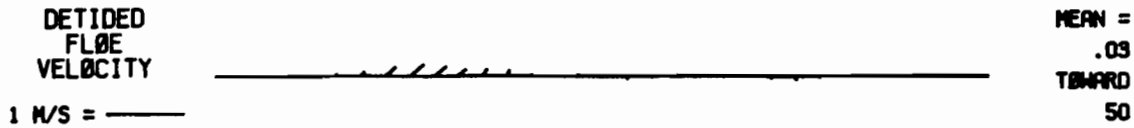
FLØE
TRACK
WITH
SURFACE
WIND

10 M/S = 

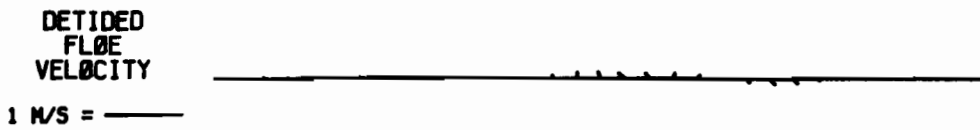


(66.0 N,
168.0 W)

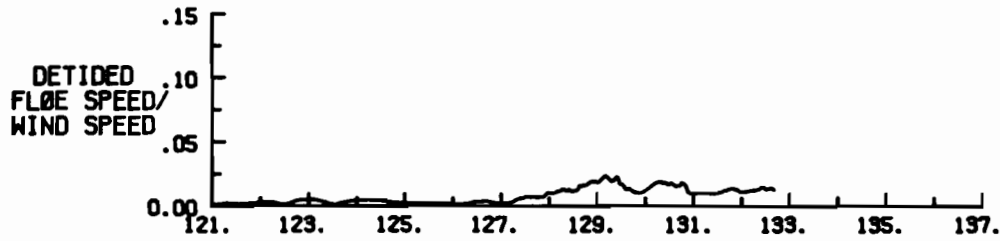
FLØE STATION 2320 APR 16-30, 1982 (JD 106 -120)



FLØ STATION 2320 MAY 01-15, 1982 (JD 121 -135)



MEAN =
.01
TOWARD
27



MEAN =
.0080
SIGMA=
.0061

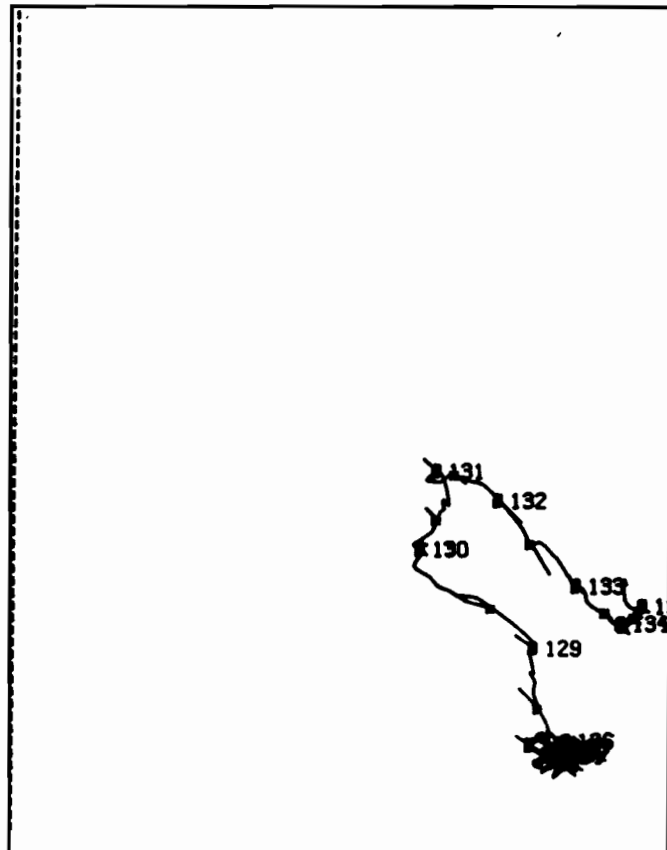


MEAN =
14.2
SIGMA=
73.7

(67.5 N,
165.0 W)

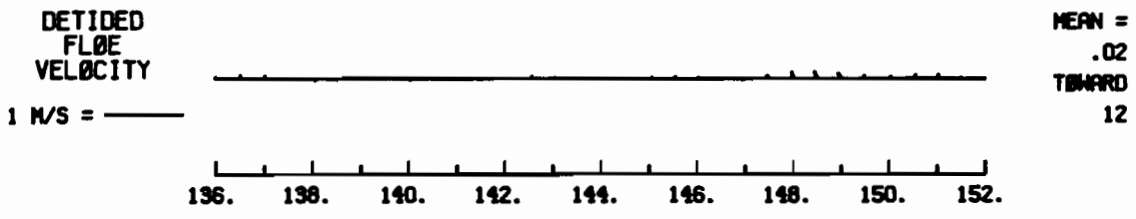
FLØ
TRACK
WITH
SURFACE
WIND

10 M/S =
—

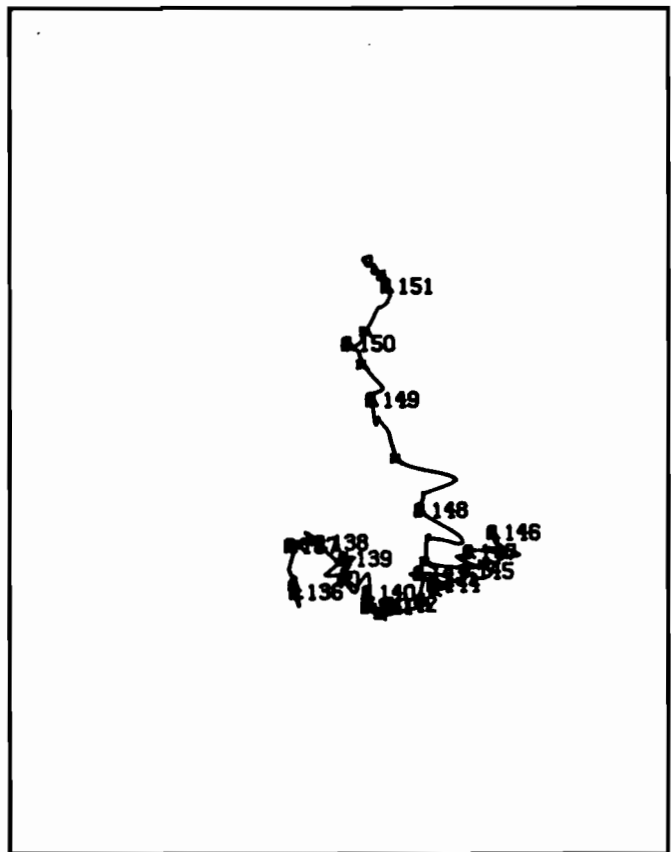


(67.0 N,
166.0 W)

FLØE STATION 2320 MAY 16-31, 1982 (JD 136 -151)



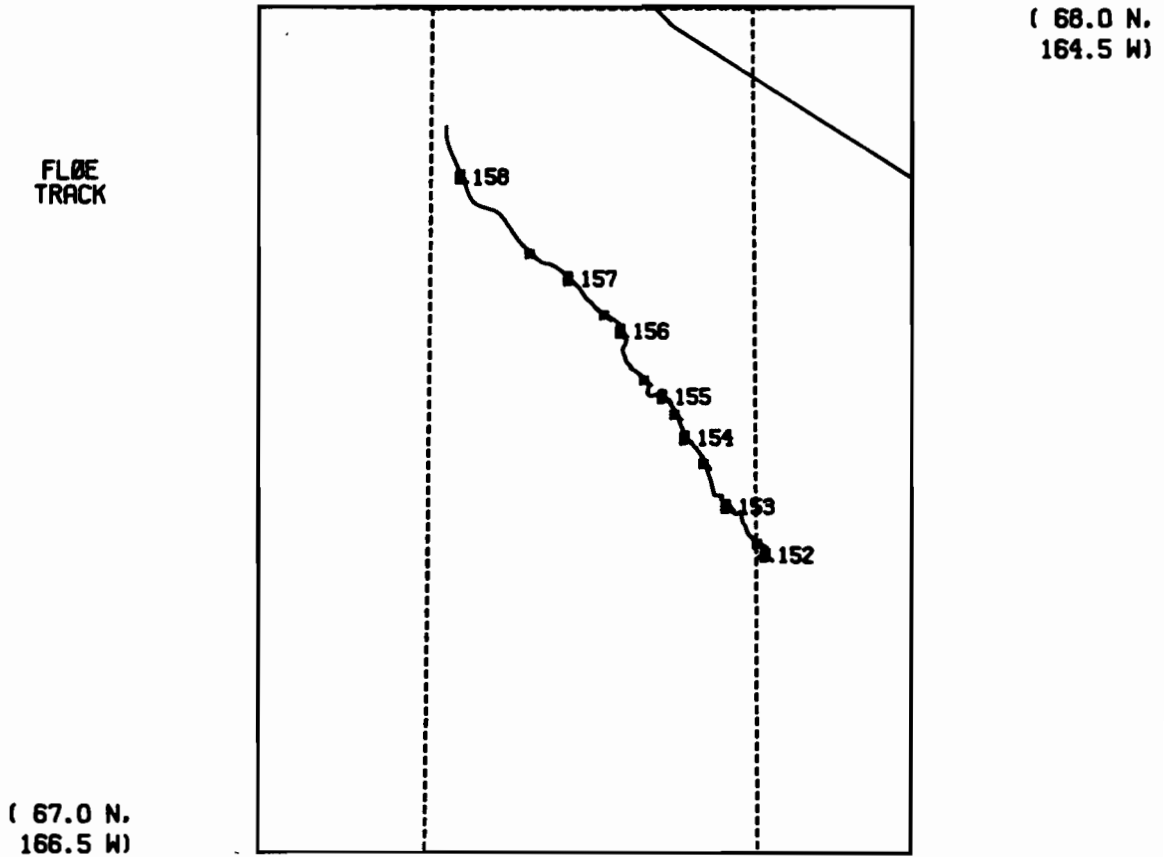
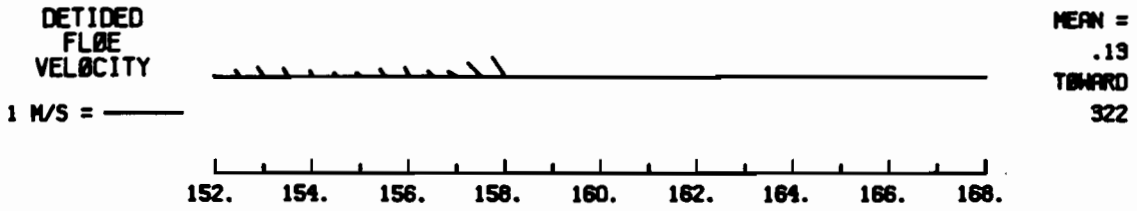
FLØE
TRACK



(67.5 N,
164.5 W)

(67.0 N,
165.5 W)

FLØE STATION 2320 JUN 01-15, 1982 (JD 152 -166)

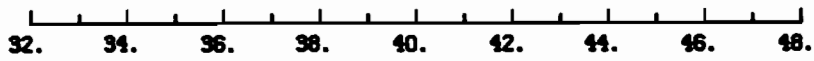


A2. Station 2321B

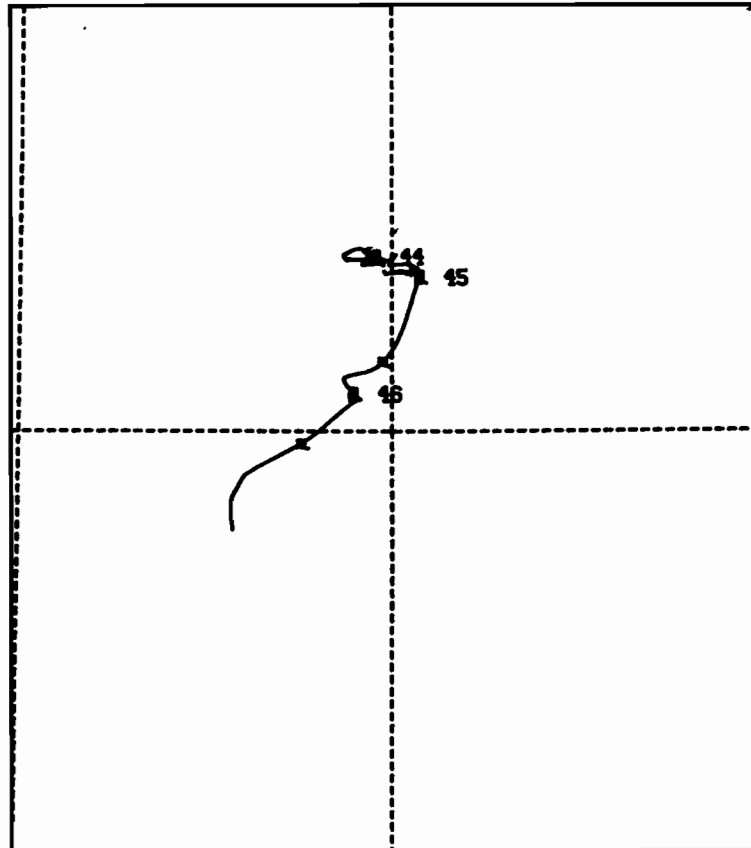
FLØE STATION 2321B FEB 01-15, 1982 (JD 32 - 46)

DETERMINED
FLØE
VELOCITY
1 M/S = 

MEAN =
.12
TOWARD
207



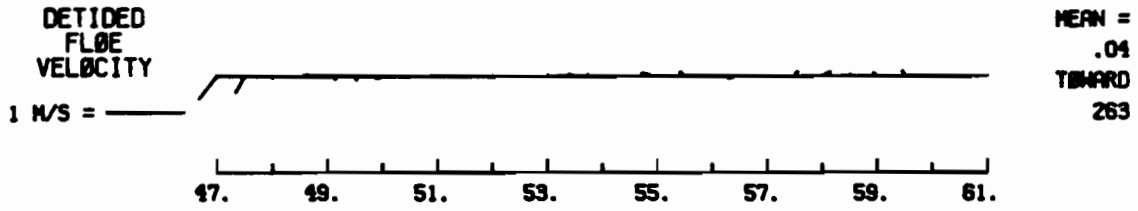
FLØE
TRACK



(64.5 N.
163.0 W)

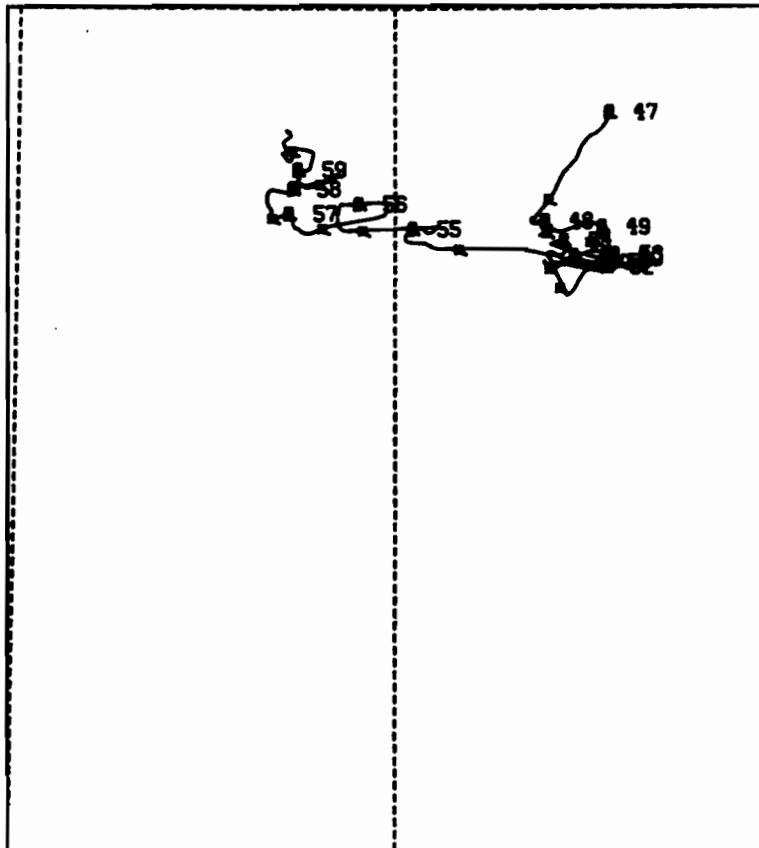
(63.5 N.
165.0 W)

FLØE STATION 2321B FEB 16-28, 1982 (JD 47 - 59)

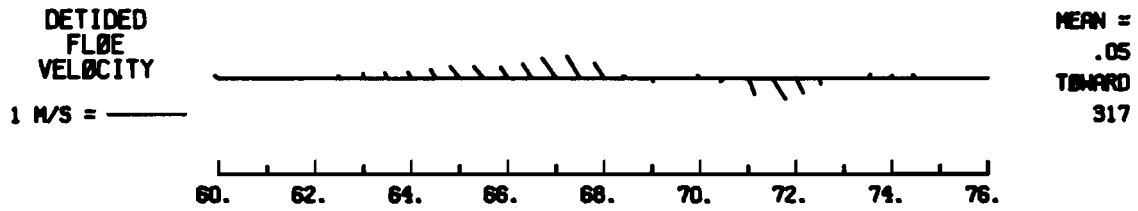


FLØE
TRACK

(63.0 N.
166.0 W)

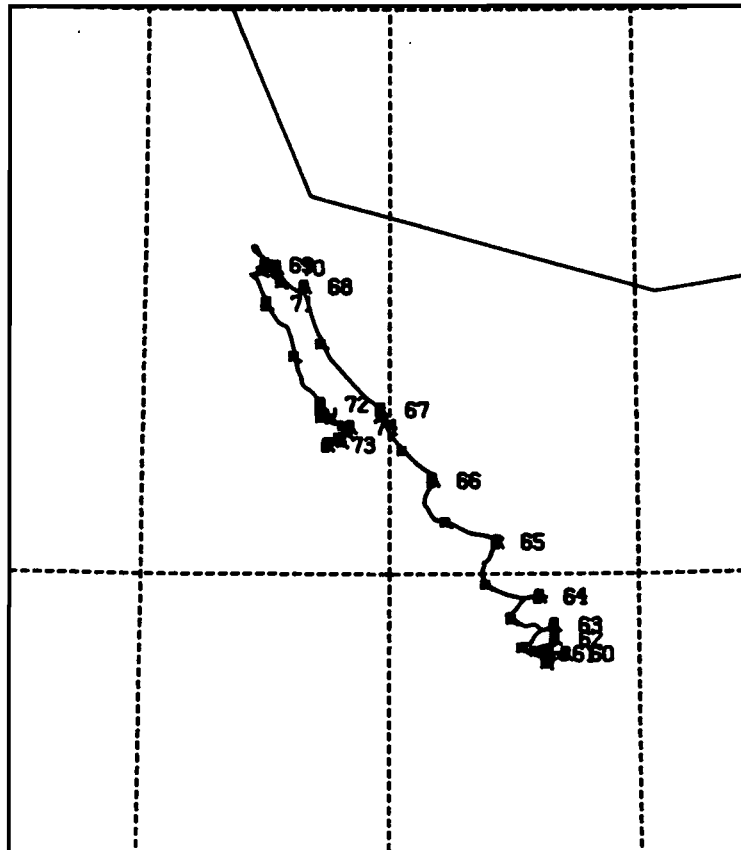


FLØ STATION 2321B MAR 01-15, 1982 (JD 60 - 74)



FLØ
TRACK

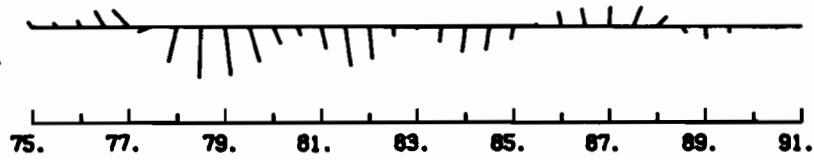
(63.5 N.
167.5 W)



(65.0 N.
164.5 W)

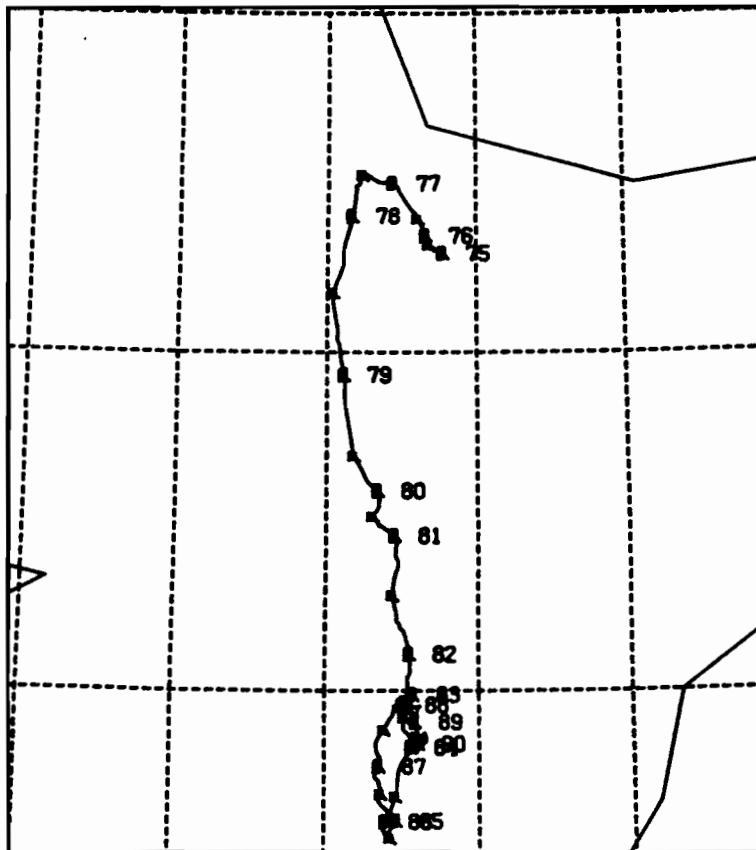
FLØE STATION 2321B MAR 16-31, 1982 (JD 75 - 90)

DETIDED
FLØE
VELOCITY
1 M/S = _____



MEAN =
.12
TOWARD
182

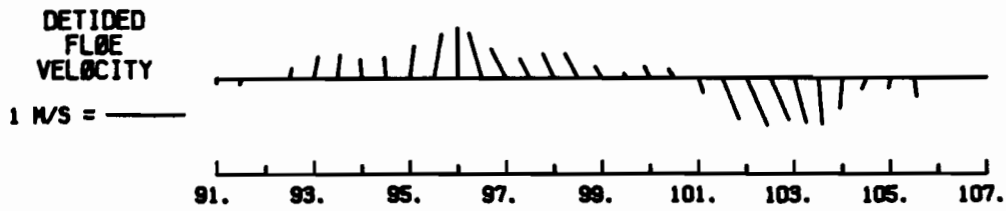
FLØE
TRACK



(65.0 N,
164.0 W)

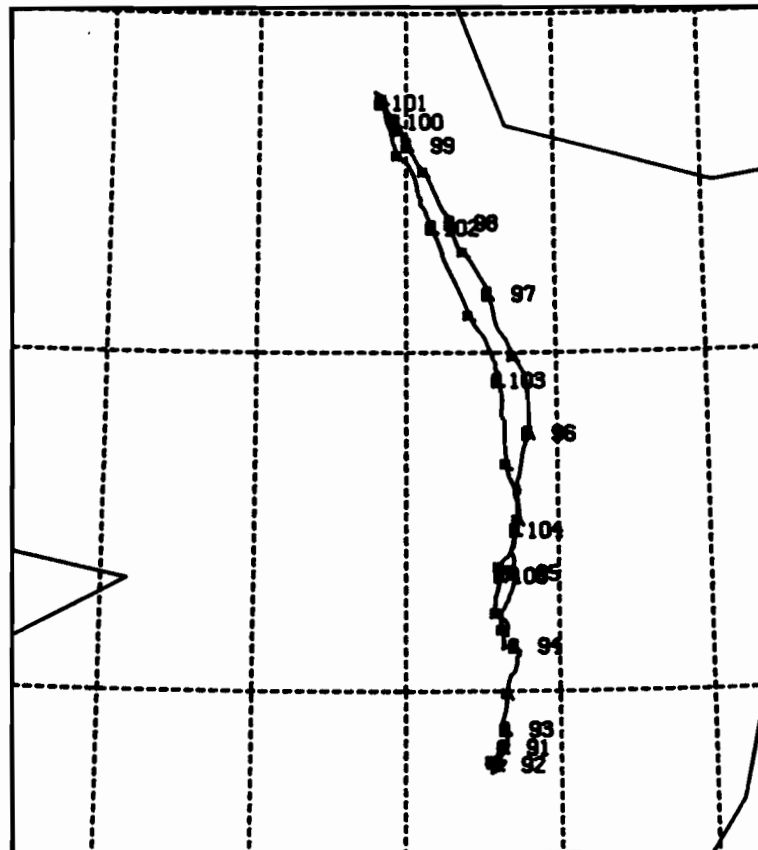
(62.5 N,
169.0 W)

FLØE STATION 2321B APR 01-15, 1982 (JD 91 -105)



MEAN =
.03
TOWARD
3

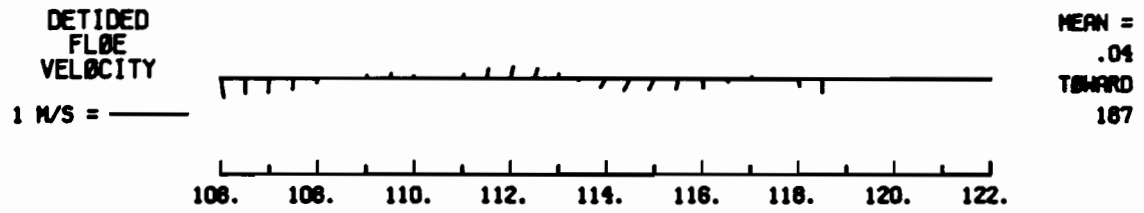
FLØE
TRACK



(65.0 N,
164.5 W)

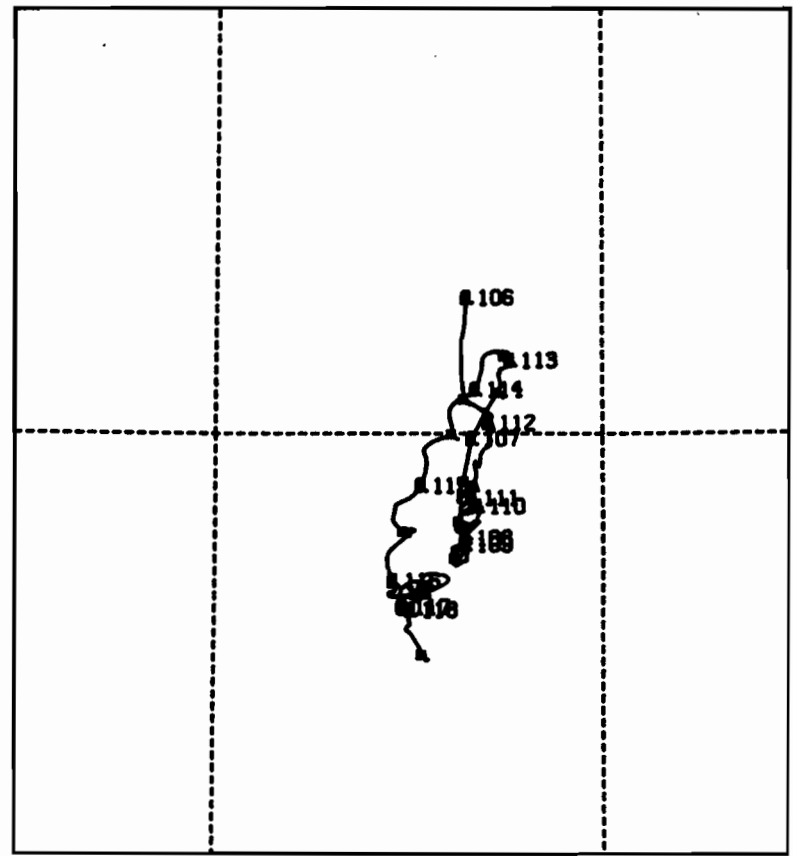
(62.5 N,
169.5 W)

FLØE STATION 2321B APR 16-30, 1982 (JD 106 -120)



FLØE
TRACK

(62.5 N,
167.5 W)



(63.5 N,
165.5 W)

A3. Station 2322B

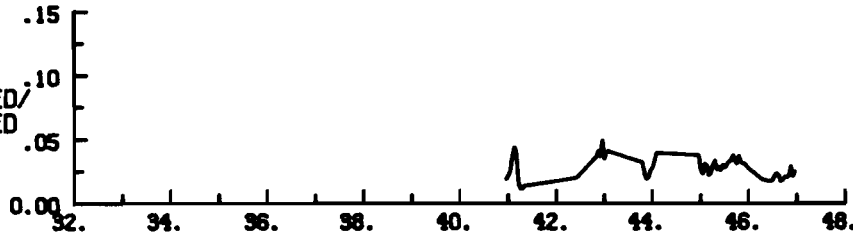
FLØE STATION 2322B FEB 01-15, 1982 (JD 32 - 46)

DETIDED
FLØE
VELOCITY
1 M/S = _____



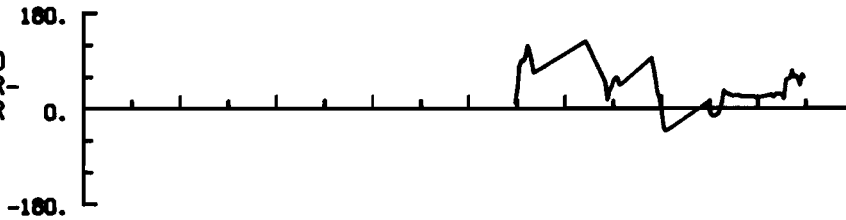
MEAN =
.09
TOWARD
194

DETIDED
FLØE SPEED/
WIND SPEED



MEAN =
.0277
SIGMA=
.0086

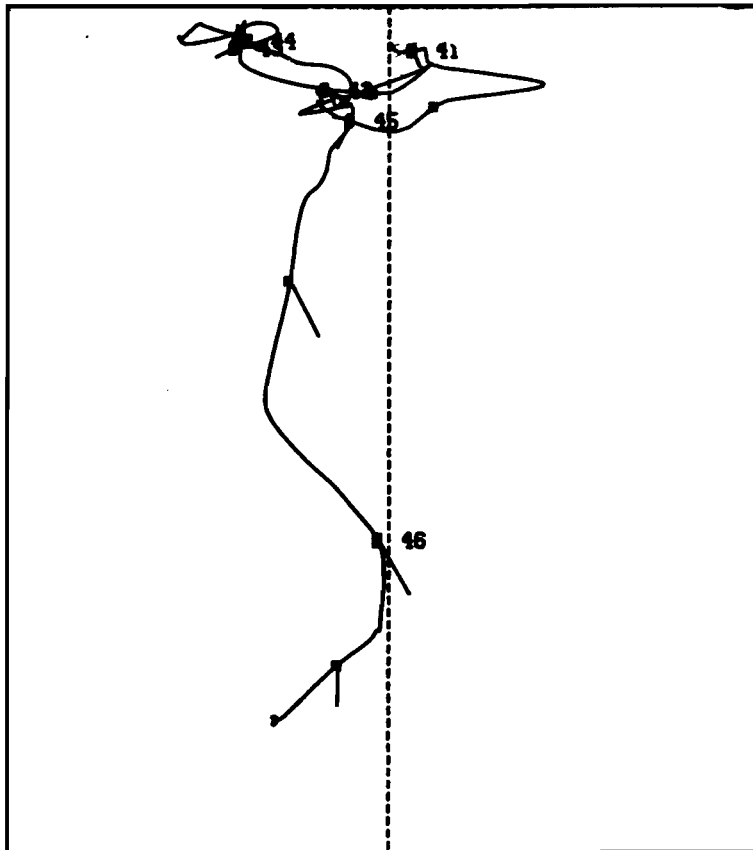
DETIDED
FLØE DIR-
AIR DIR
(DEG)



MEAN =
37.7
SIGMA=
34.9

FLØE
TRACK
WITH
SURFACE
WIND

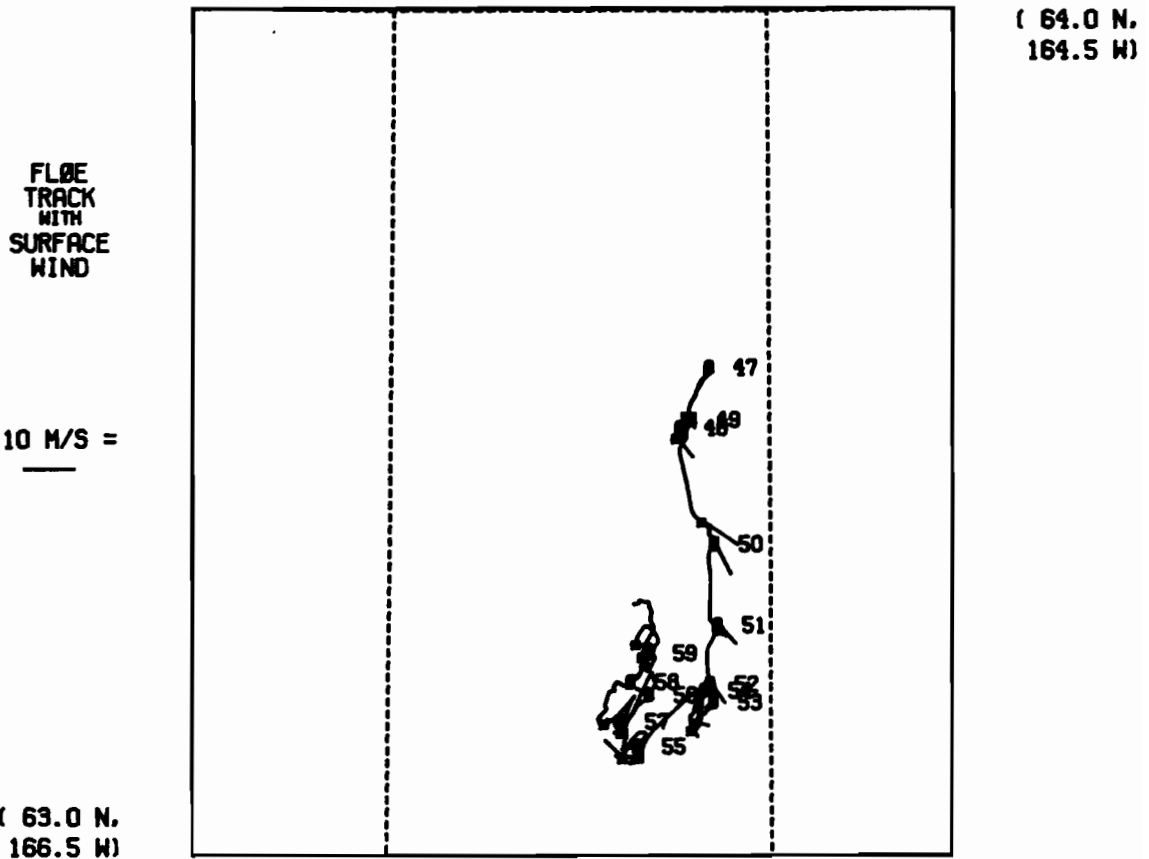
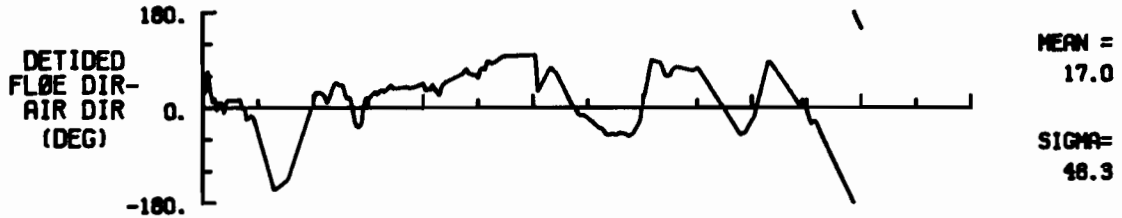
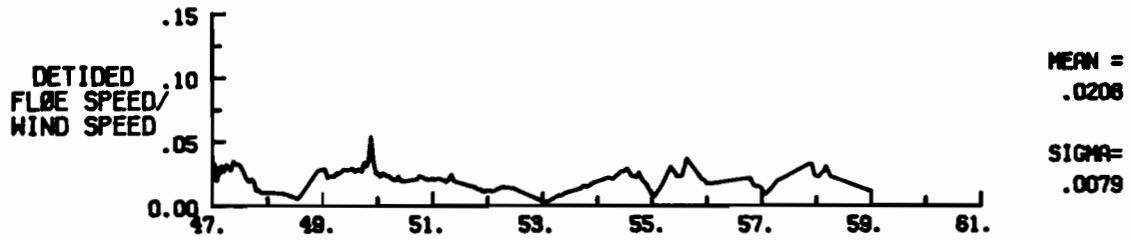
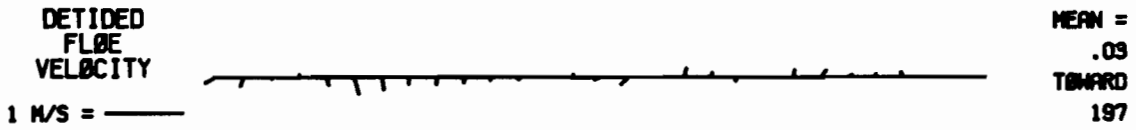
10 M/S = _____



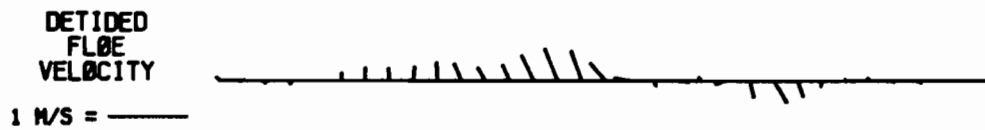
(64.0 N.
164.5 W)

(63.5 N.
165.5 W)

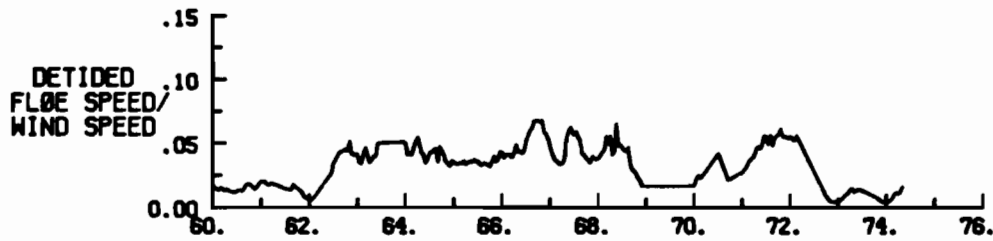
FLØE STATION 2322B FEB 16-28, 1982 (JD 47 - 59)



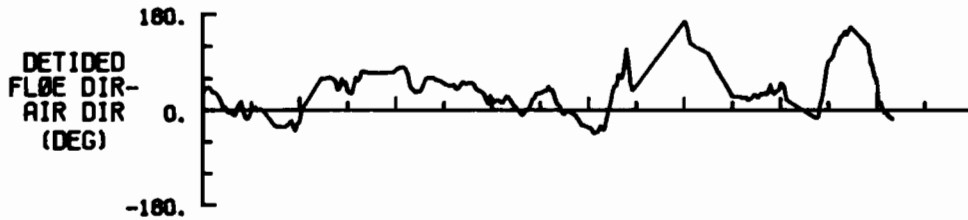
FLØE STATION 2322B MAR 01-15, 1982 (JD 60 - 74)



MEAN =
.07
TOWARD
330



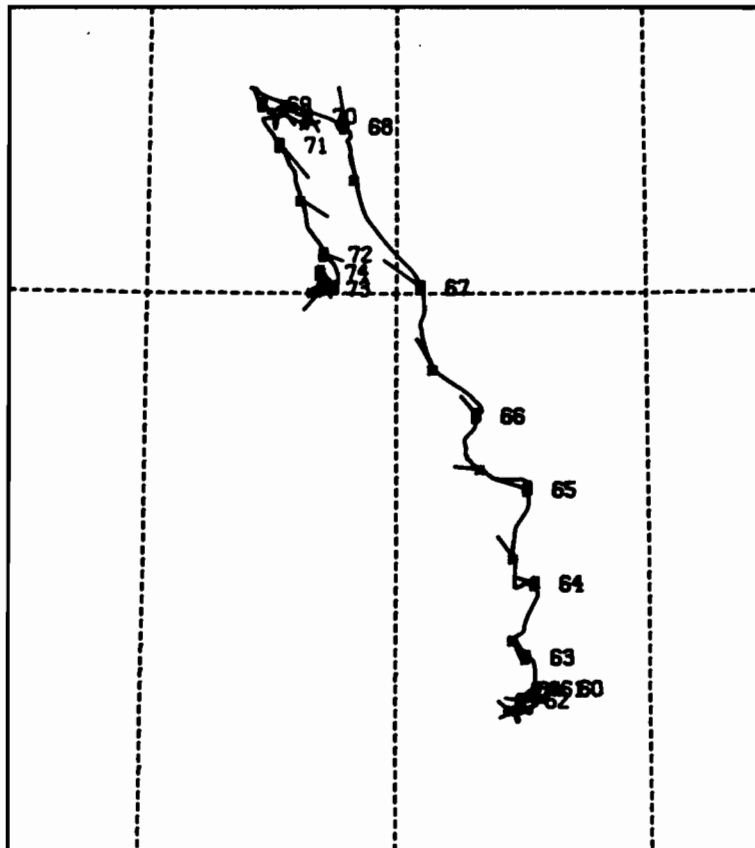
MEAN =
.0341
SIGMA=
.0169



MEAN =
32.7
SIGMA=
41.1

FLØE
TRACK
WITH
SURFACE
WIND

10 M/S =

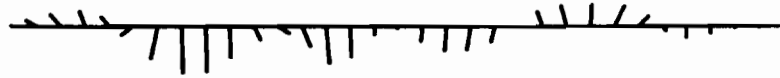


(64.5 N,
164.5 W)

(63.0 N,
167.5 W)

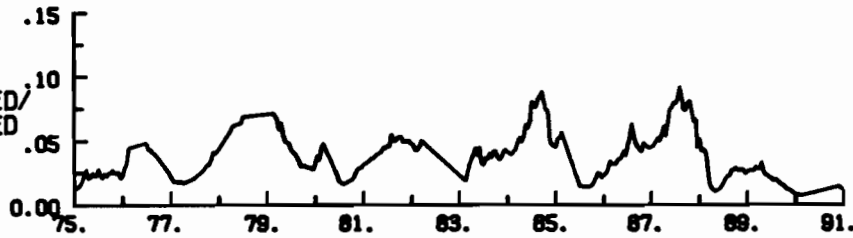
FLØE STATION 2322B MAR 16-31, 1982 (JD 75 - 90)

DETIDED
FLØE
VELOCITY
1 M/S = 



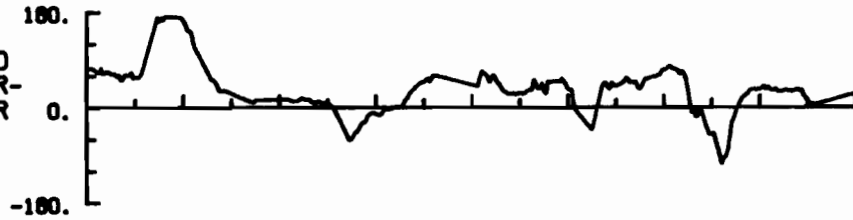
MEAN =
.11
TOWARD
185

DETIDED
FLØE SPEED/
WIND SPEED



MEAN =
.0374
SIGMA=
.0185

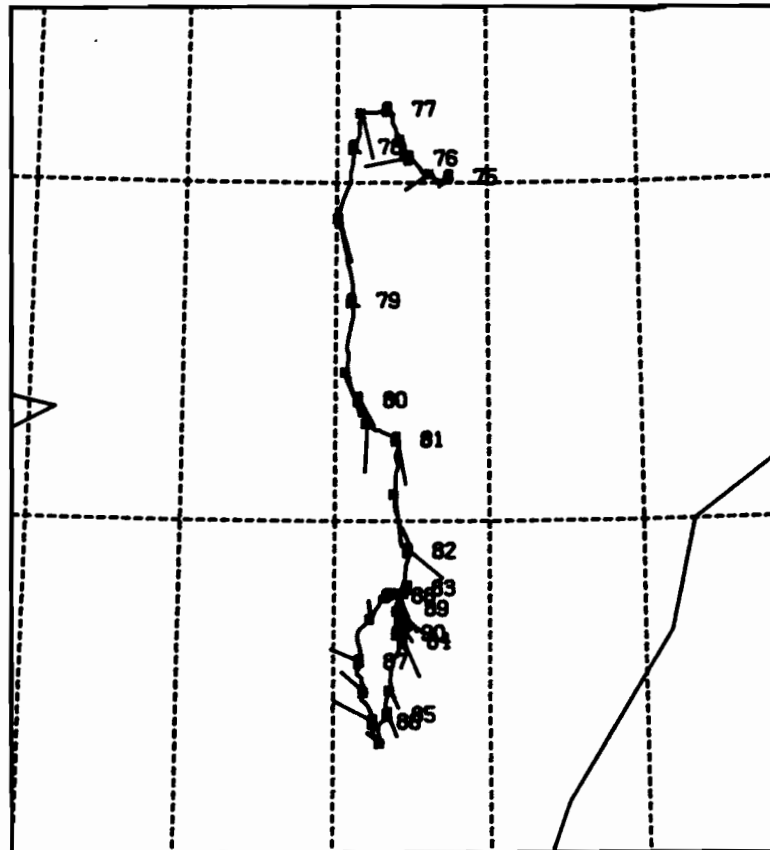
DETIDED
FLØE DIR-
AIR DIR
(DEG)



MEAN =
32.6
SIGMA=
44.1

FLØE
TRACK
WITH
SURFACE
WIND

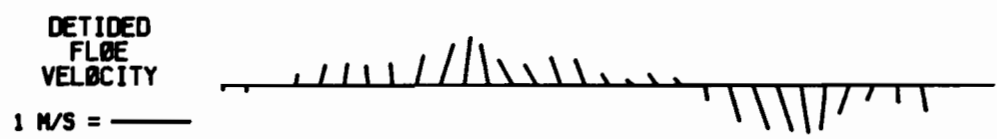
10 M/S = 



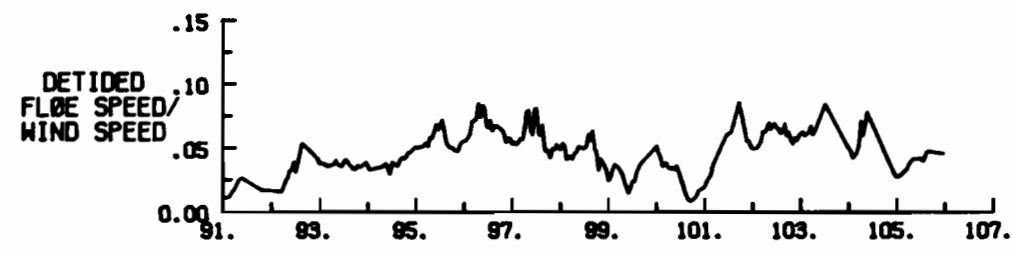
(64.5 N,
164.0 W)

(62.0 N,
169.0 W)

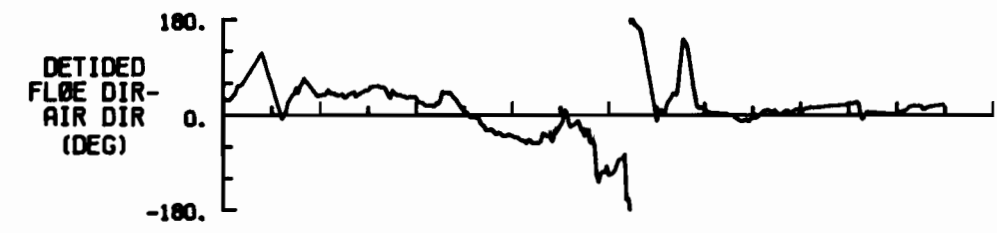
FLØE STATION 2322B APR 01-15, 1982 (JD 91 -105)



MEAN =
.02
TOWARD
344



MEAN =
.0469
SIGMA=
.0172

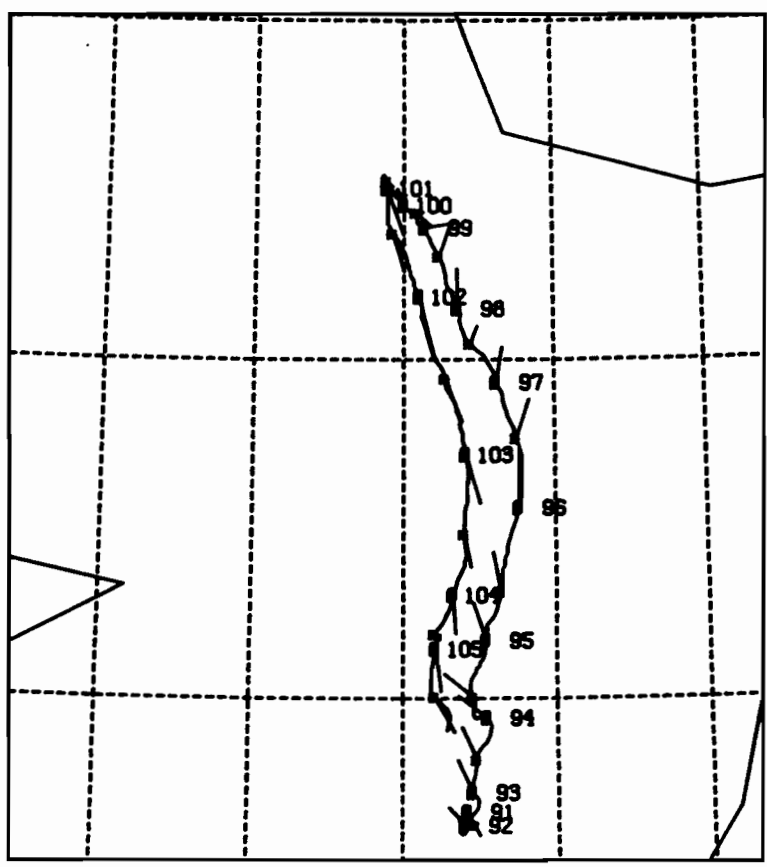


MEAN =
6.6
SIGMA=
49.5

(65.0 N,
164.5 W)

FLØE TRACK WITH SURFACE WIND

10 M/S =



(62.5 N,
169.5 W)

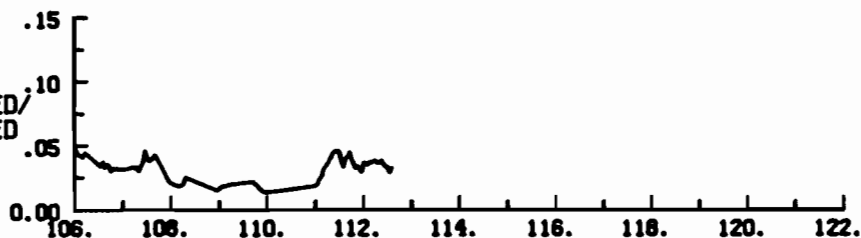
FLØE STATION 2322B APR 16-30, 1982 (JD 106 -120)

DETIDED
FLØE
VELOCITY
1 M/S = _____



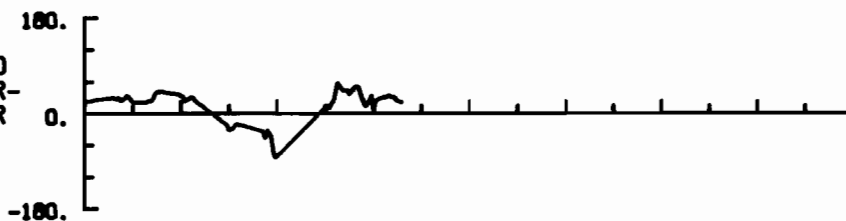
MEAN =
.10
TOWARD
185

DETIDED
FLØE SPEED/
WIND SPEED



MEAN =
.0315
SIGMA=
.0091

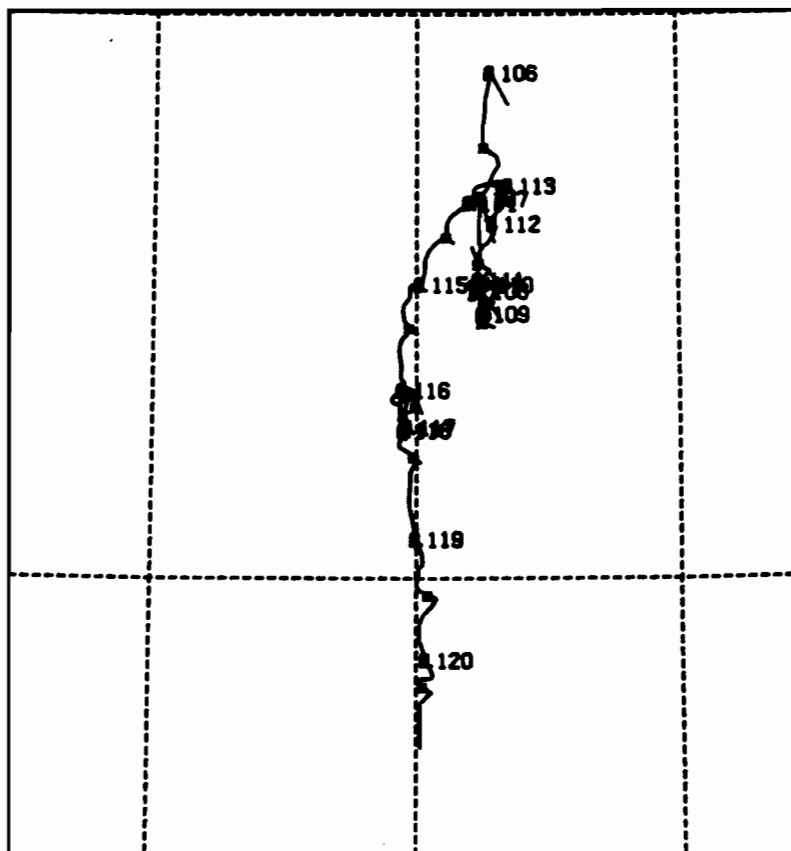
DETIDED
FLØE DIR-
AIR DIR
(DEG)



MEAN =
19.0
SIGMA=
27.5

FLØE
TRACK
WITH
SURFACE
WIND

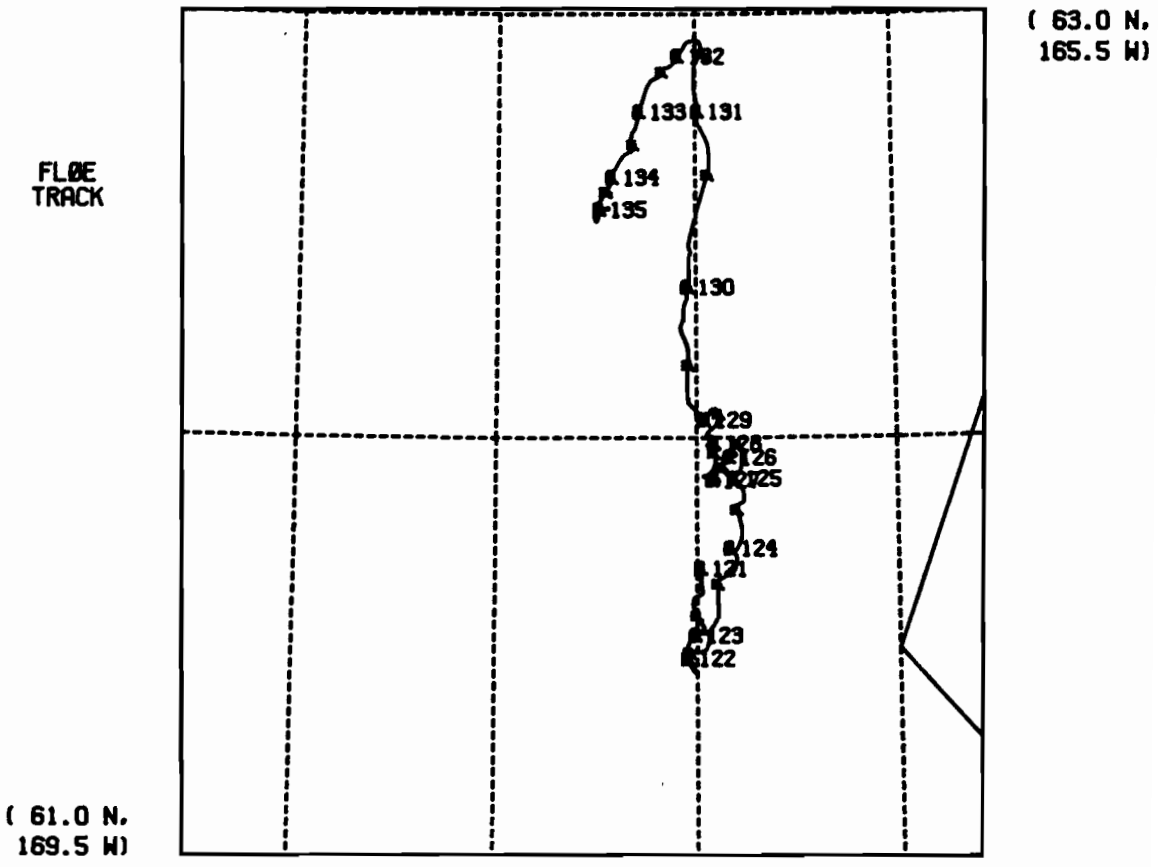
10 M/S = _____



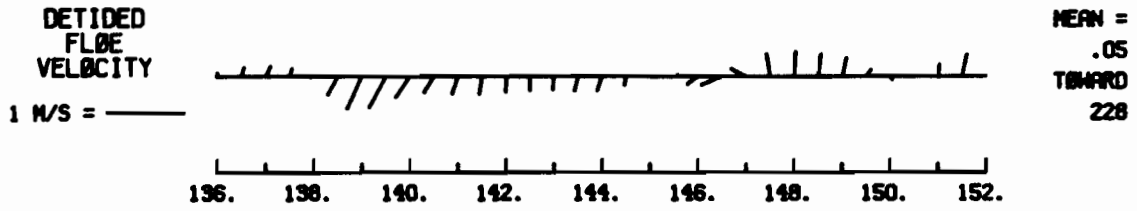
(63.0 N,
165.5 W)

(61.5 N,
168.5 W)

FLØE STATION 2322B MAY 01-15, 1982 (JD 121 -135)

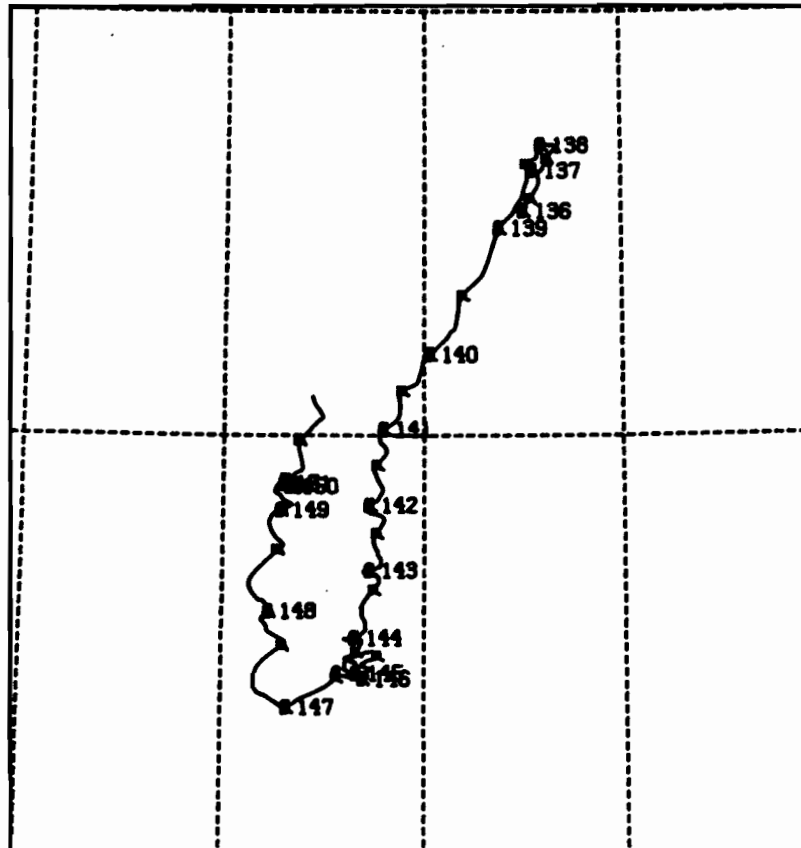


FLØE STATION 2322B MAY 16-31, 1982 (JD 136 -151)

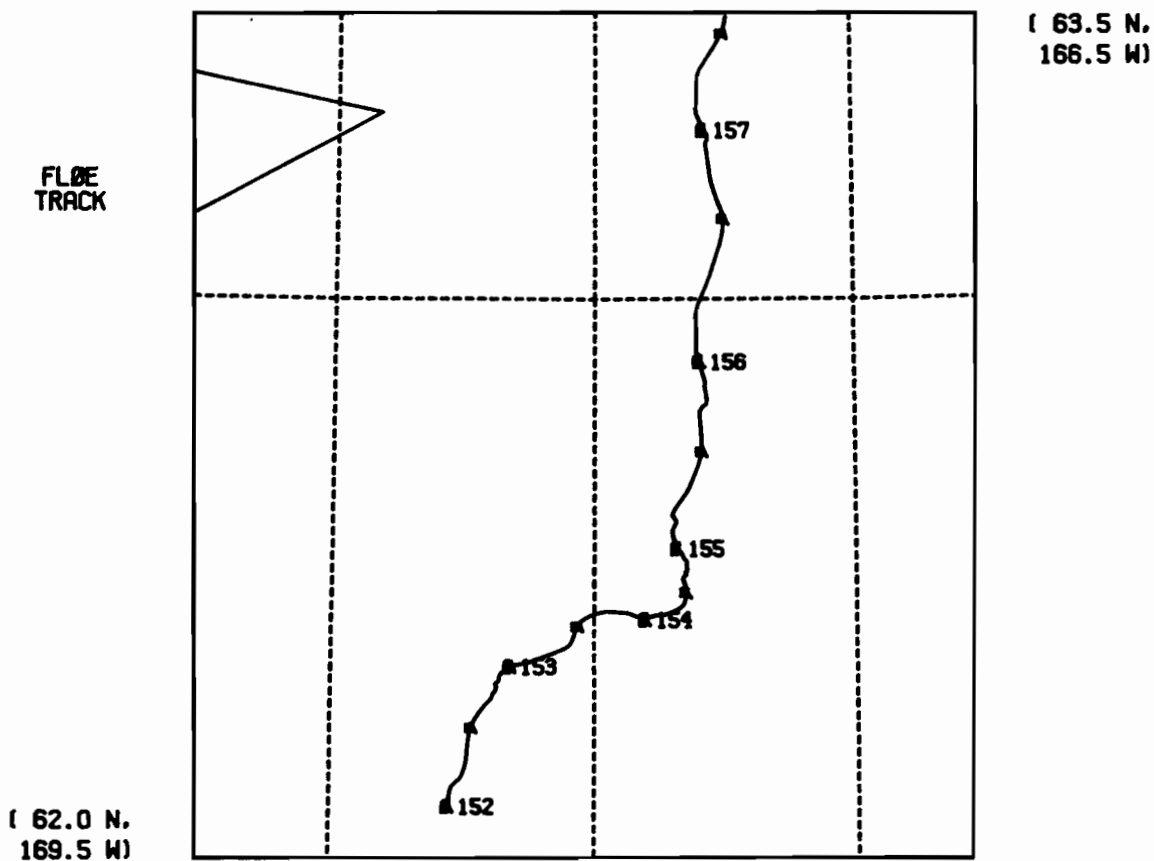
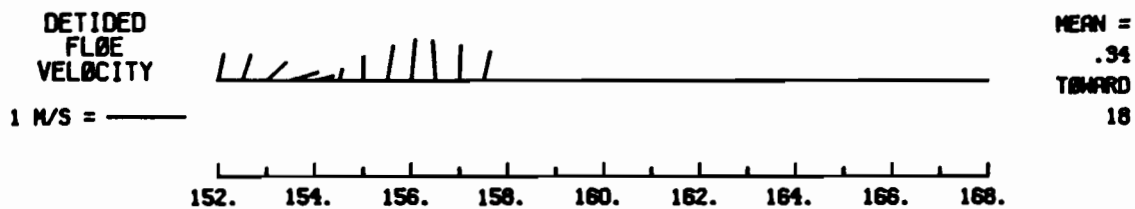


FLØE
TRACK

(61.0 N,
170.0 W)



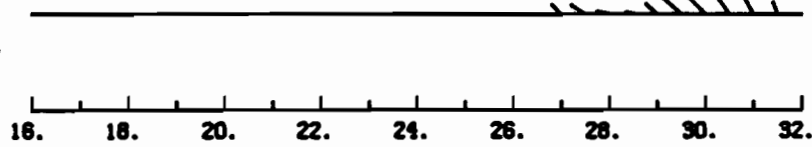
FLØE STATION 2322B JUN 01-15, 1982 (JD 152 -166)



A4. Station 2323

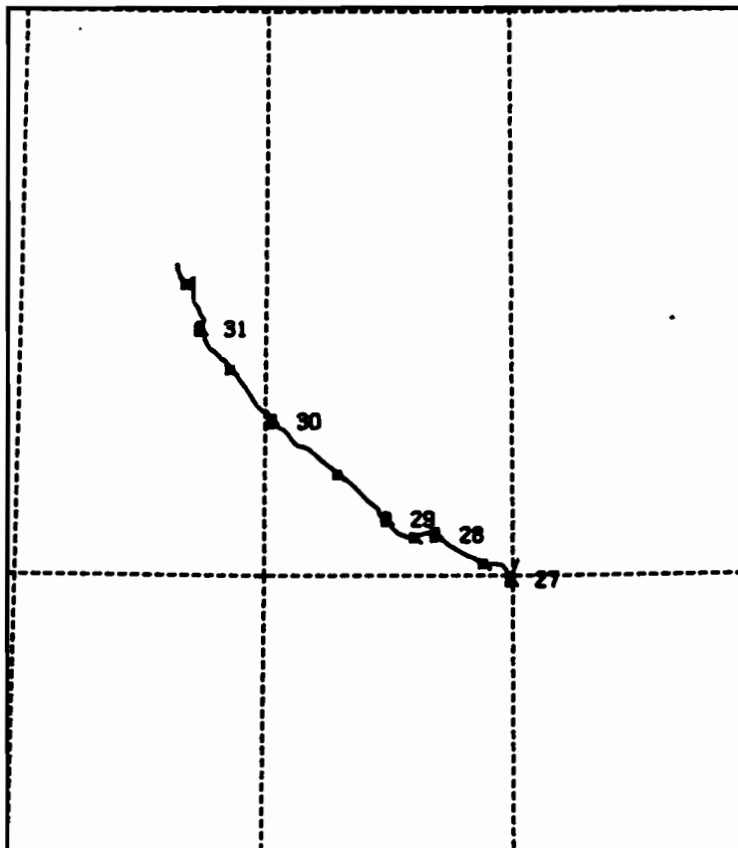
FLØE STATION 2323 JAN 16-31, 1982 (JD 16 - 31)

DETIDED
FLØE
VELOCITY
1 M/S = _____



MEAN =
.21
TOWARD
313

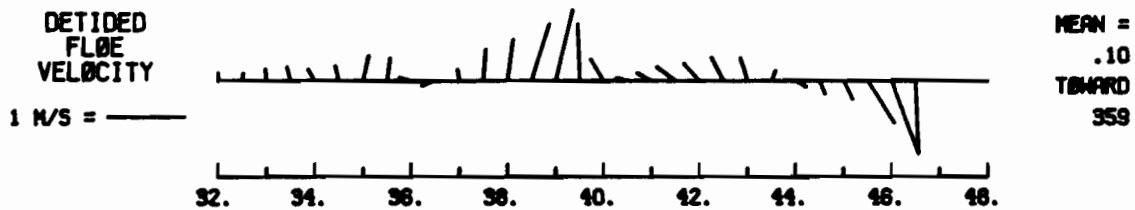
FLØE
TRACK



(65.0 N.
167.0 W)

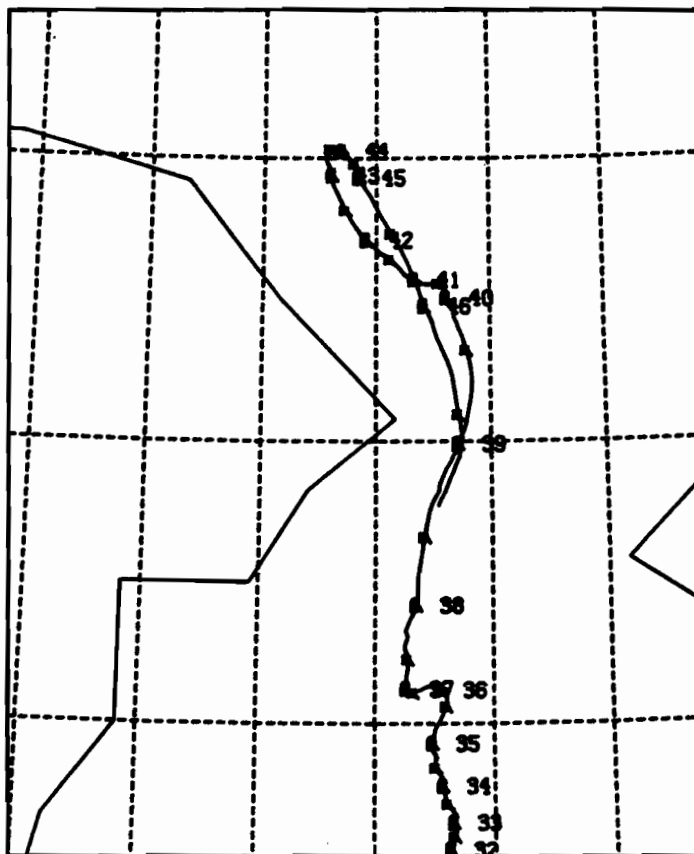
(63.5 N.
170.0 W)

FLØE STATION 2323 FEB 01-15, 1982 (JD 32 - 46)



FLØE
TRACK

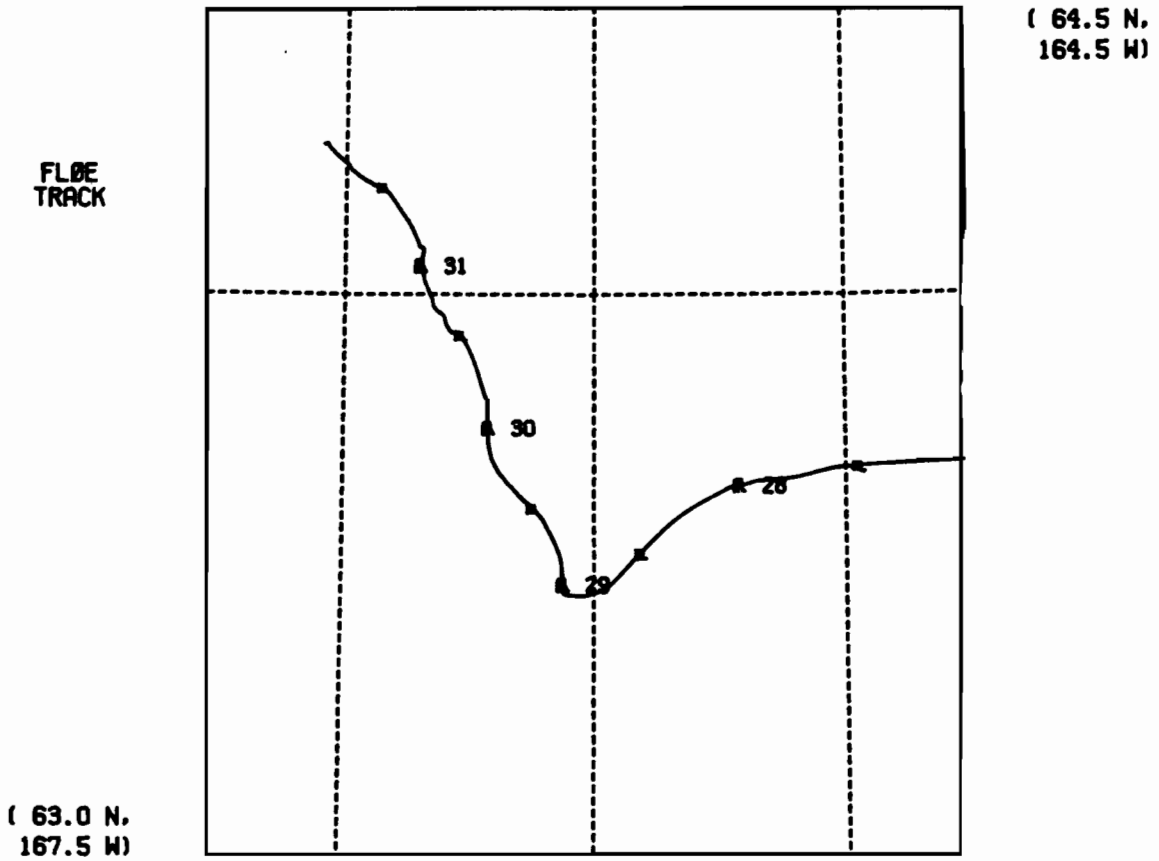
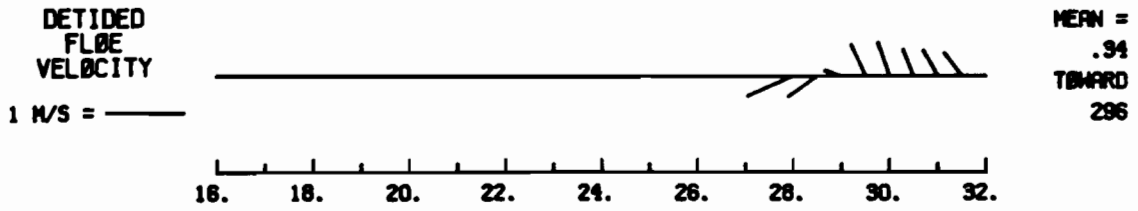
(64.5 N,
173.0 W)



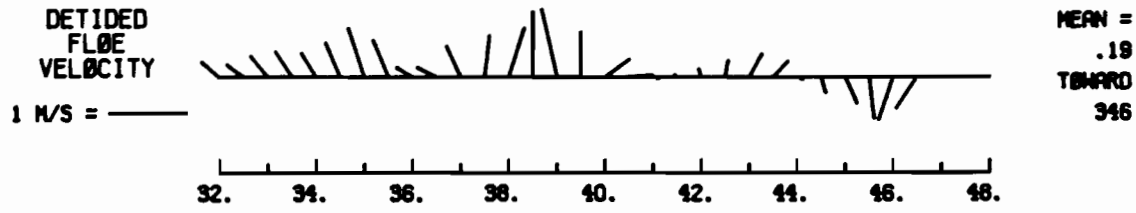
(67.5 N,
167.0 W)

A5. Station 2324

FLØE STATION 2324 JAN 16-31, 1982 (JD 16 - 31)

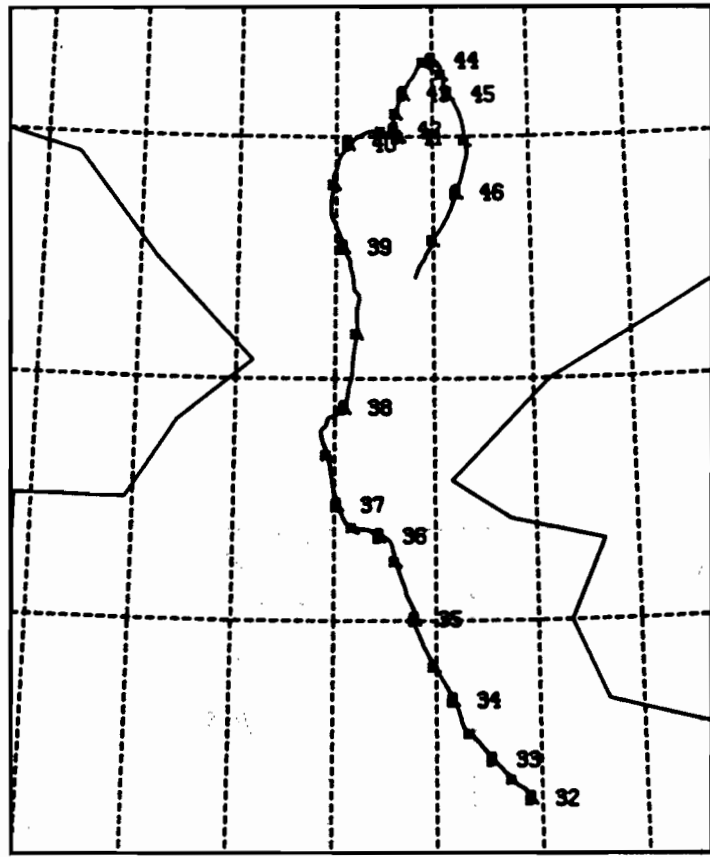


FLØ STATION 2324 FEB 01-15, 1982 (JD 32 - 46)



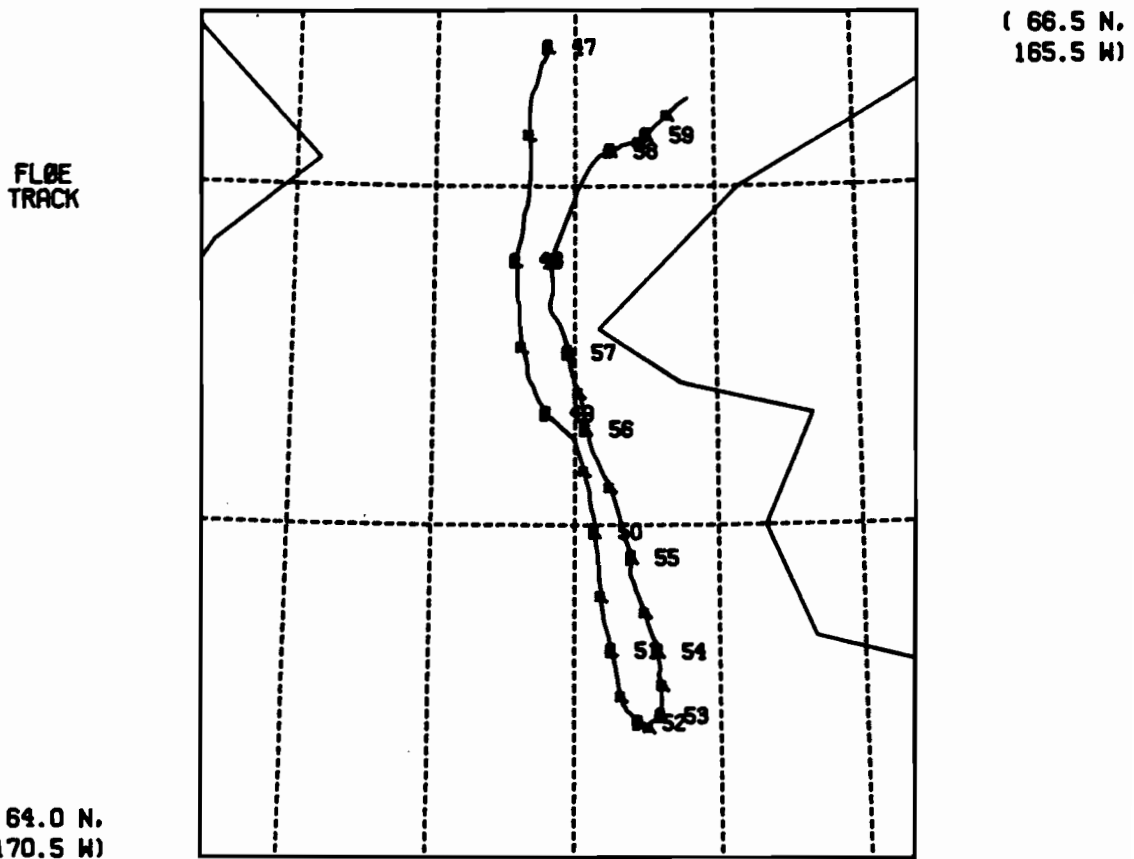
FLØ
TRACK

(64.0 N,
172.0 W)

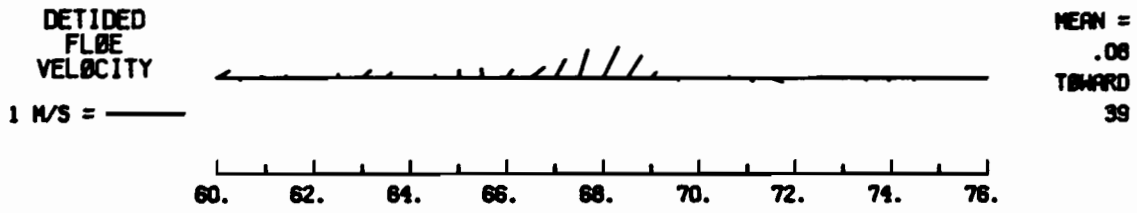


(67.5 N,
165.0 W)

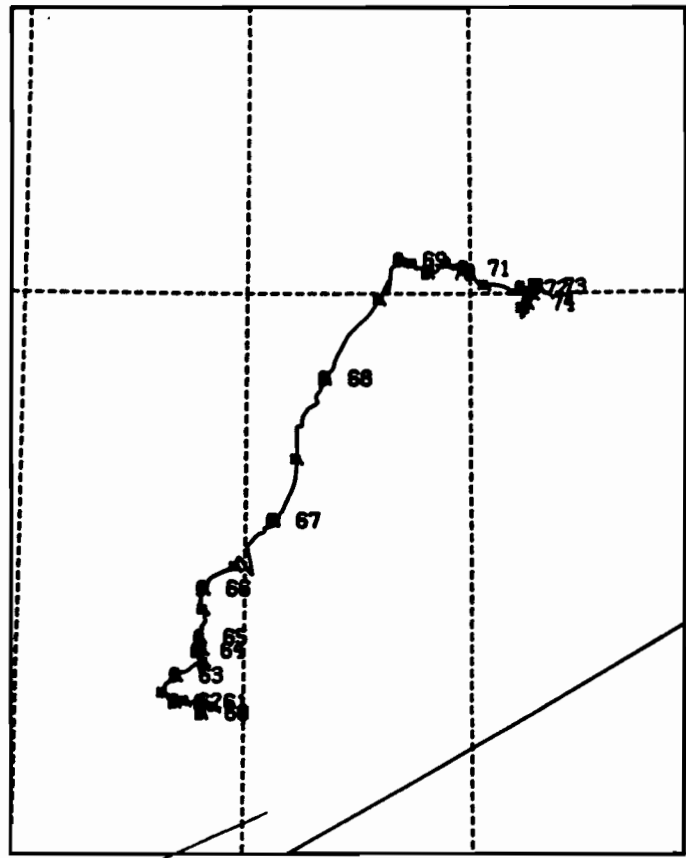
FLØE STATION 2324 FEB 16-28, 1982 (JD 47 - 59)



FLØ STATION 2324 MAR 01-15, 1982 (JD 60 - 74)



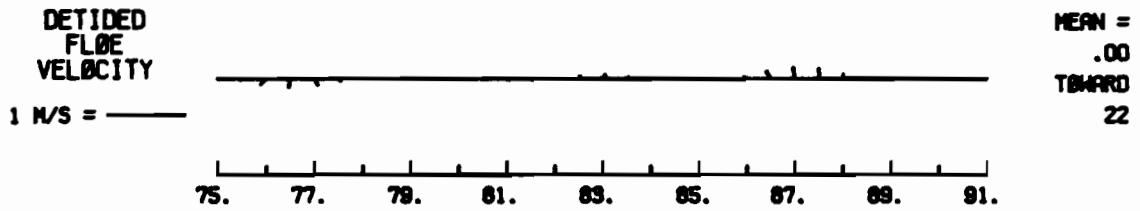
FLØ
TRACK



(67.5 N,
165.0 W)

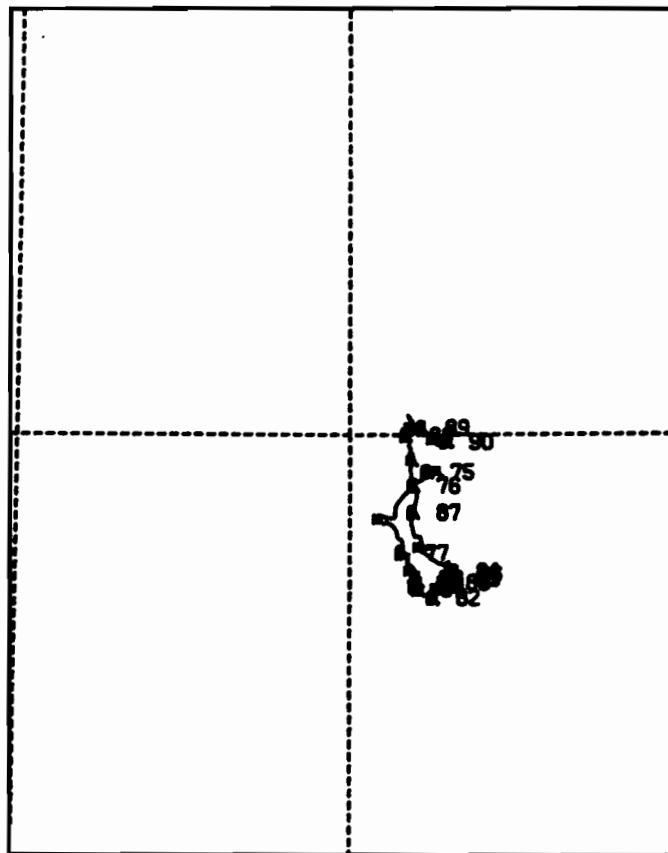
(66.0 N,
168.0 W)

FLØE STATION 2324 MAR 16-31, 1982 (JD 75 - 90)

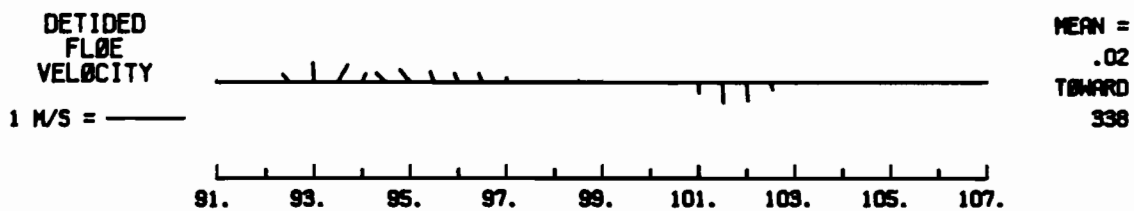


FLØE
TRACK

(66.5 N,
167.0 W)

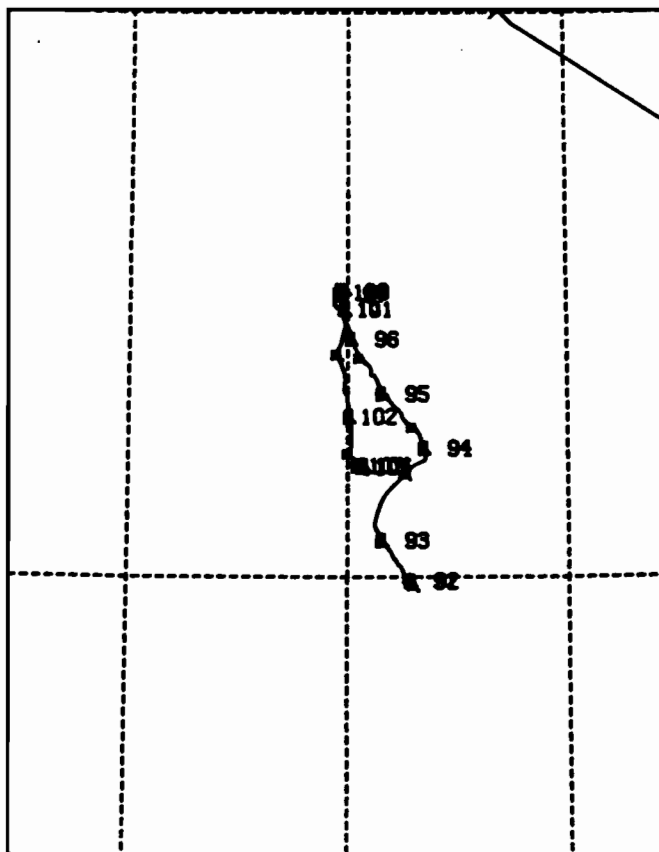


FLØE STATION 2324 APR 01-15, 1982 (JD 91 -105)



FLØE
TRACK

(66.5 N,
167.5 W)



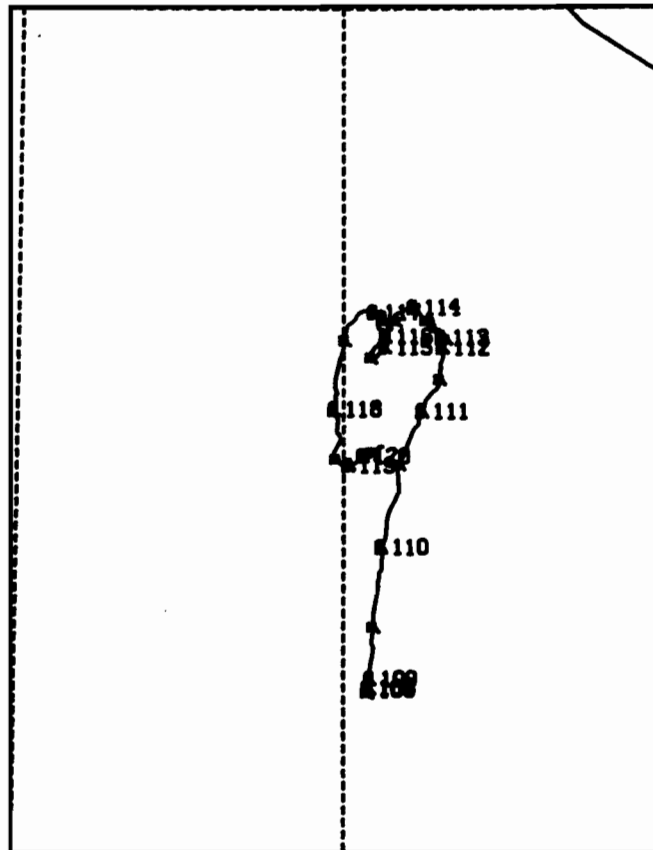
(68.0 N,
164.5 W)

FLØE STATION 2324 APR 16-30, 1982 (JD 106 -120)

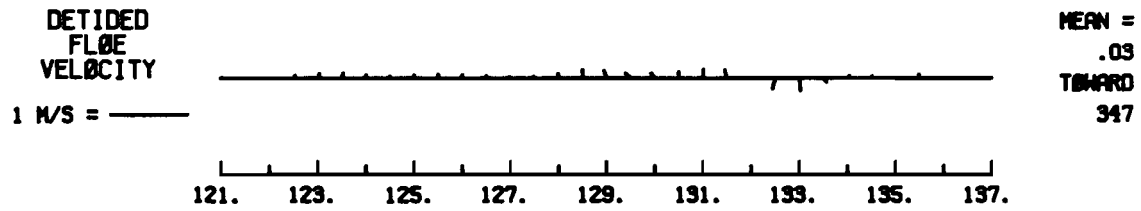


FLØE
TRACK

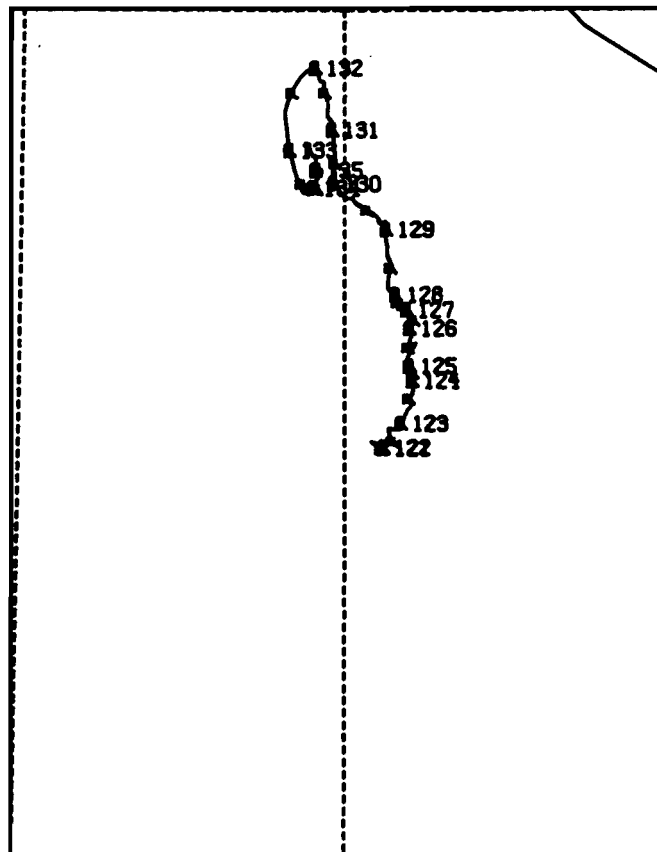
(67.0 N,
167.0 W)



FLØE STATION 2324 MAY 01-15, 1982 (JD 121 -135)



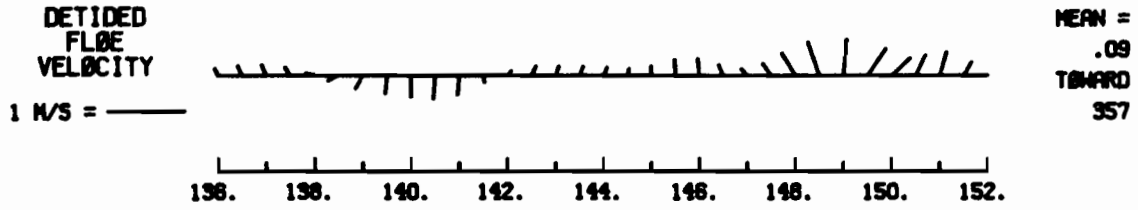
FLØE
TRACK



(68.0 N.
165.0 W)

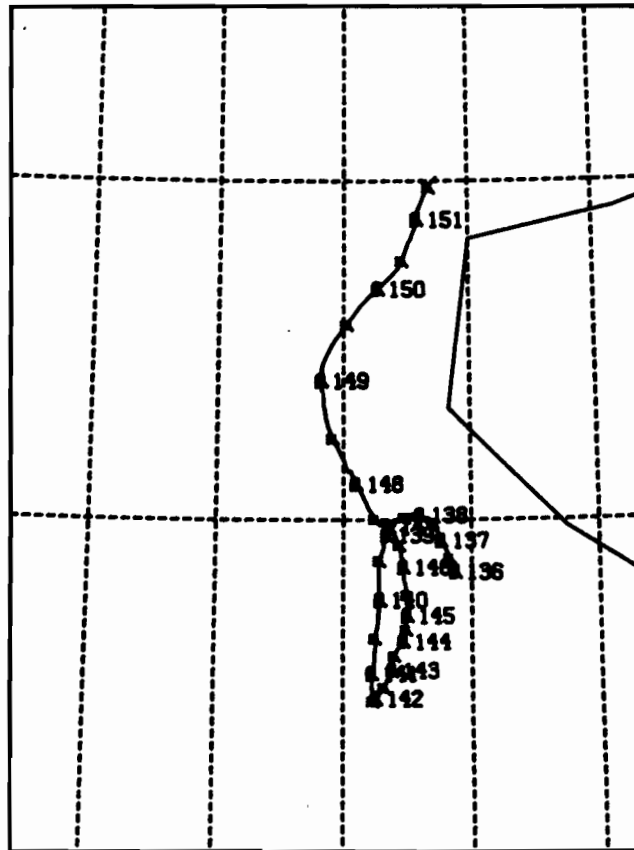
(67.0 N.
167.0 W)

FLØE STATION 2324 MAY 16-31, 1982 (JD 136 -151)



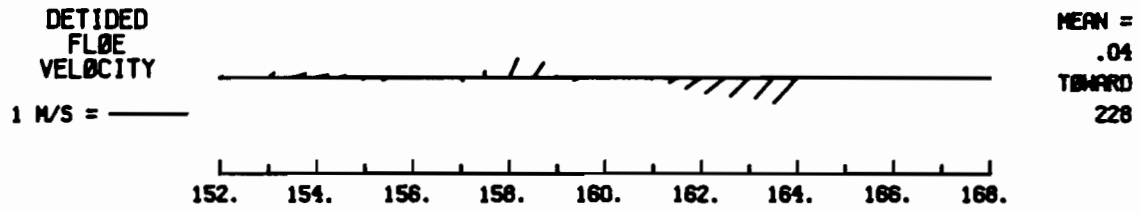
FLØE
TRACK

(67.0 N,
169.5 W)

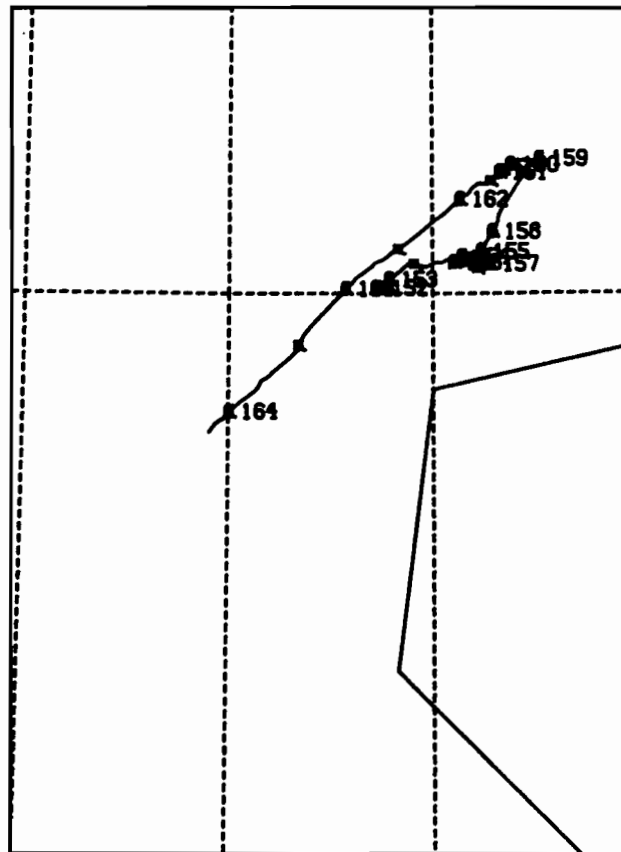


(69.5 N,
164.5 W)

FLØE STATION 2324 JUN 01-15, 1982 (JD 152 -166)



FLØE
TRACK

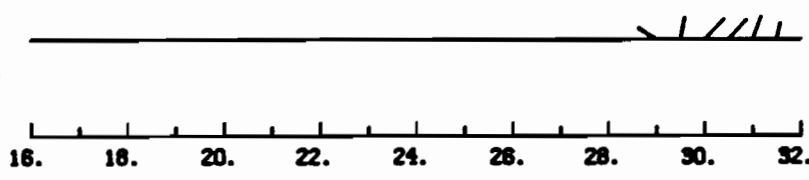


(68.0 N.
168.0 W)

A6. Station 2325

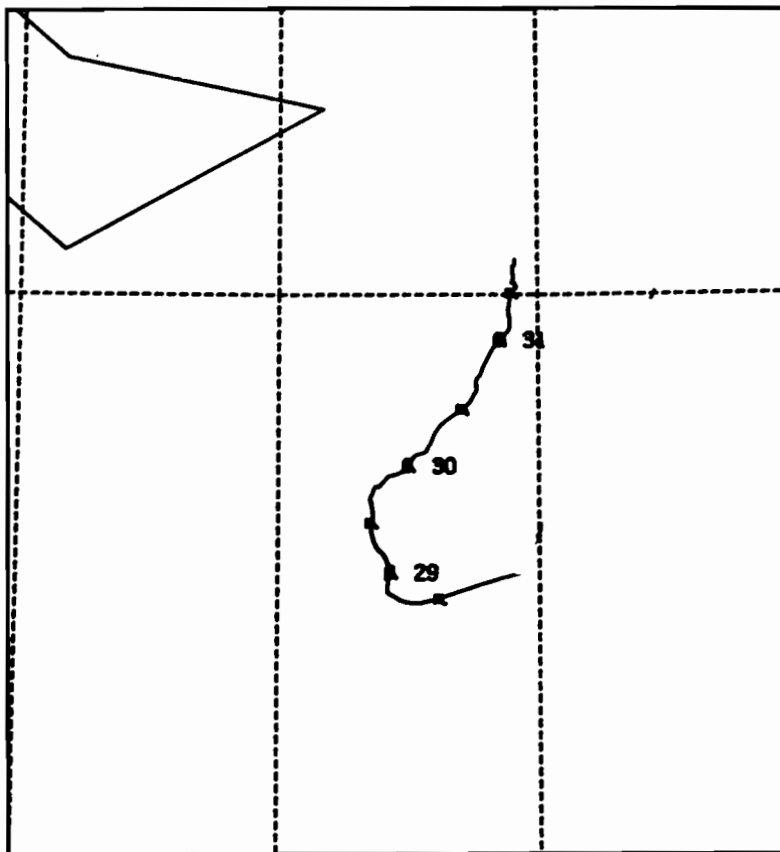
FLØE STATION 2325 JAN 16-31, 1982 (JD 16 - 31)

DETERMINED
FLØE
VELOCITY
1 M/S = _____



MEAN =
.18
TOWARD
358

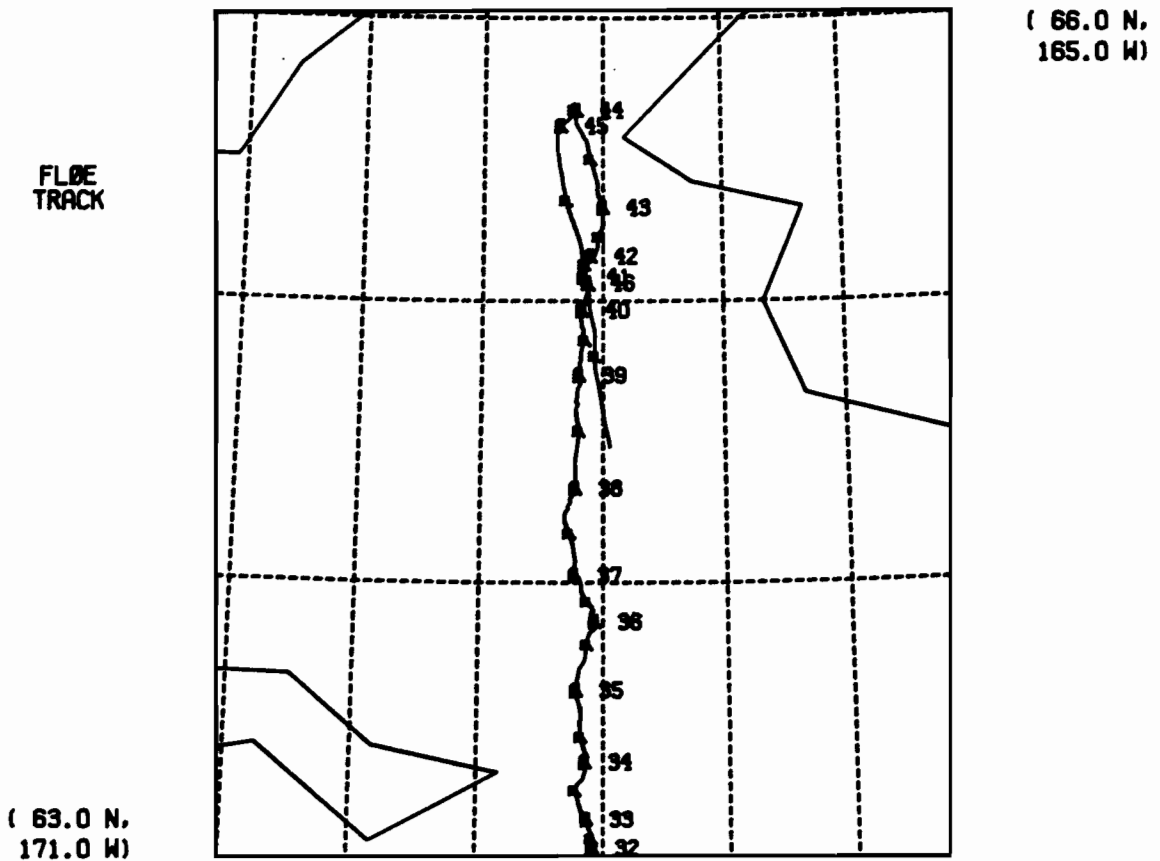
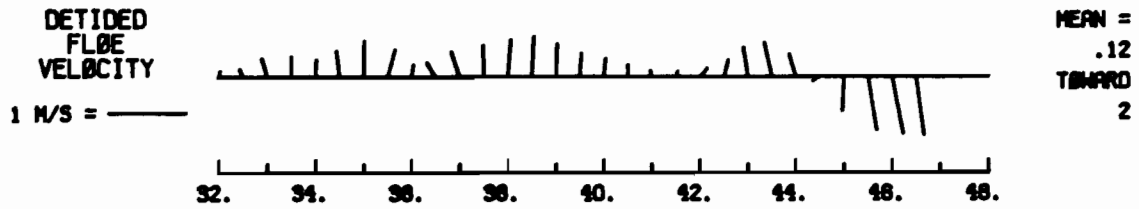
FLØE
TRACK



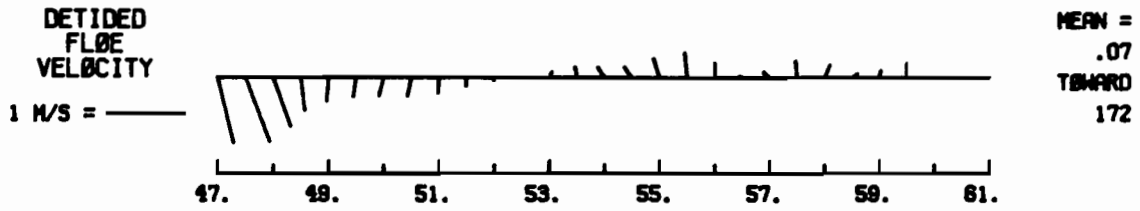
(63.5 N,
167.0 W)

(62.0 N,
170.0 W)

FLØE STATION 2325 FEB 01-15, 1982 (JD 32 - 46)

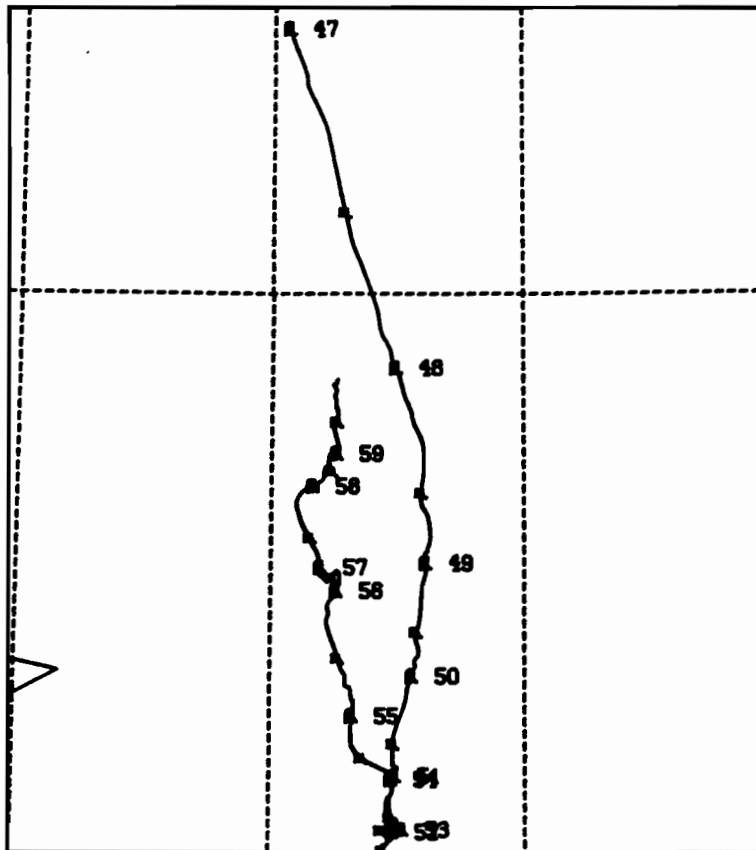


FLØE STATION 2325 FEB 16-28, 1982 (JD 47 - 59)



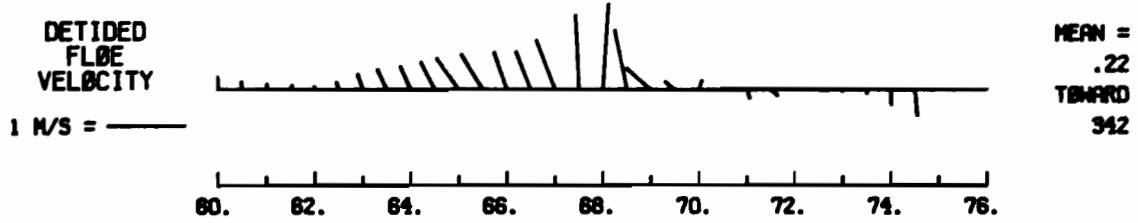
FLØE
TRACK

(63.0 N.
169.0 W)



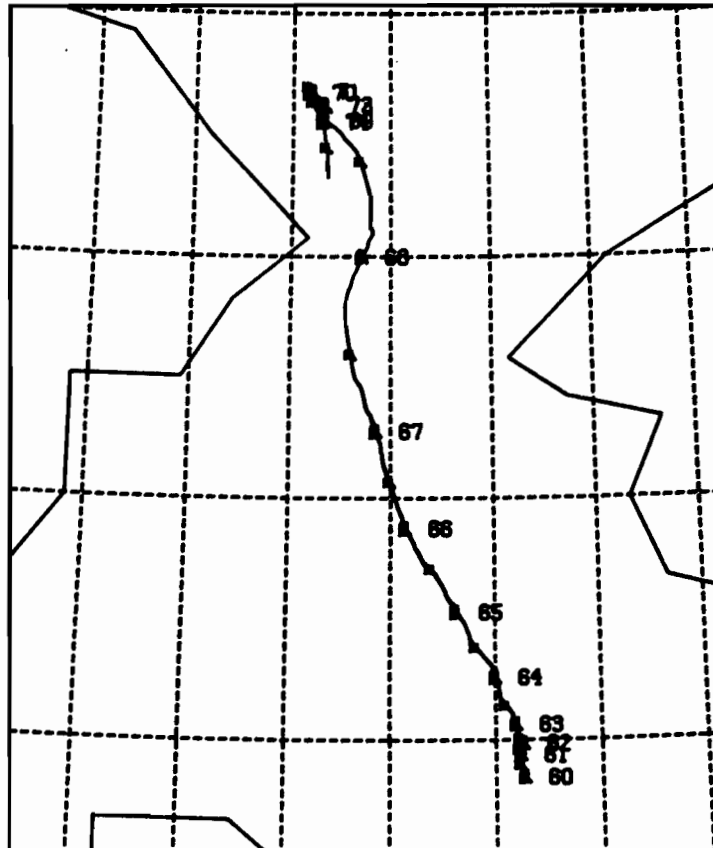
(64.5 N.
166.0 W)

FLØE STATION 2325 MAR 01-15, 1982 (JD 60 - 74)

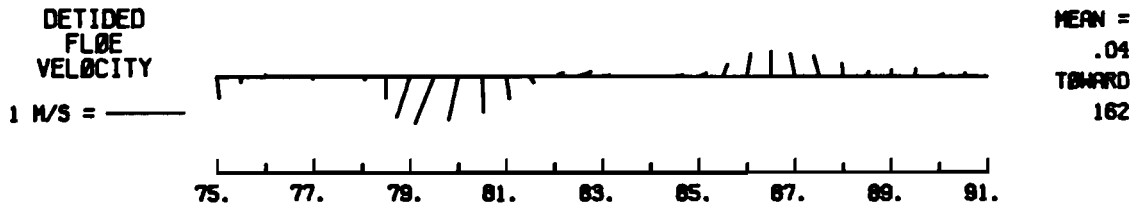


FLØE
TRACK

(63.5 N.
172.5 W)

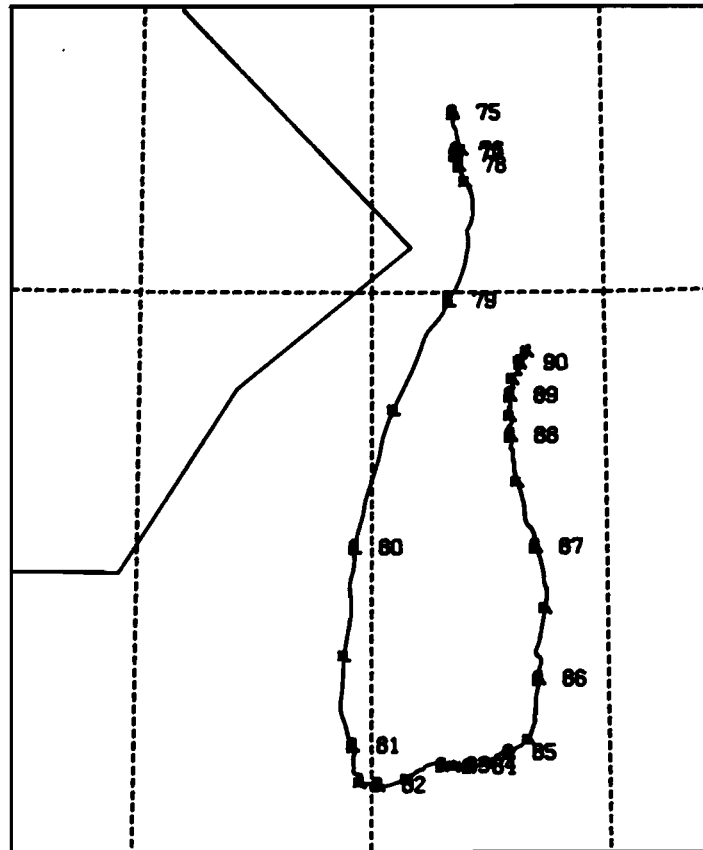


FLØE STATION 2325 MAR 16-31, 1982 (JD 75 - 90)

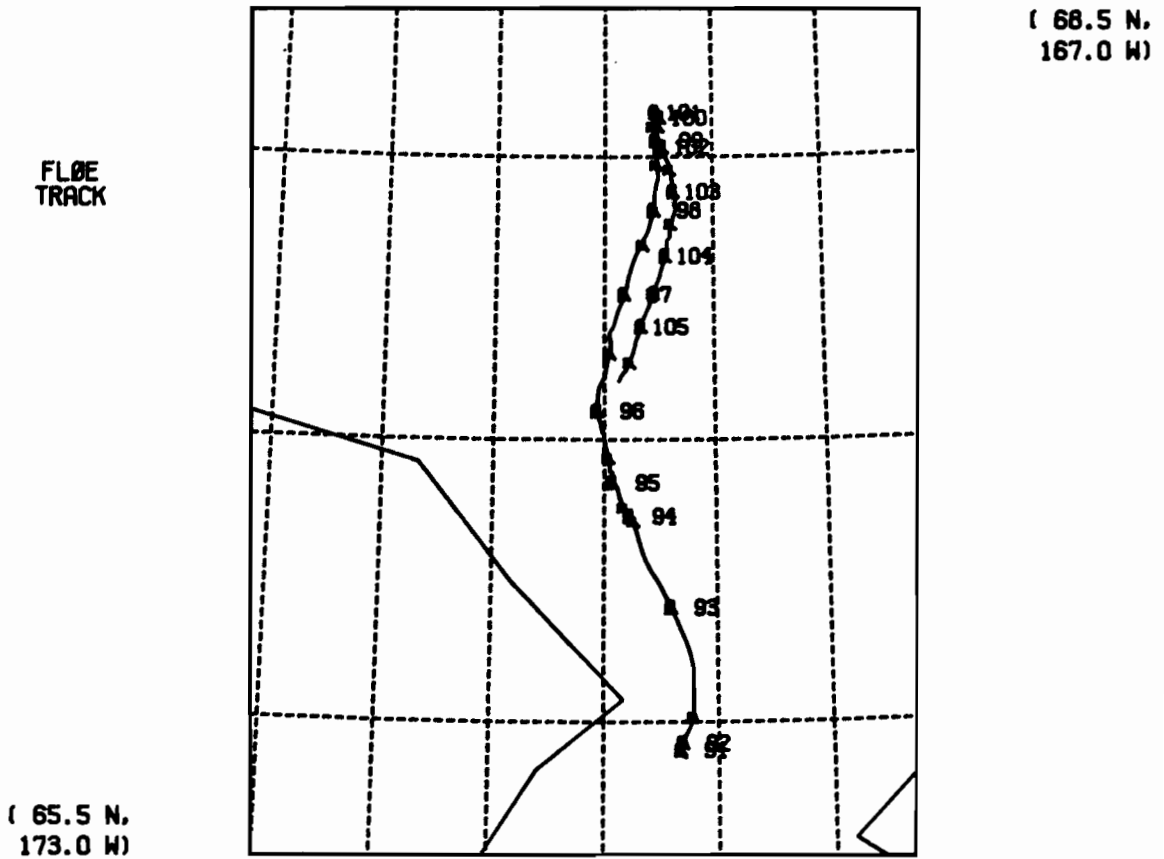
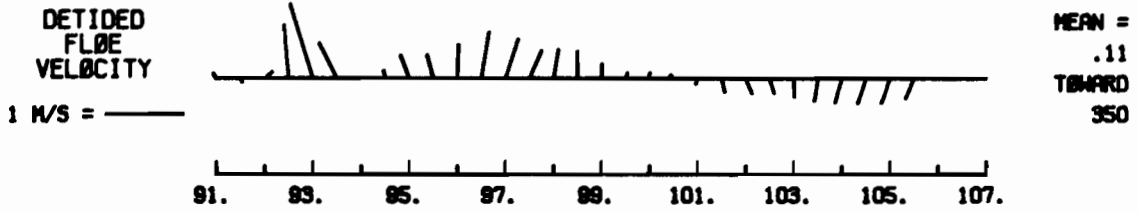


FLØE
TRACK

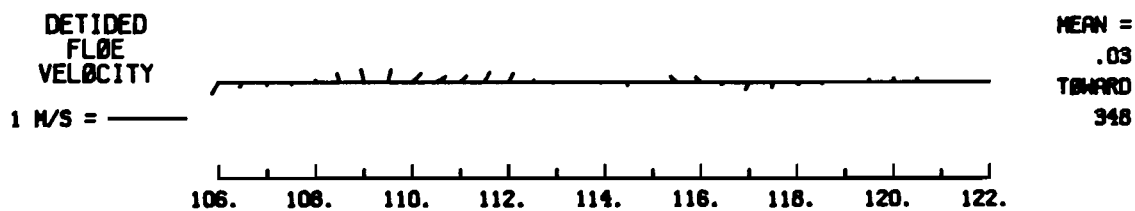
(65.0 N,
171.5 W)



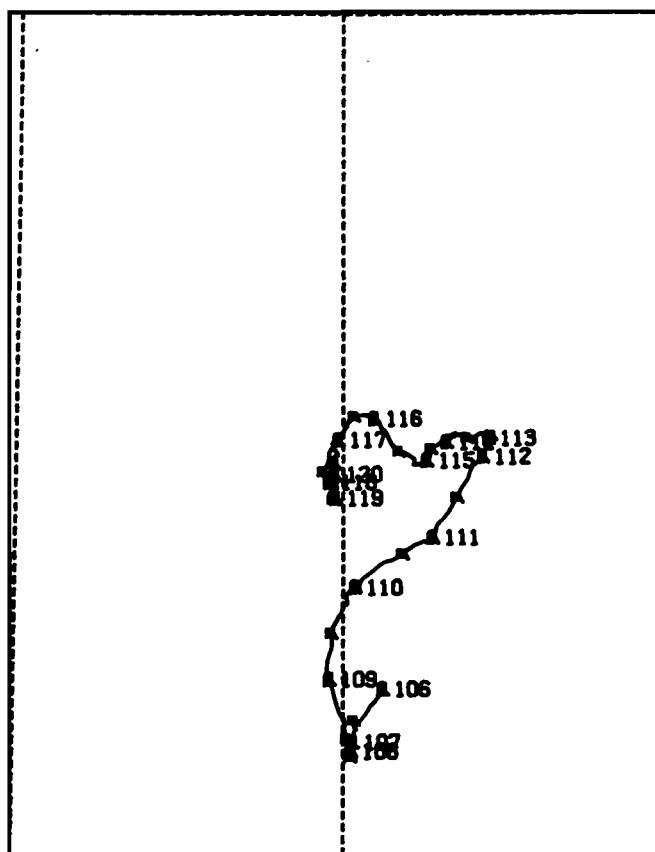
FLØE STATION 2325 APR 01-15, 1982 (JD 91 -105)



FLØE STATION 2325 APR 16-30, 1982 (JD 106 -120)

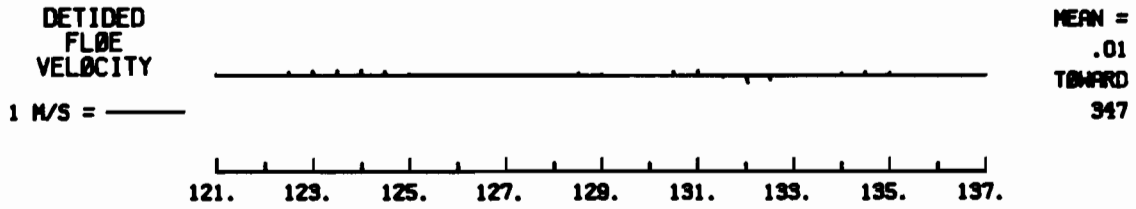


FLØE
TRACK



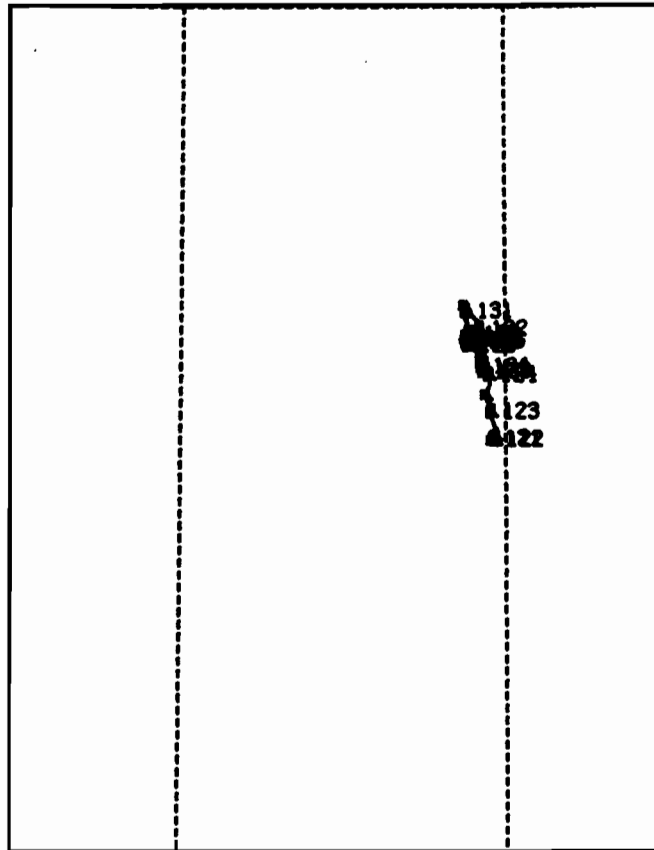
(67.0 N.
171.0 W)

FLØE STATION 2325 MAY 01-15, 1982 (JD 121 -135)



FLØE
TRACK

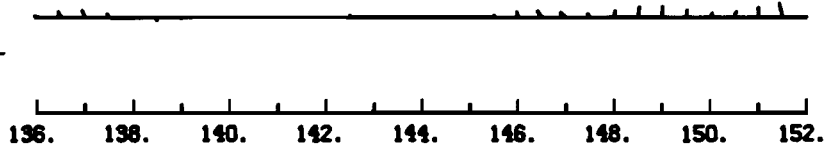
(67.0 N,
171.5 W)



(68.0 N,
169.5 W)

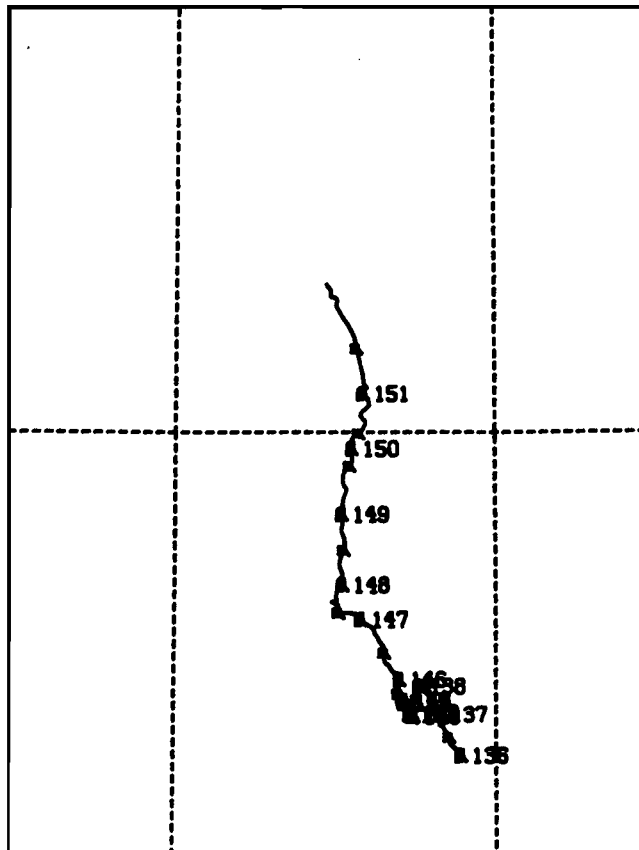
FLØ STATION 2325 MAY 16-31, 1982 (JD 136 -151)

DETIDED
FLØ
VELOCITY
1 M/S = _____



MEAN =
.05
TOWARD
344

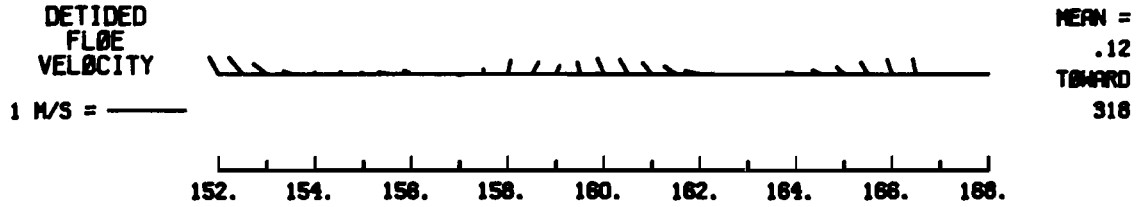
FLØ
TRACK



(68.5 N,
169.5 W)

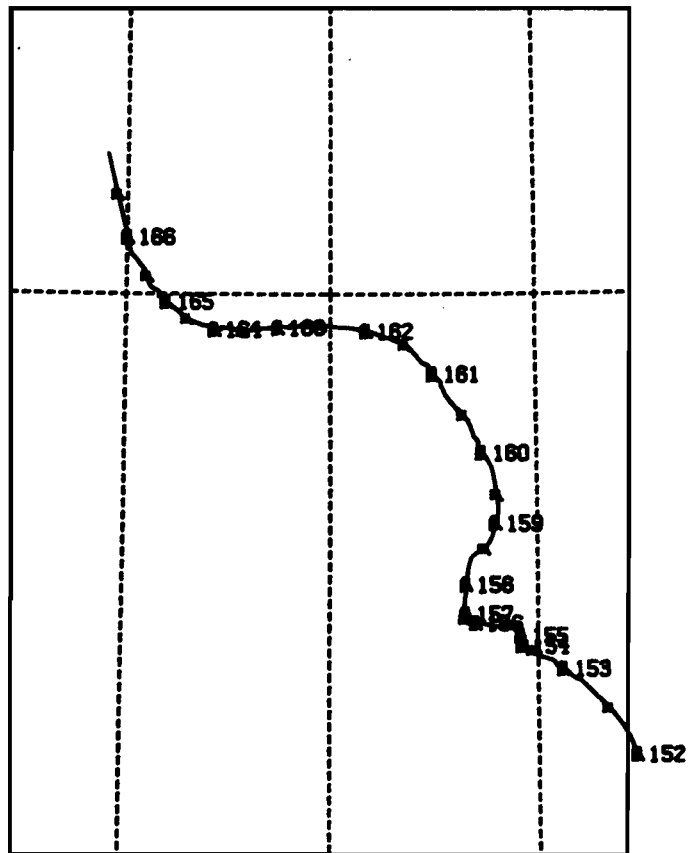
(67.5 N,
171.5 W)

FLØE STATION 2325 JUN 01-15, 1982 (JD 152 -166)

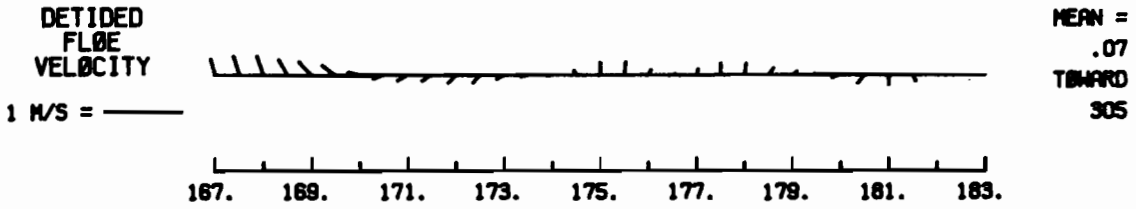


FLØE
TRACK

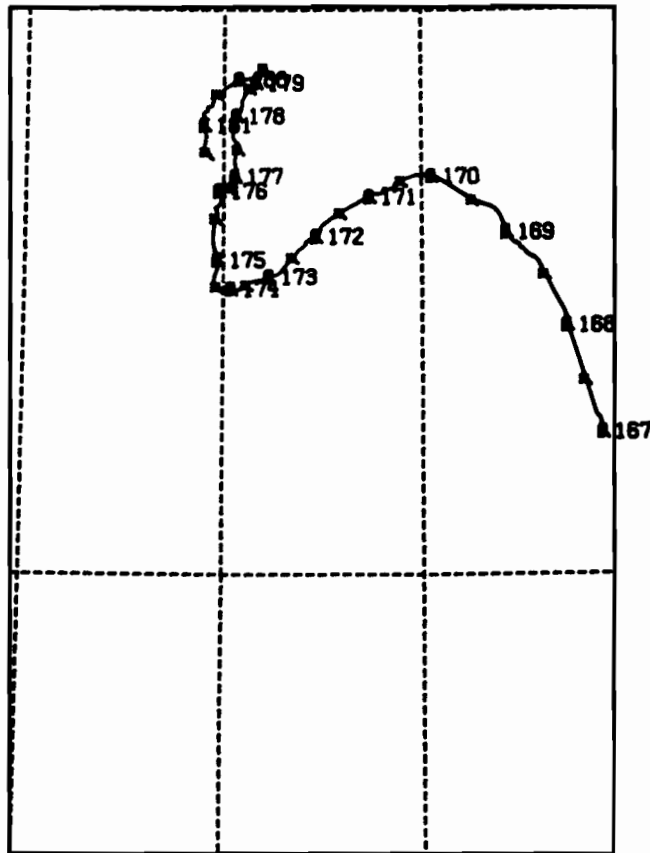
(68.0 N,
173.5 W)



FLØE STATION 2325 JUN 16-30, 1982 (JD 167 -181)



FLØE
TRACK



APPENDIX B

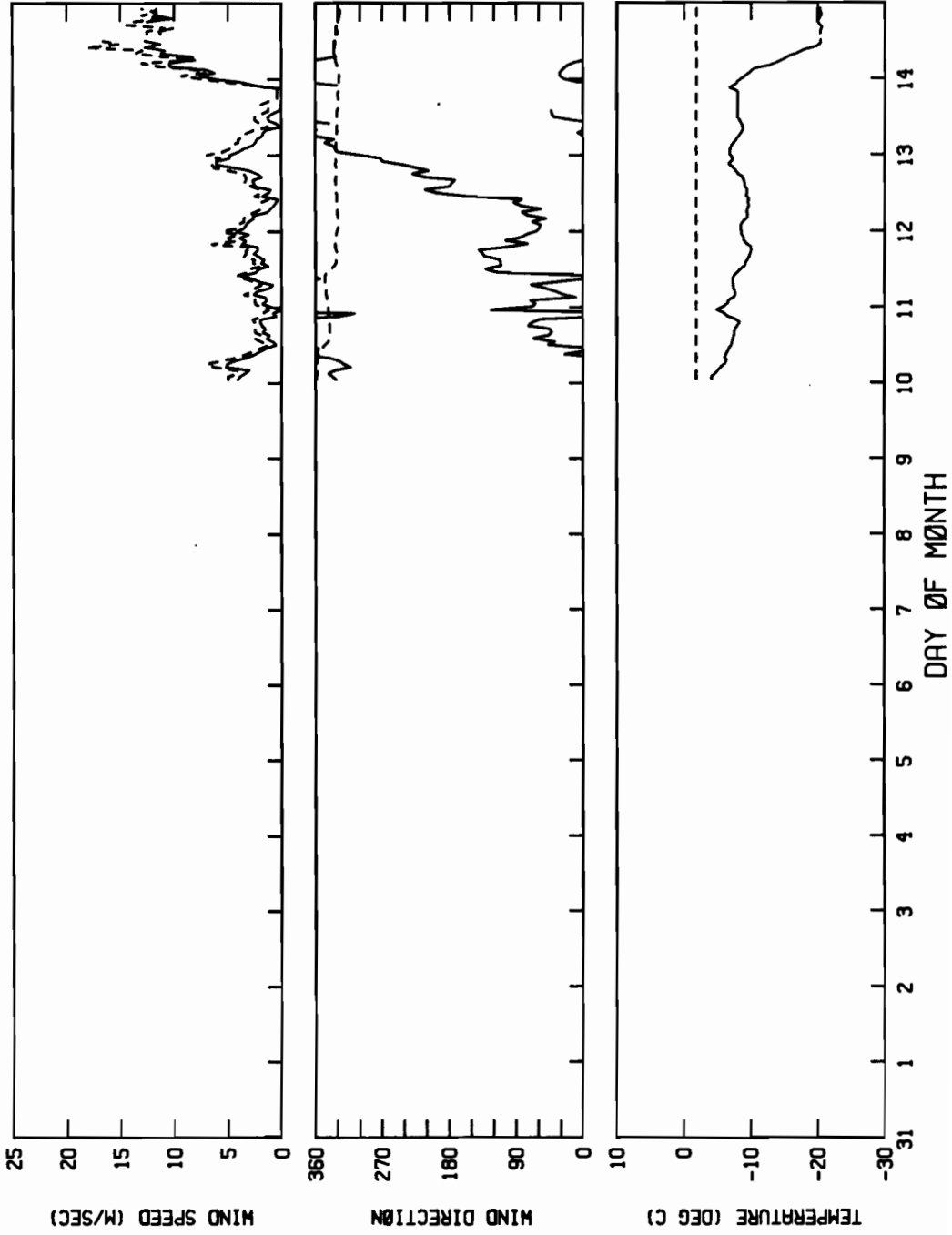
Meteorological Data

1. Data were sampled hourly. Plots here show all data considered good in raw form. Bad points occurred because of telemetry problems or instrument failure. Otherwise, data is shown here and some consideration should be given to environmental errors (frozen sensors, etc.).
2. In wind speed plot, the solid line is the vector average wind for a 20-minute sample period. The dashed line is the maximum gust observed during the sample period.
3. In the direction plot, the solid line is the vector-mean wind direction (relative to True North) and the dashed line is the compass heading which was sampled once in each sample period.
4. In the temperature plot, the solid line is the air temperature at 3 m height and the dashed line is the water temperature.

B1. Meteorological Station 010C (ARGOS 2322B)

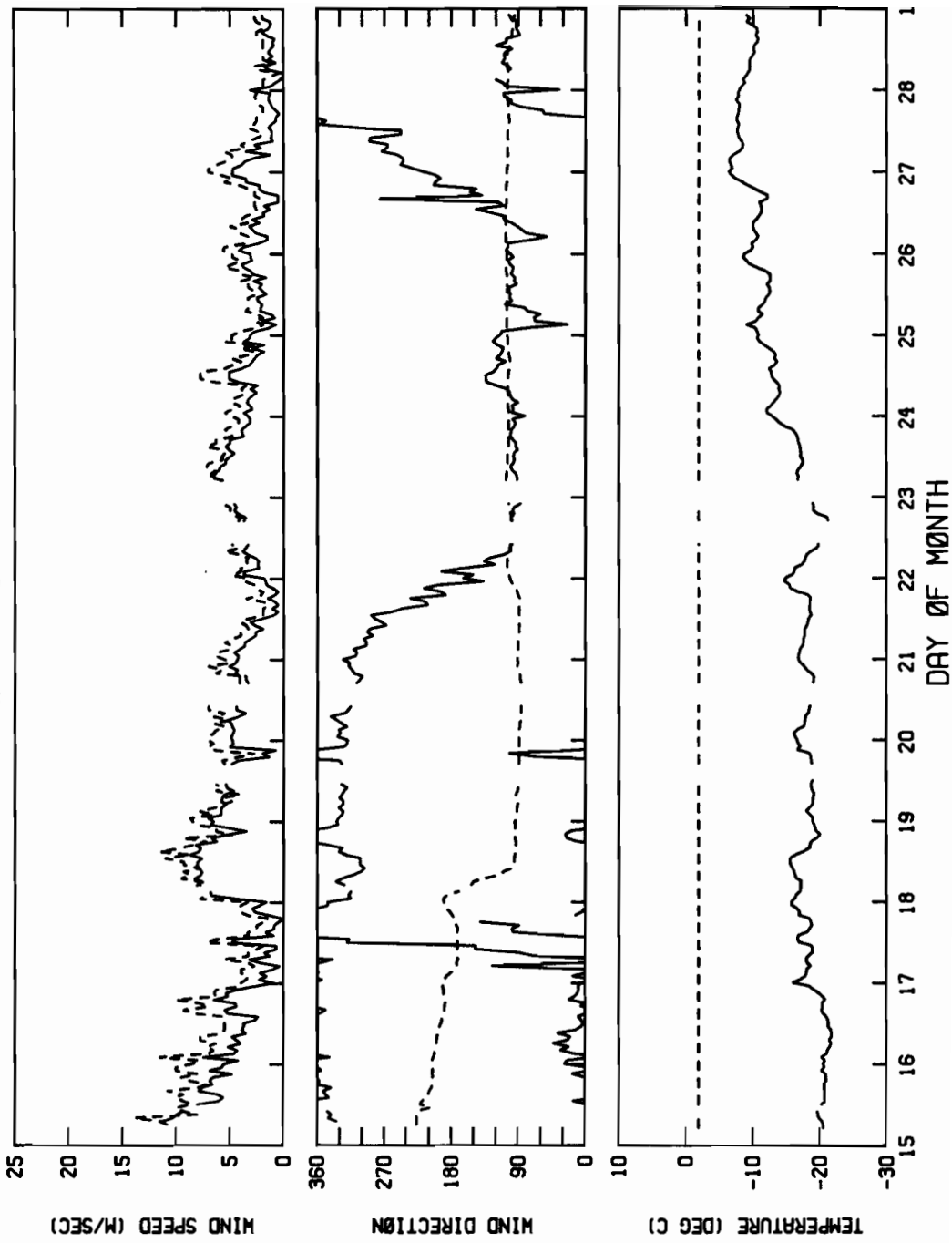
TIME SERIES PLOT FOR BERING 82 STA 010C

31 JAN 82 T0 14 FEB 82 INTERVAL= 60.0MINS



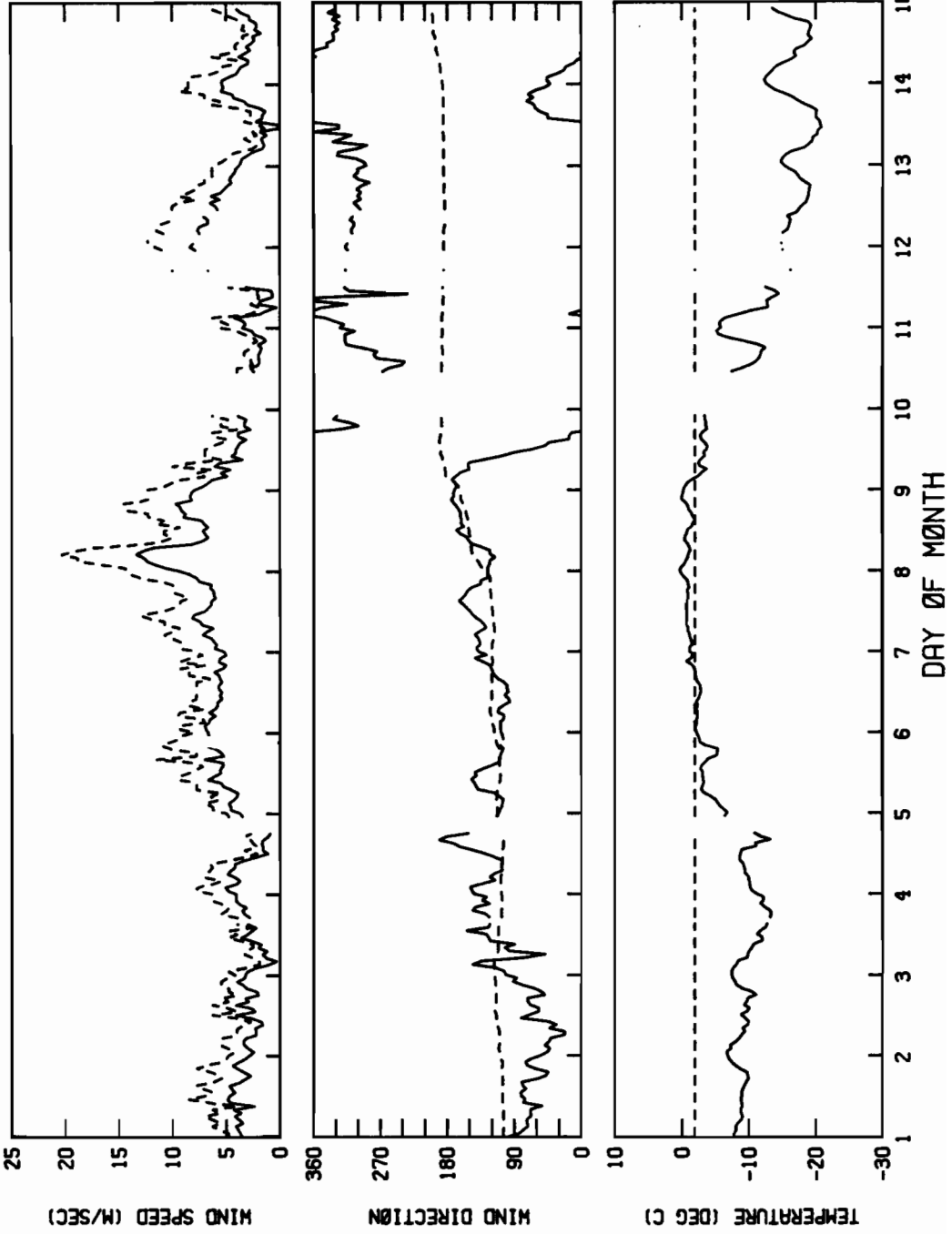
TIME SERIES PLOT FOR BERING 82 STA 010C

15 FEB 82 TO 1 MAR 82 INTERVAL= 60.0MINS



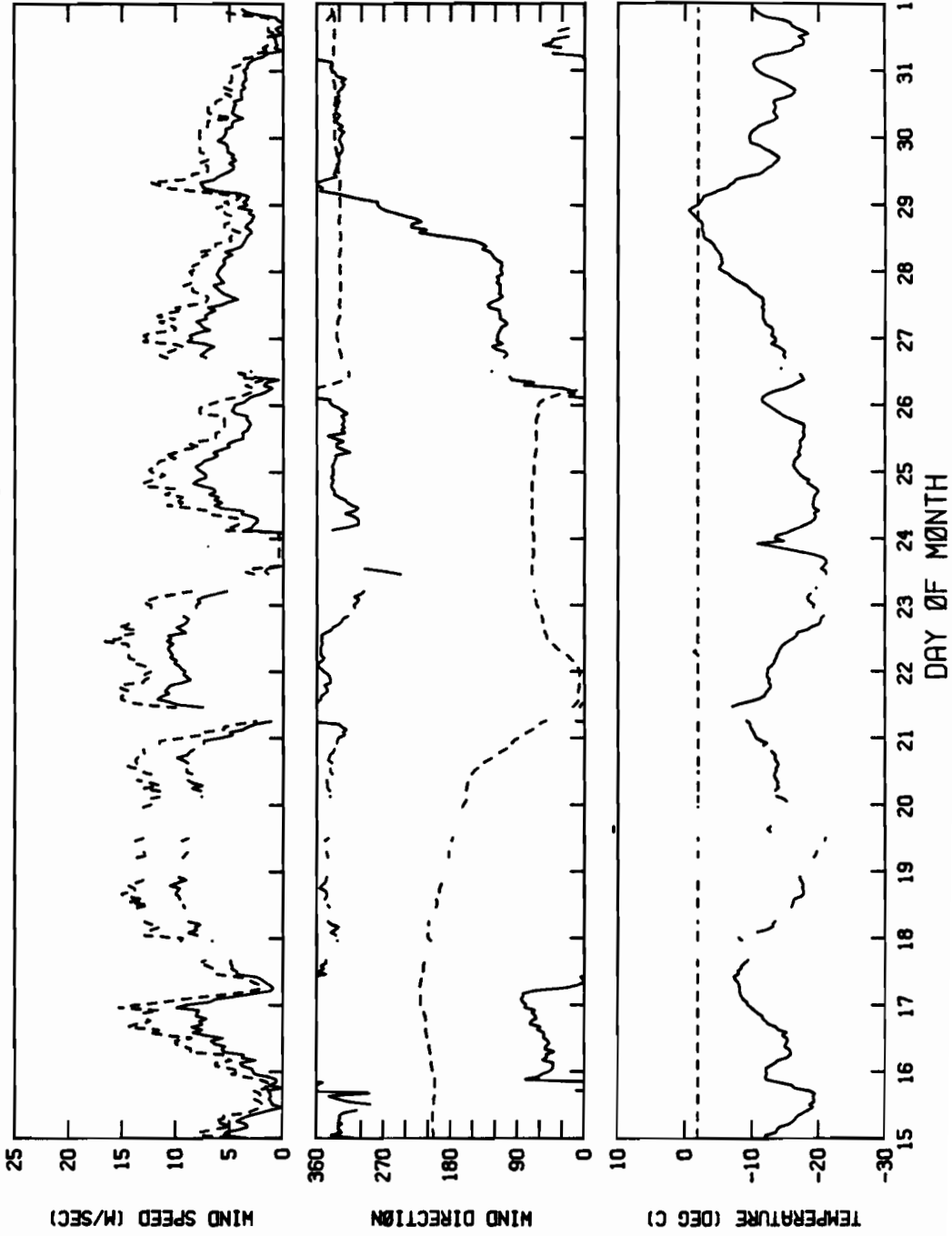
TIME SERIES PLOT FOR BERING 82 STA 010C

1 MAR 82 TO 15 MAR 82 INTERVAL= 60.0MINS



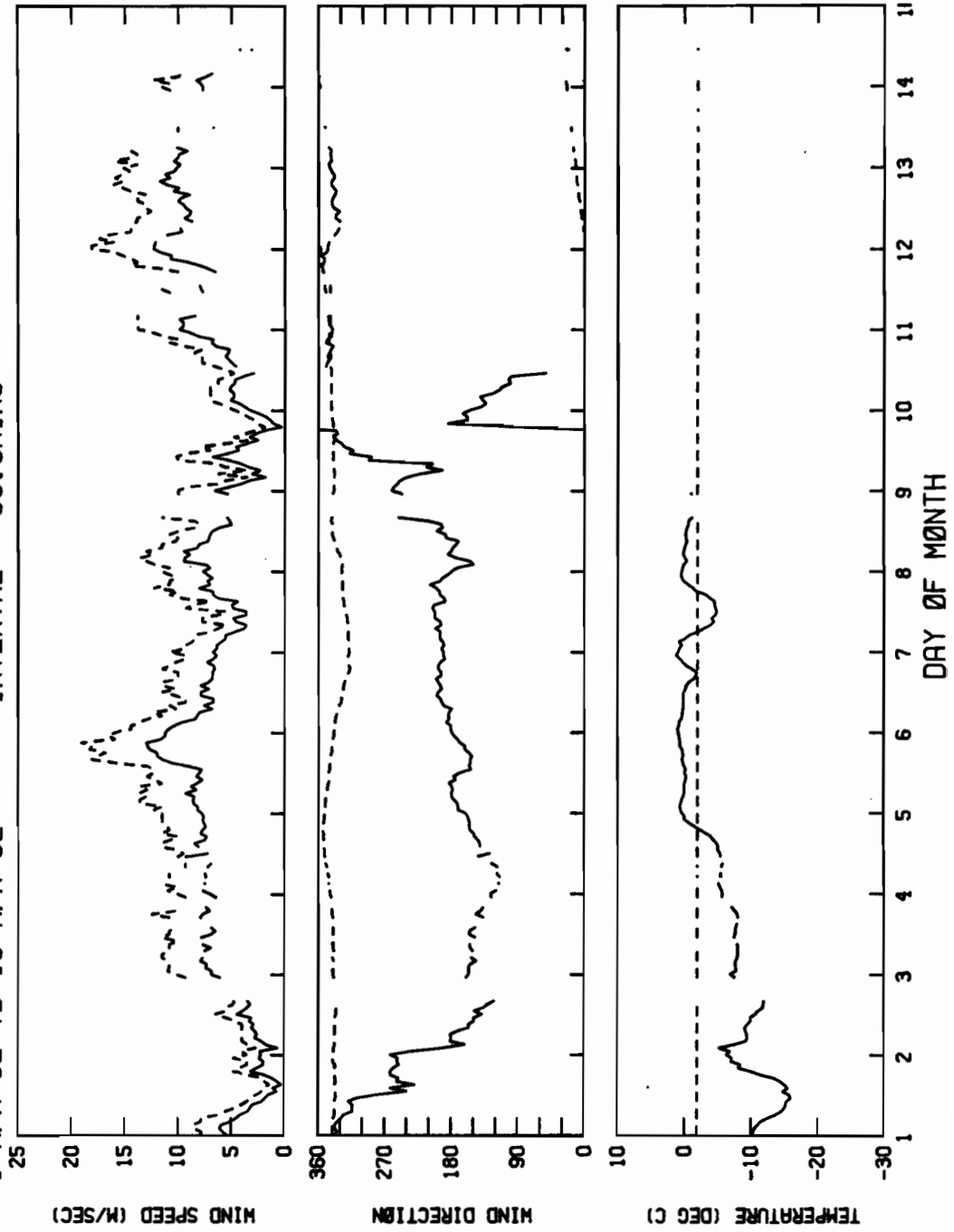
TIME SERIES PLOT FOR BERING 82 STA 010C

15 MAR 82 TO 1 APR 82 INTERVAL= 60.0MINS



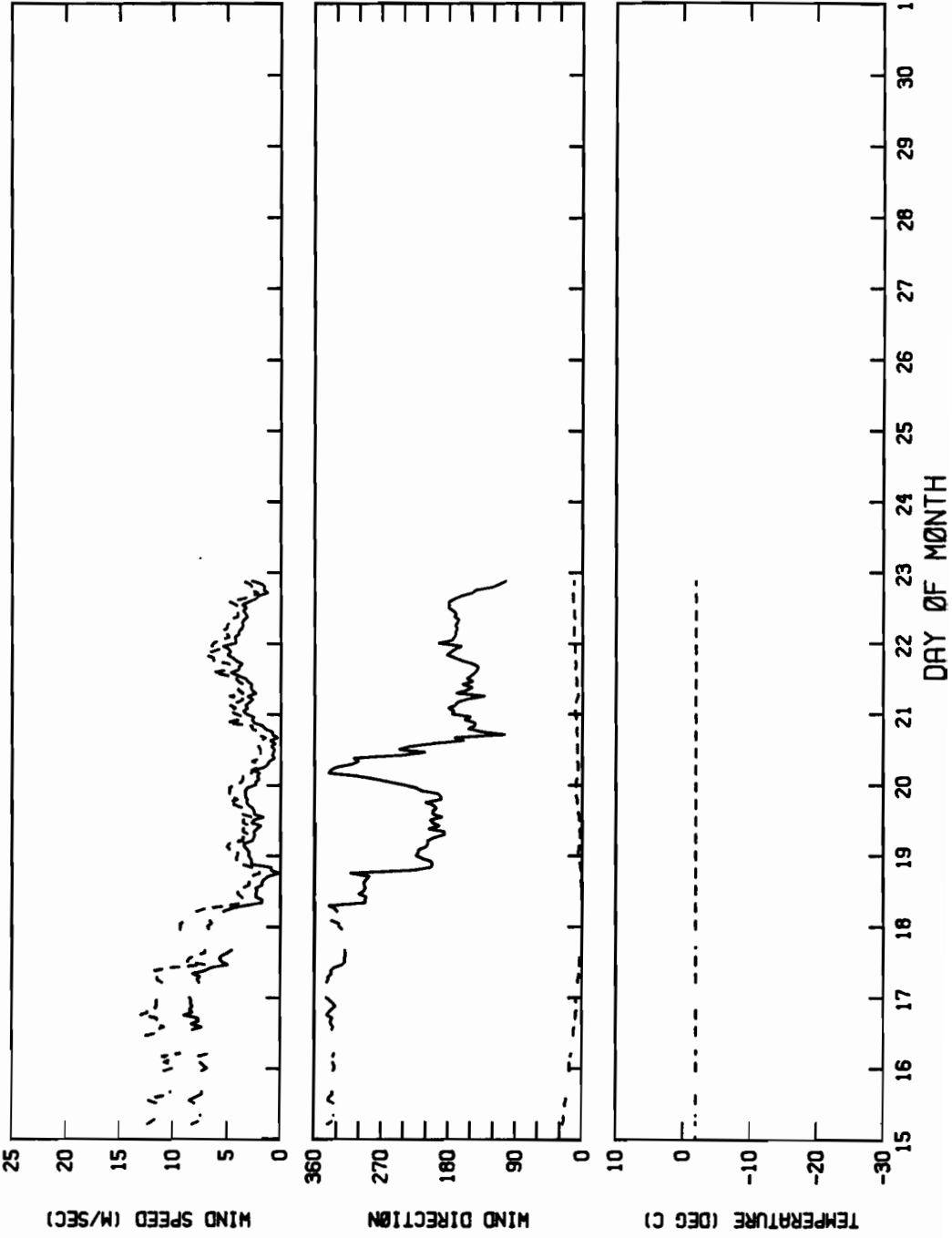
TIME SERIES PLOT FOR BERING 82 STA 010C

1 APR 82 TO 15 APR 82 INTERVAL= 60.0MINS



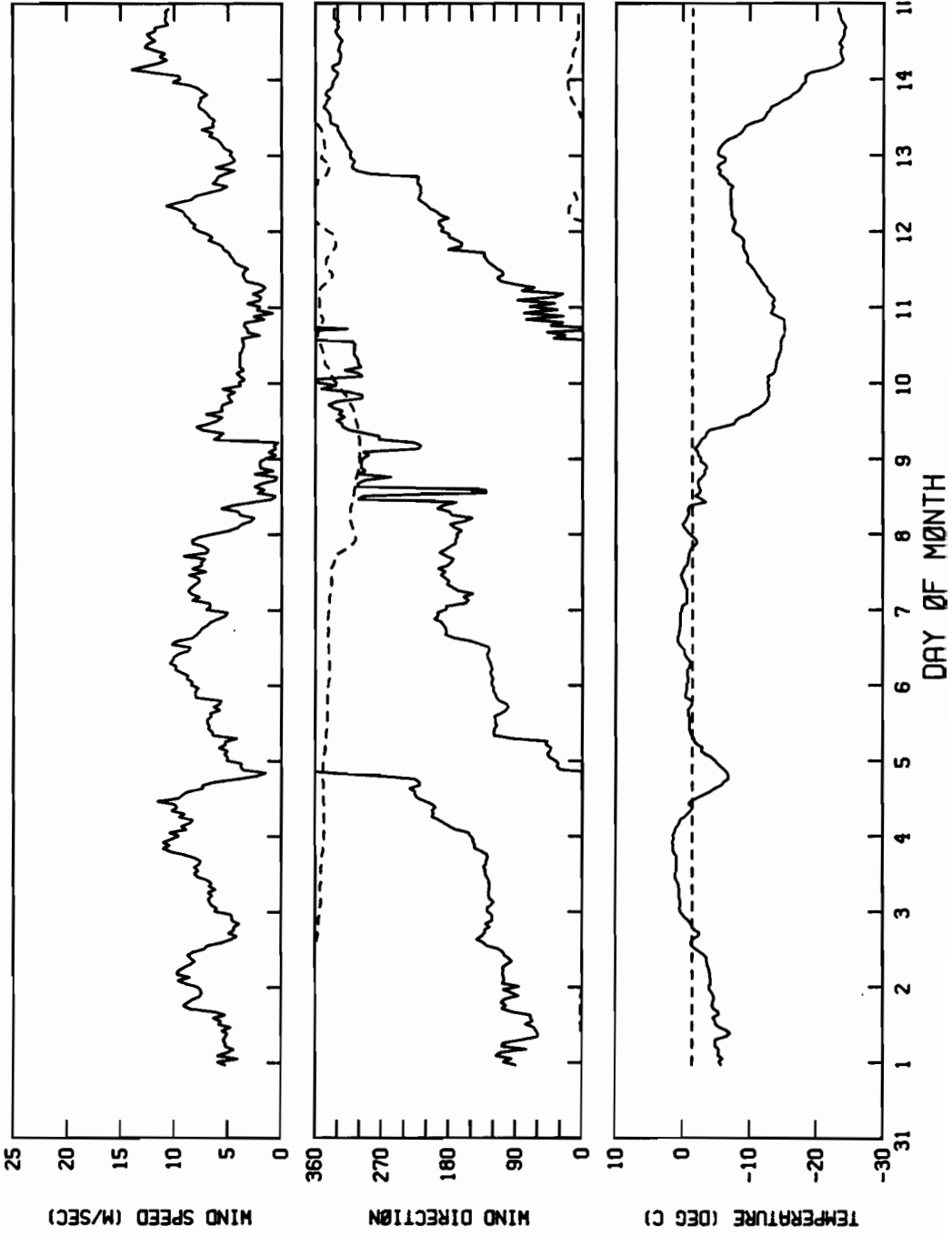
TIME SERIES PLOT FOR BERING 82 STA 010C

15 APR 82 TO 1 MAY 82 INTERVAL= 60.0MINS

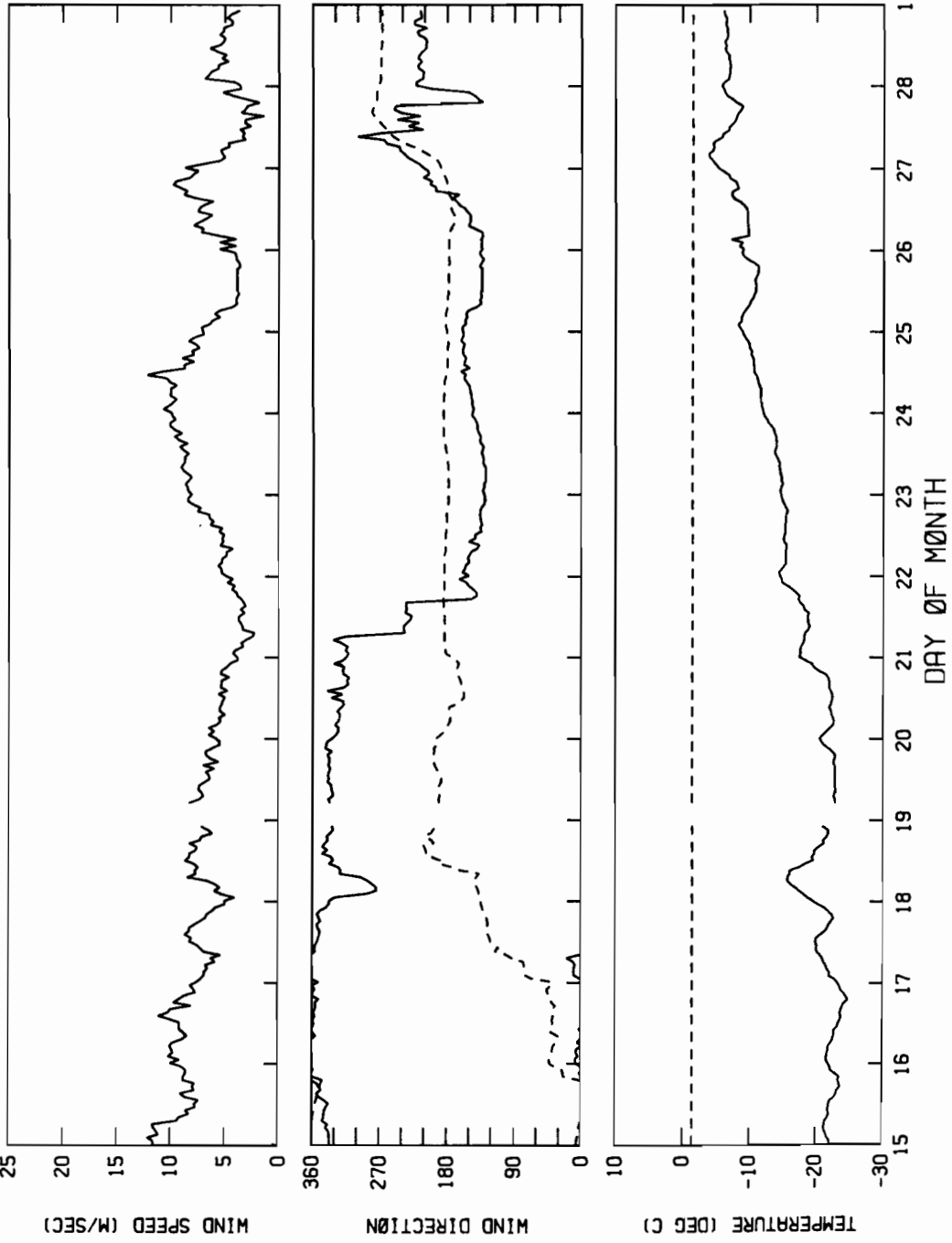


B2. Meteorological Station 5170 (ARGOS 2320)

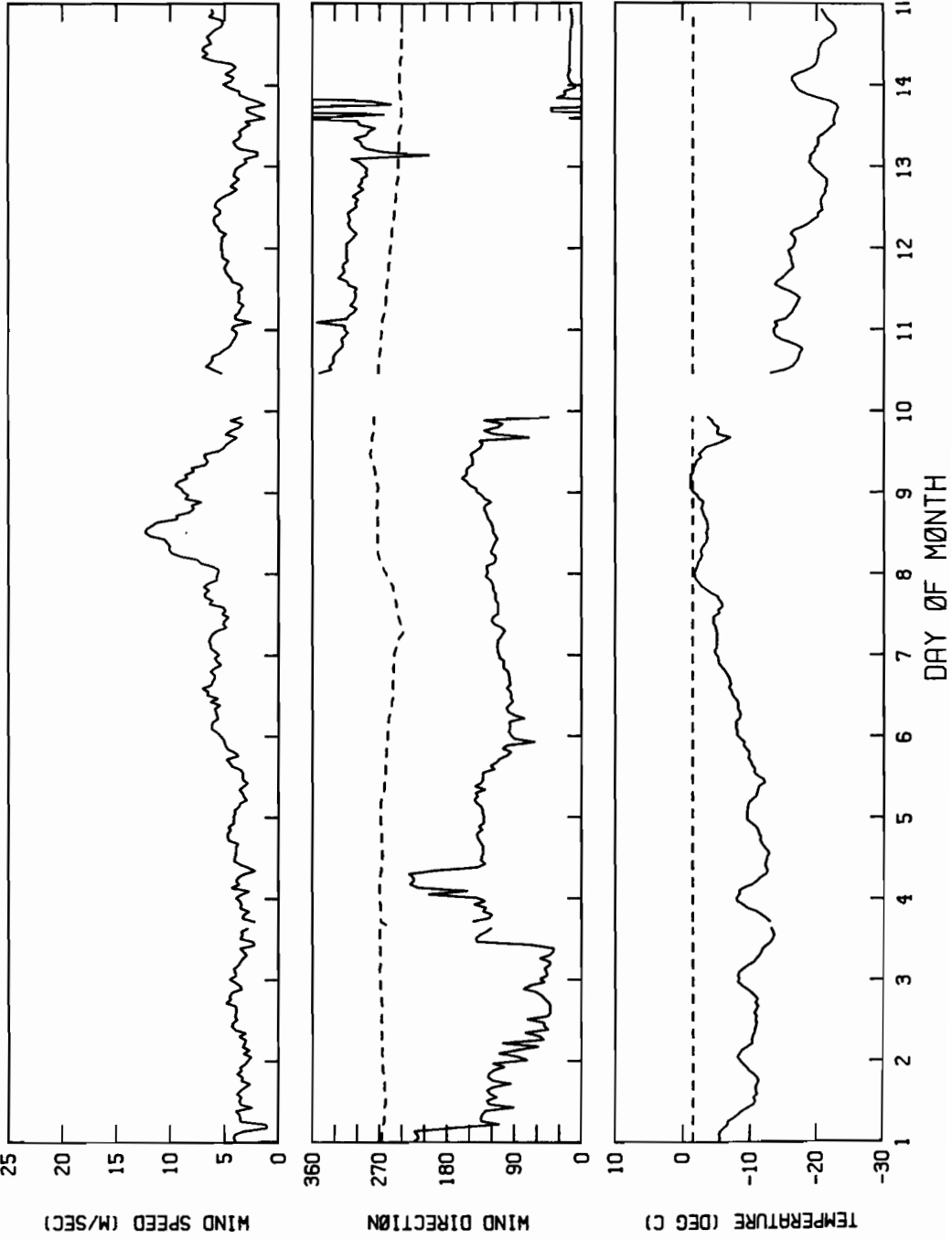
TIME SERIES PLOT FOR BERING 82 STA 5170
31 JAN 82 TO 15 FEB 82 INTERVAL= 60.0MINS



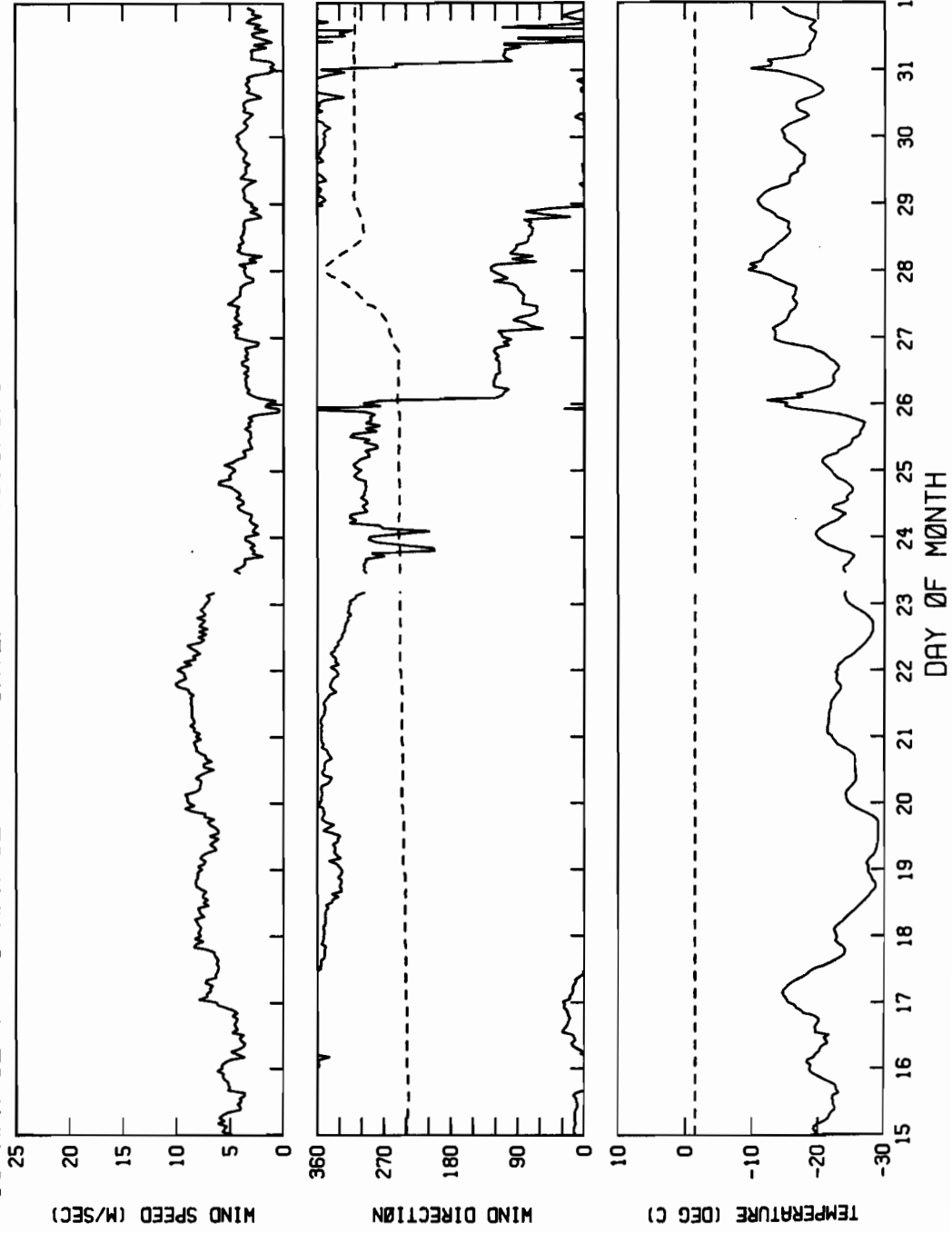
TIME SERIES PLOT FOR BERING 82 STA 5170
15 FEB 82 TO 1 MAR 82 INTERVAL= 60.0MINS



TIME SERIES PLOT FOR BERING 82 STA 5170
1 MAR 82 TØ 15 MAR 82 INTERVAL= 60.0MINS

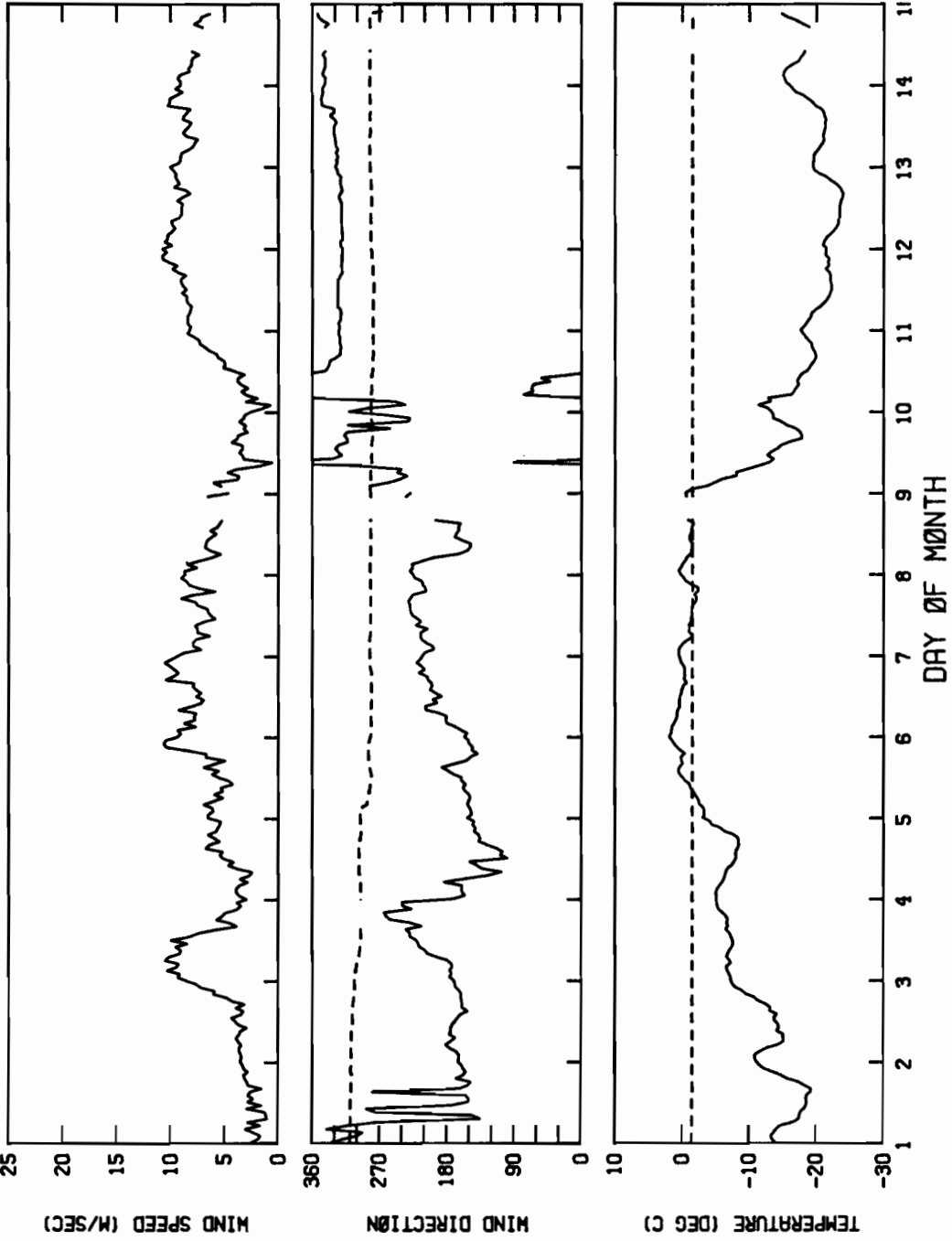


TIME SERIES PLOT FOR BERING 82 STA 5170
 15 MAR 82 TO 1 APR 82 INTERVAL= 60.0MINS



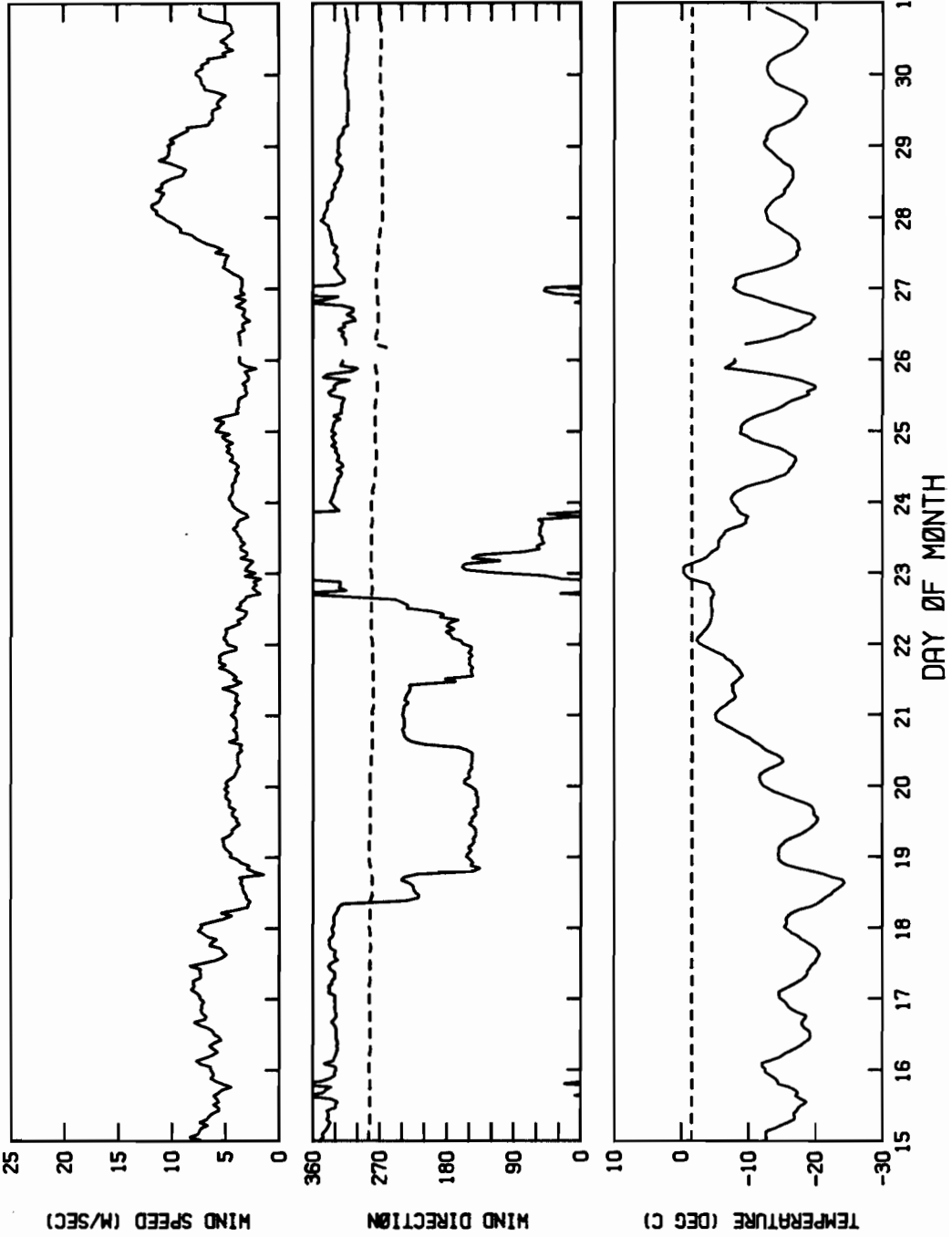
TIME SERIES PLOT FOR BERING 82 STA 5170

1 APR 82 TO 15 APR 82 INTERVAL= 60.0MINS

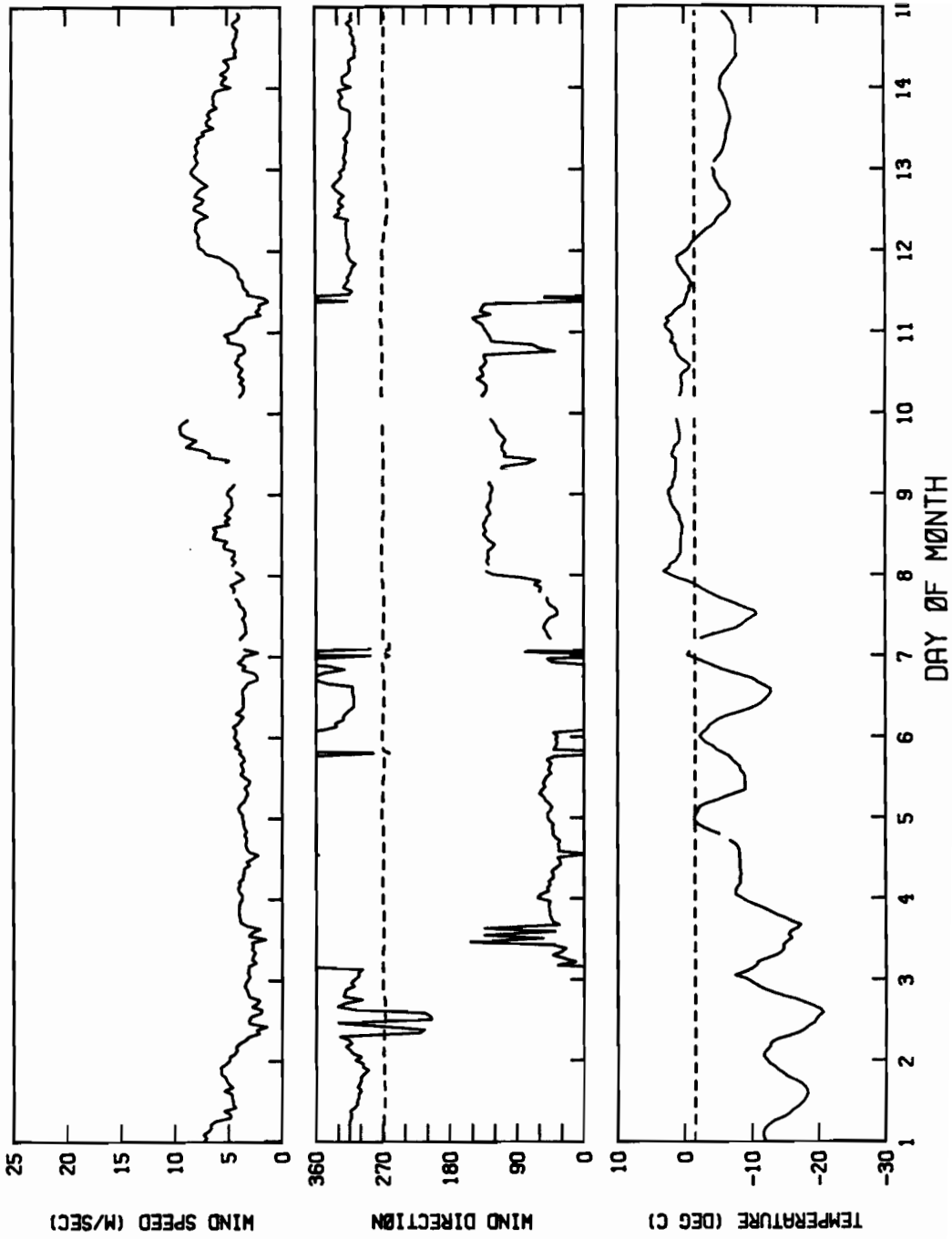


TIME SERIES PLOT FOR BERING 82 STA 5170

15 APR 82 TO 1 MAY 82 INTERVAL= 60.0MINS

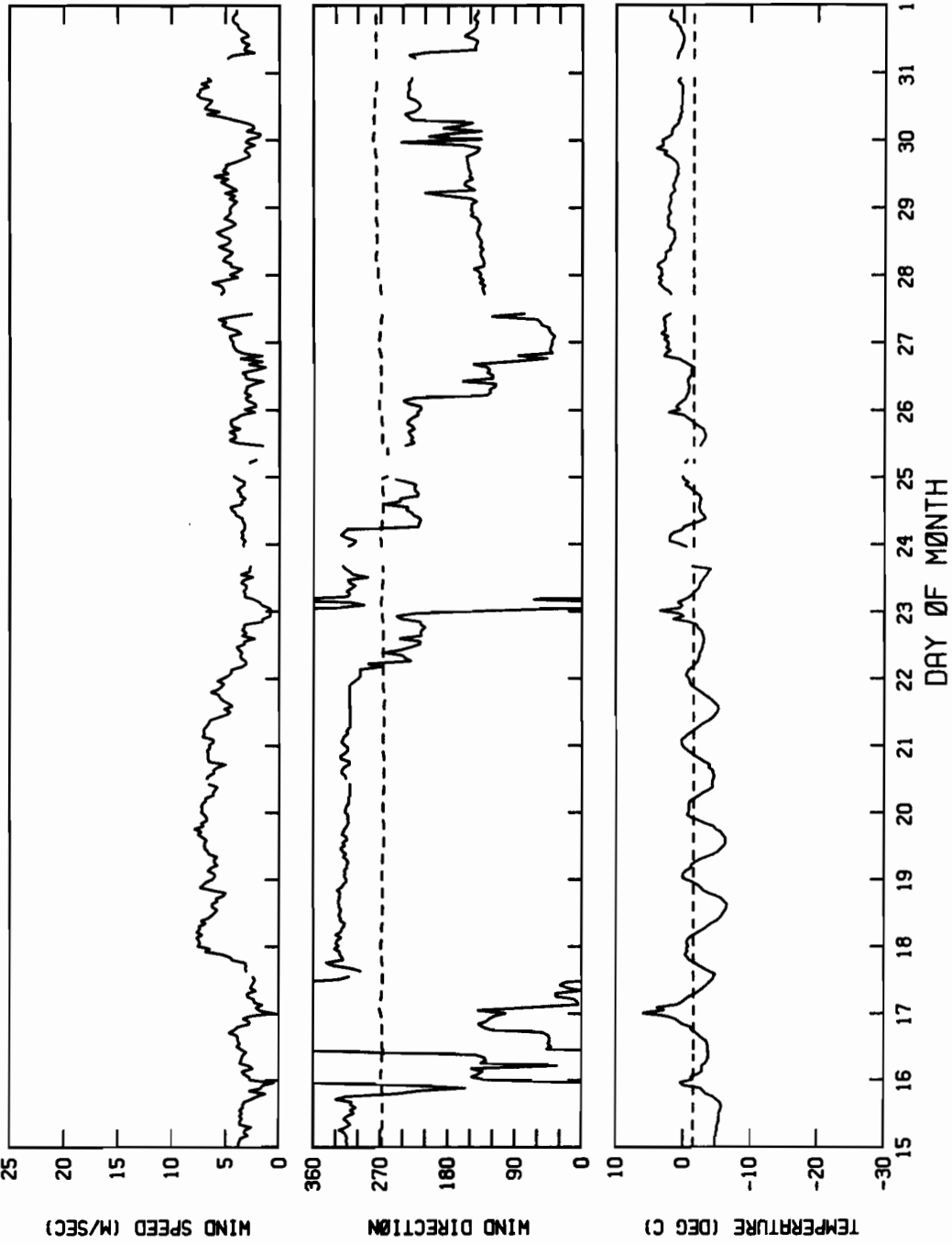


TIME SERIES PLOT FOR BERING 82 STA 5170
1 MAY 82 TO 15 MAY 82 INTERVAL = 60.0MINS



TIME SERIES PLOT FOR BERING 82 STA 5170

15 MAY 82 TO 1 JUN 82 INTERVAL= 60.0MINS



APPENDIX C.

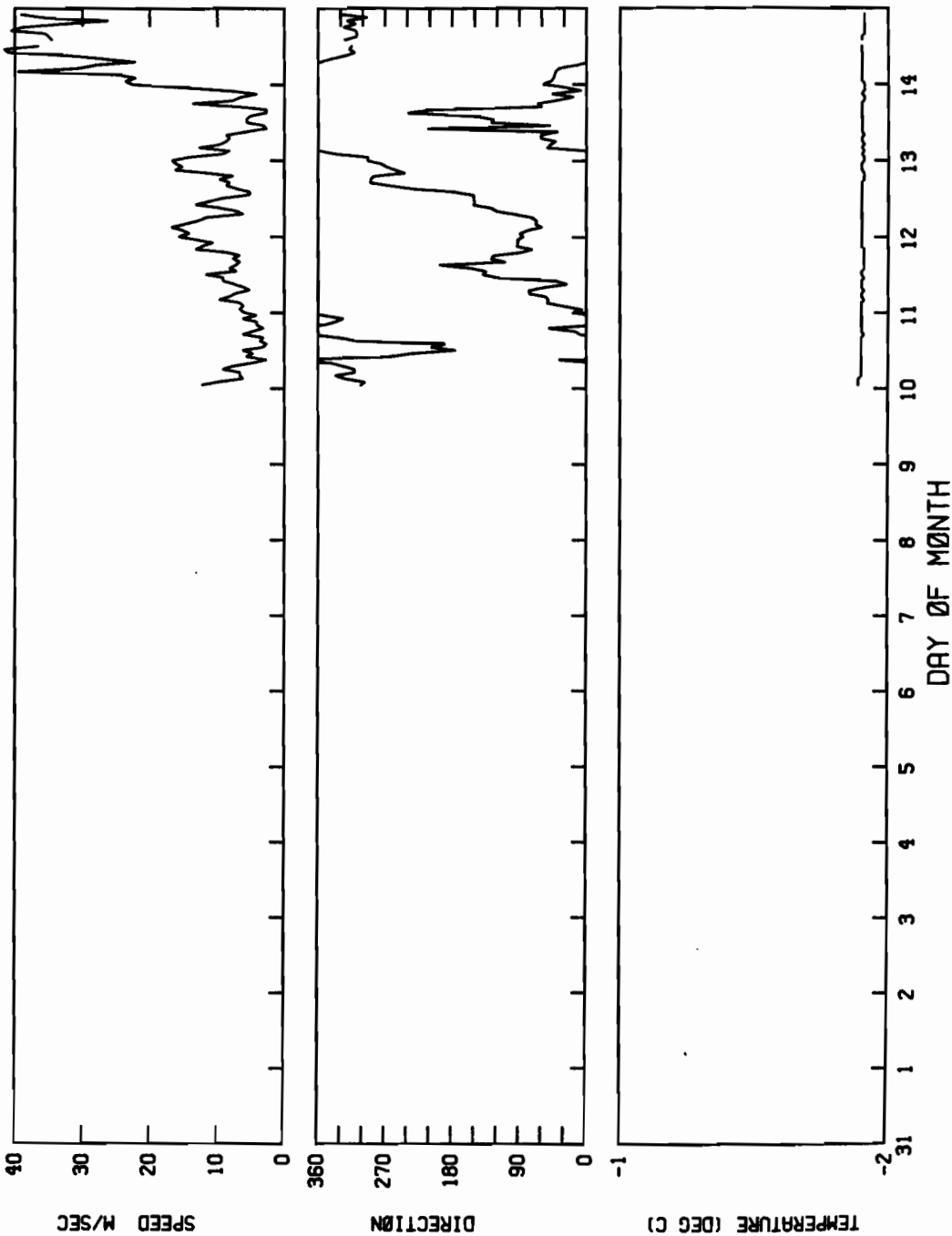
Oceanographic Data

1. Data were sampled hourly. Plots here show all data considered good in raw form. Bad points occurred because of telemetry problems or instrument failure. Otherwise, data is shown here and some consideration should be given to environmental errors (frozen sensors, etc.).
2. The speed plot is the average speed computed from the total number of rotor turns over a 20-minute period.
3. The direction is measured by instantaneously sampling the vane direction and adding that to the compass direction. More recent comparisons of this measurement to a vector average measurement show excellent agreement, and all variations in current speed and directions are probably real.
4. The temperature was measured about 2 m below the ice.

C1. Station 010C (ARGOS 2322B)

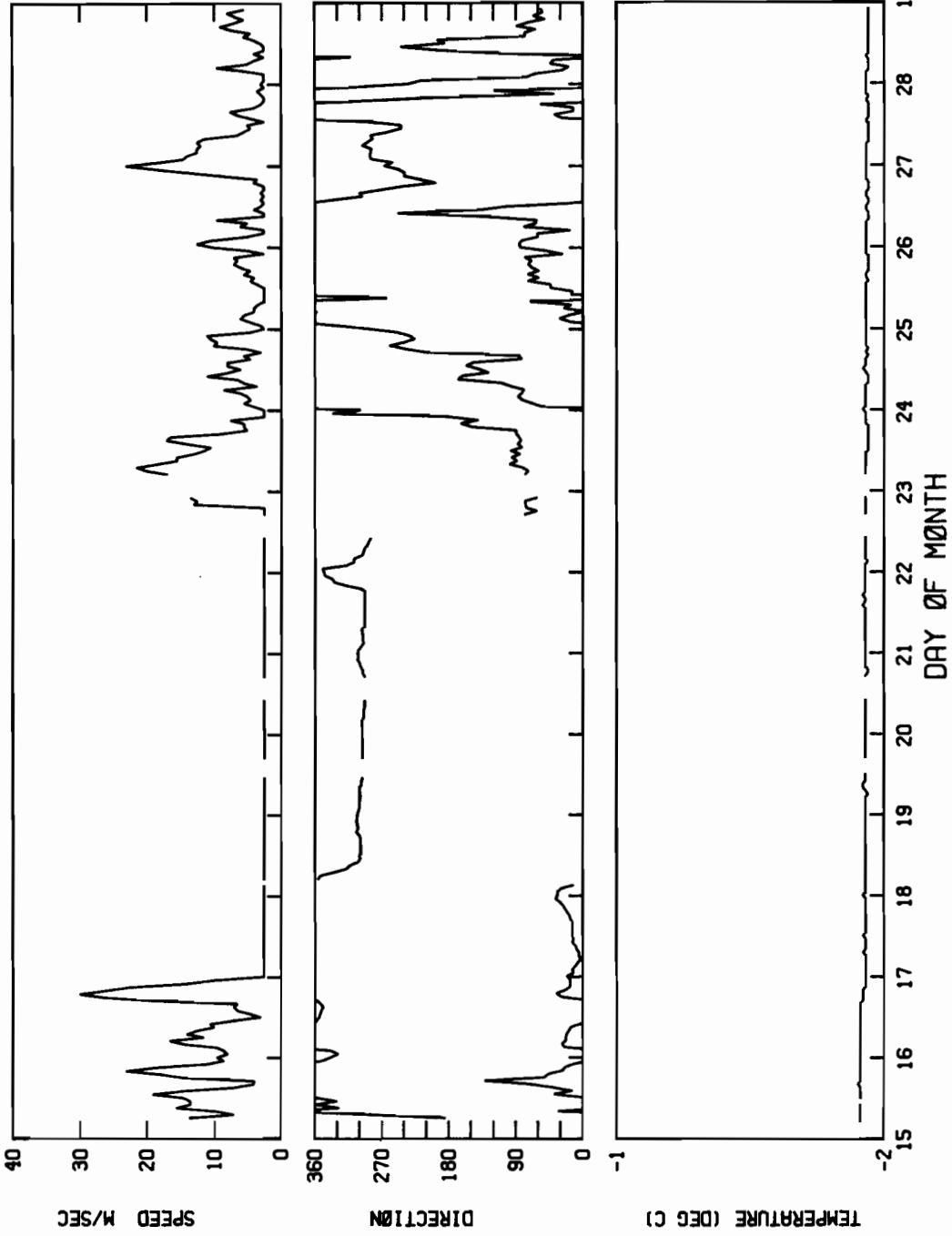
TIME SERIES PLOT FOR BERING 82 STA 010C

31 JAN 82 T0 14 FEB 82 INTERVAL= 60.0MINS



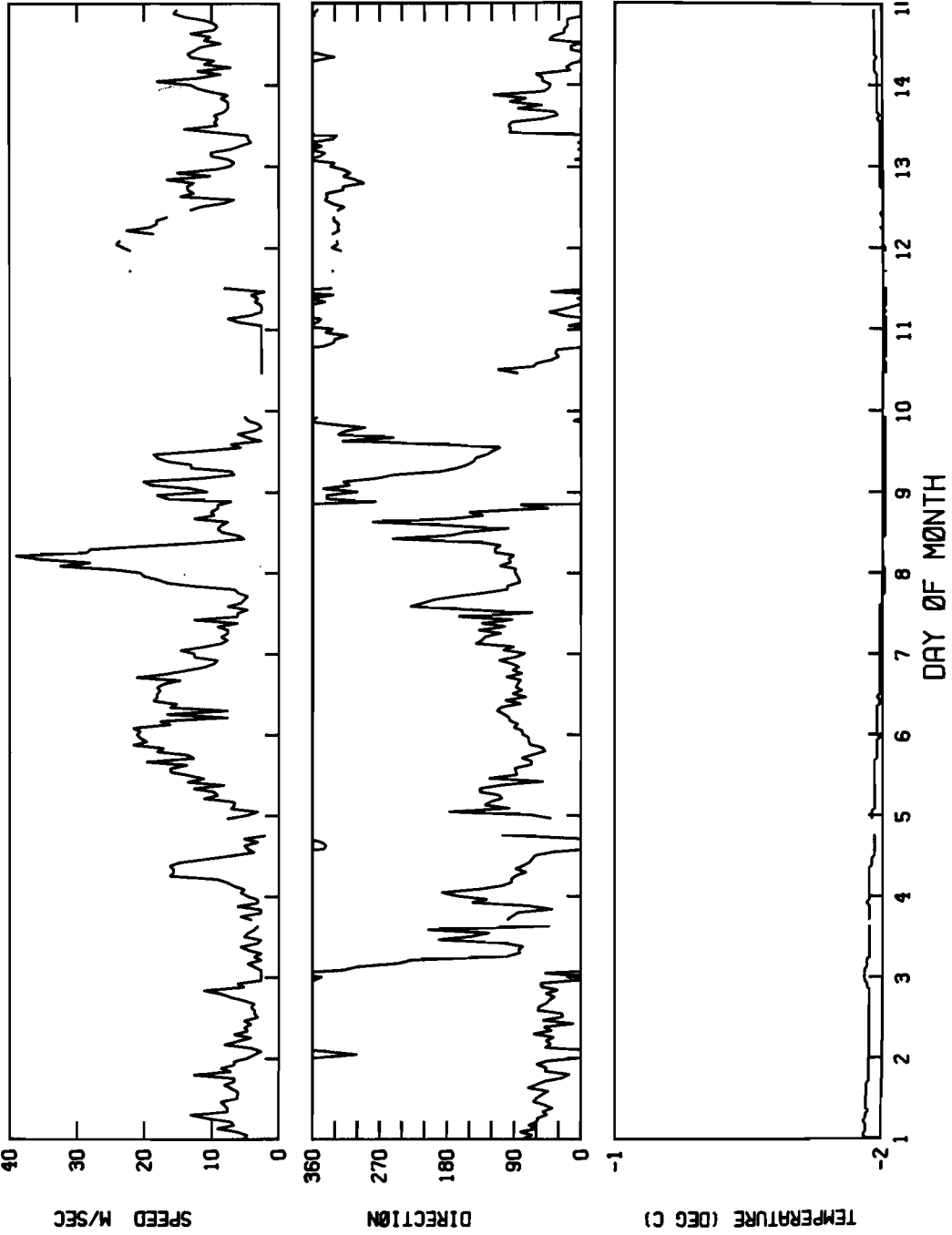
TIME SERIES PLOT FOR BERING 82 STA 010C

15 FEB 82 TO 1 MAR 82 INTERVAL = 60.0MINS



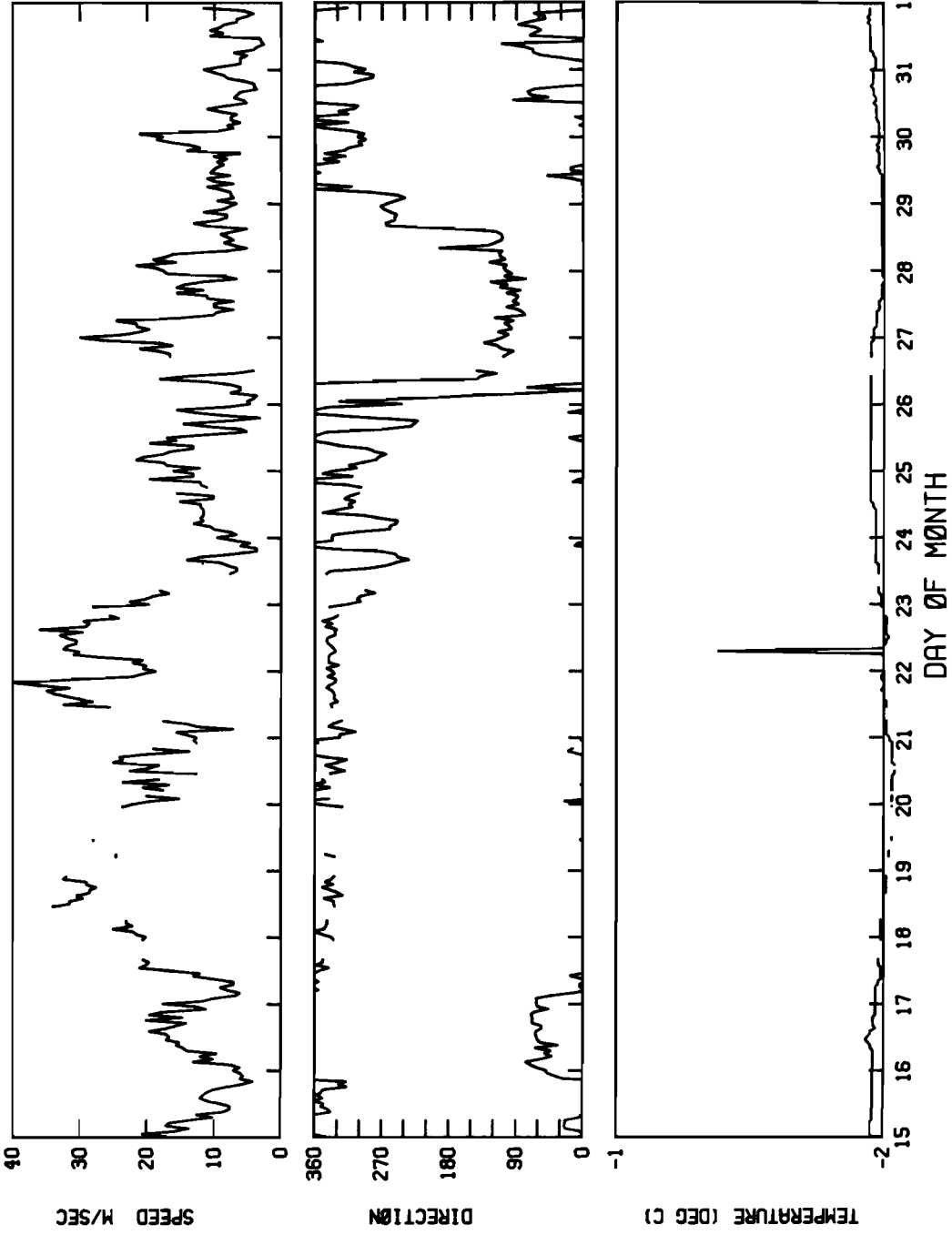
TIME SERIES PLOT FOR BERING 82 STA 010C

1 MAR 82 TO 15 MAR 82 INTERVAL= 60.0MINS



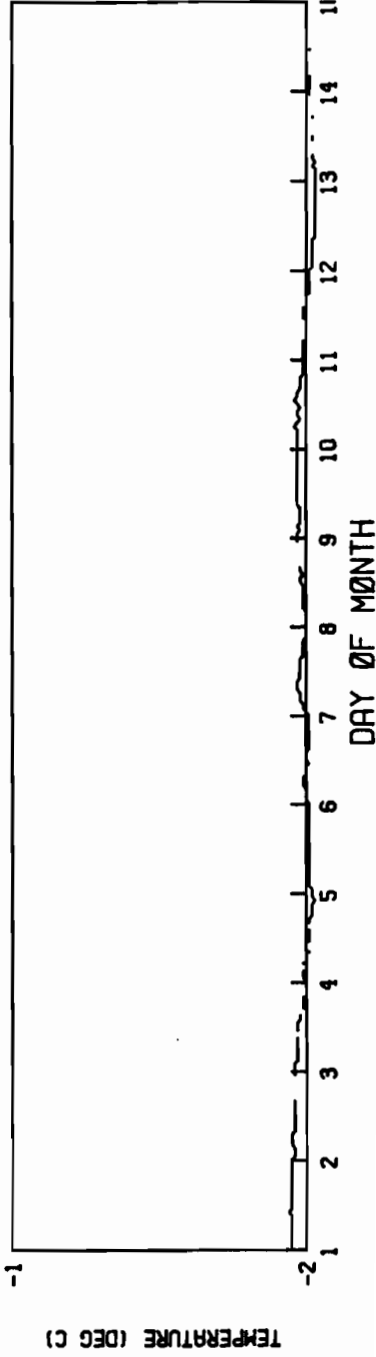
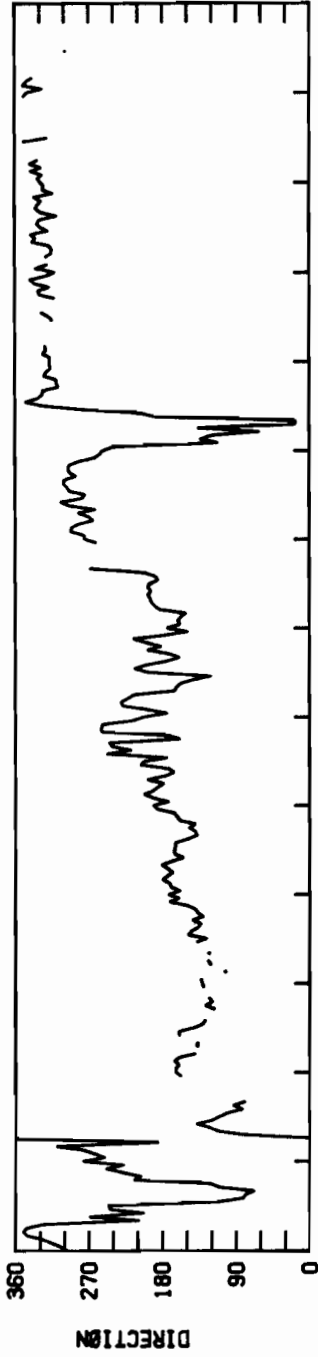
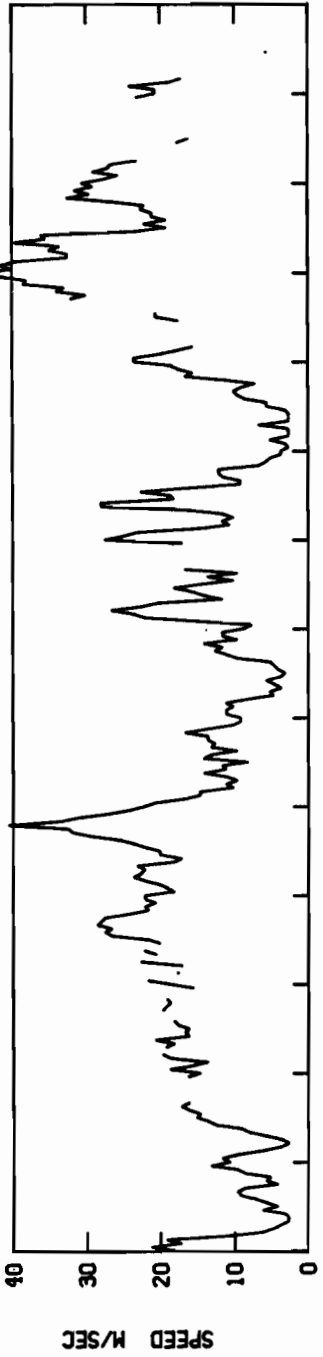
TIME SERIES PLOT FOR BERING 82 STA 010C

15 MAR 82 TO 1 APR 82 INTERVAL= 60.0MINS



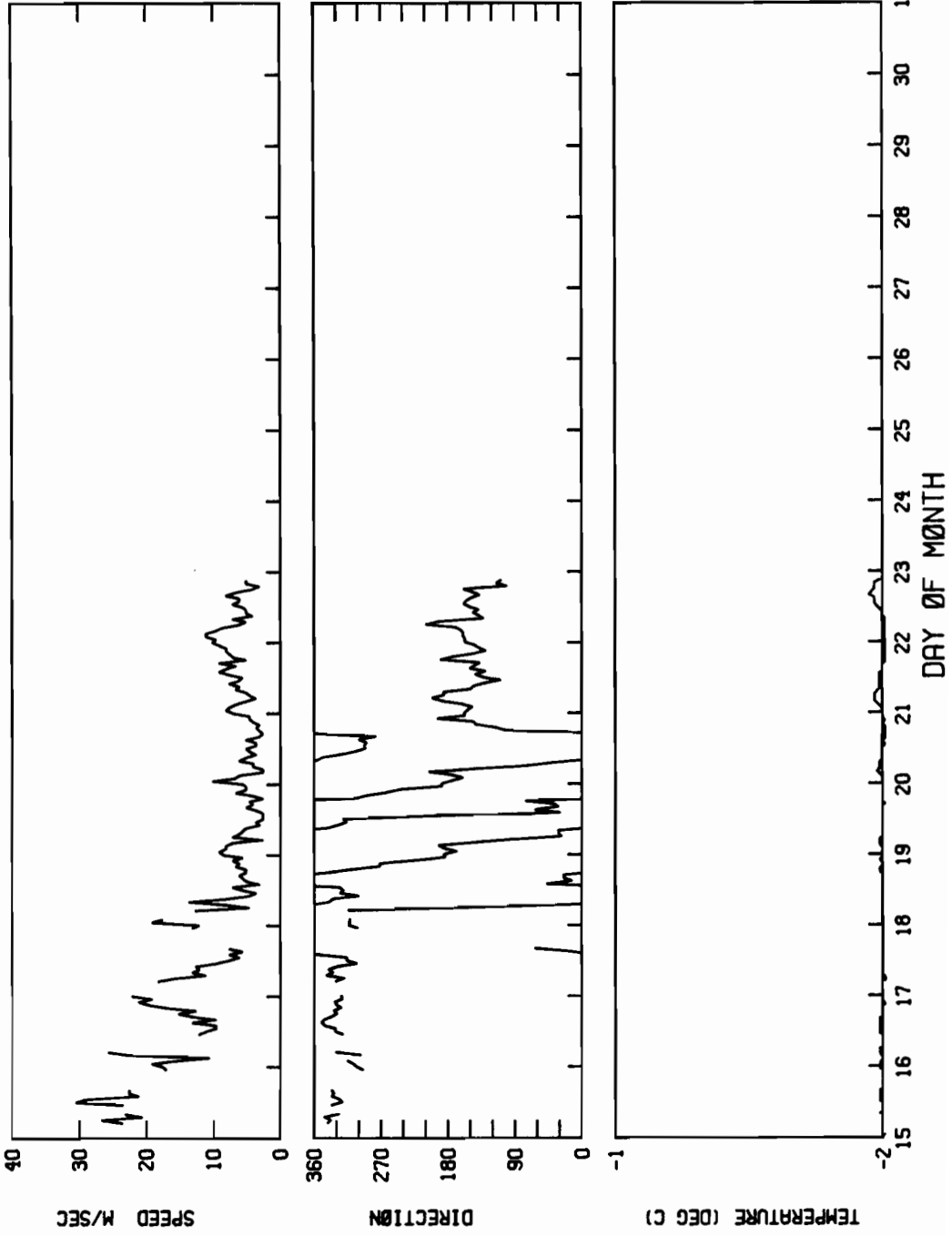
TIME SERIES PLOT FOR BERING 82 STA 010C

1 APR 82 TO 15 APR 82 INTERVAL = 60.0MINS



TIME SERIES PLOT FOR BERING 82 STA 010C

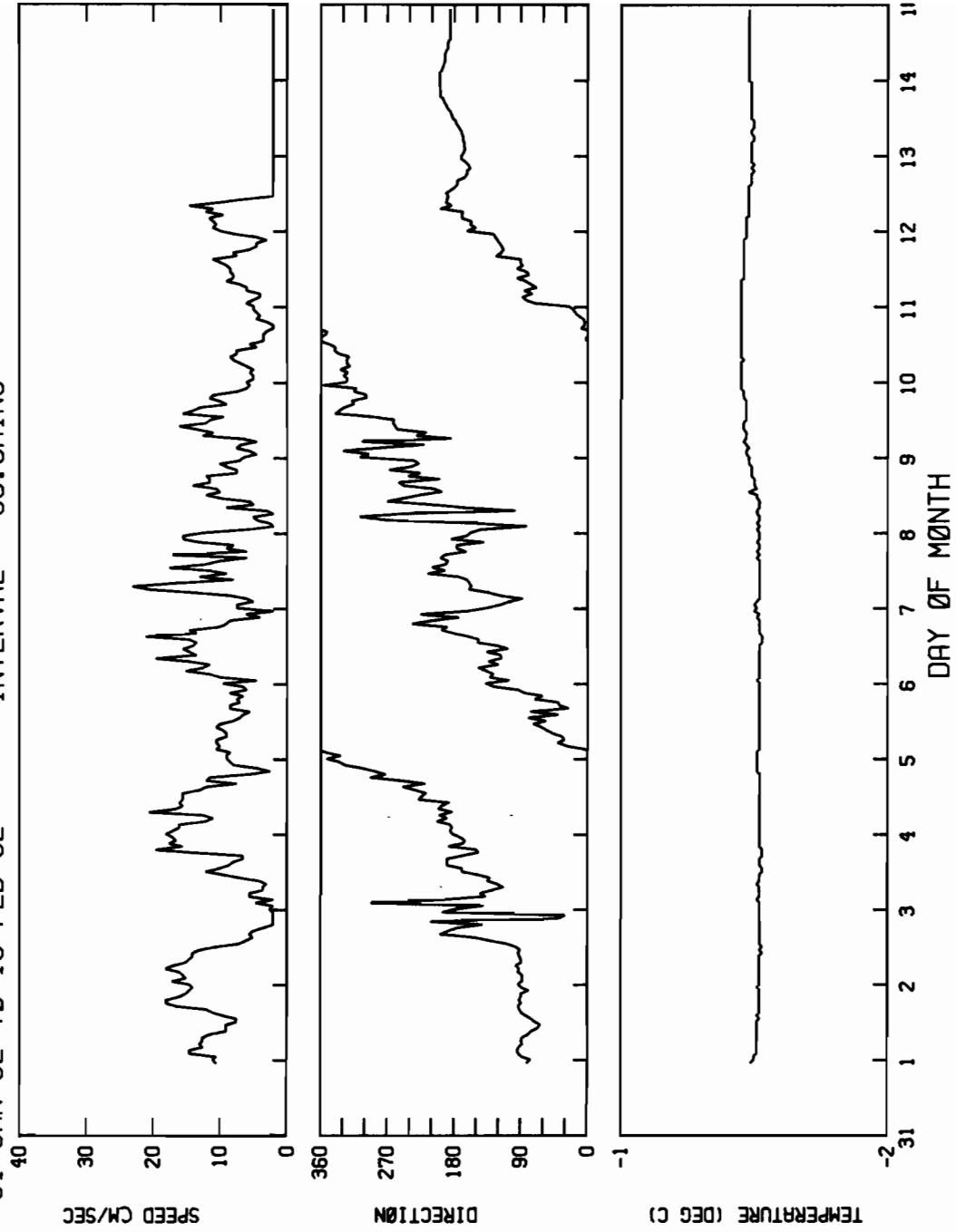
15 APR 82 TO 1 MAY 82 INTERVAL= 60.0MINS



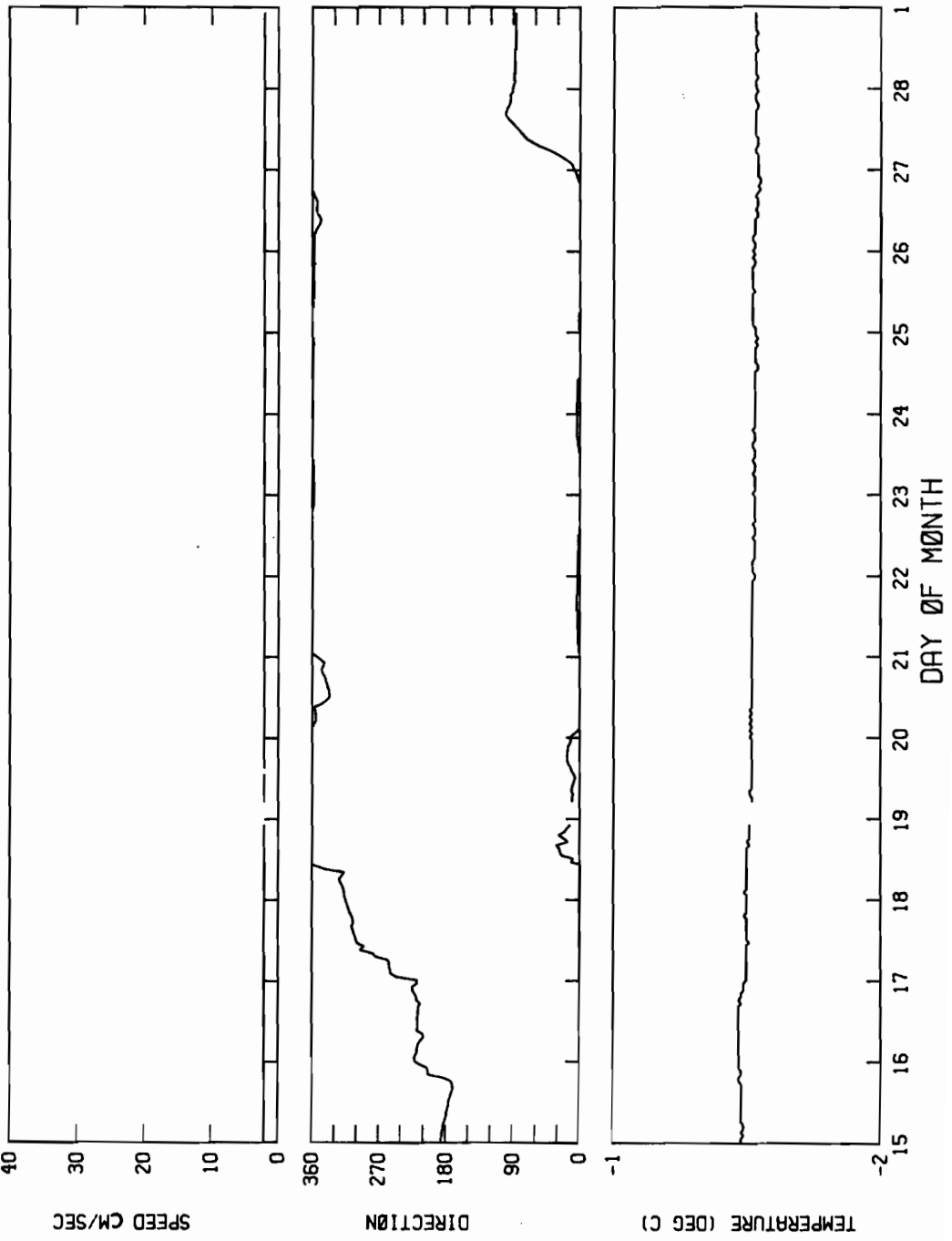
C2. Station 5170 (ARGOS 2320)

TIME SERIES PLOT FØR BERING 82 STA 5170

31 JAN 82 TØ 15 FEB 82 INTERVAL= 60.0MINS

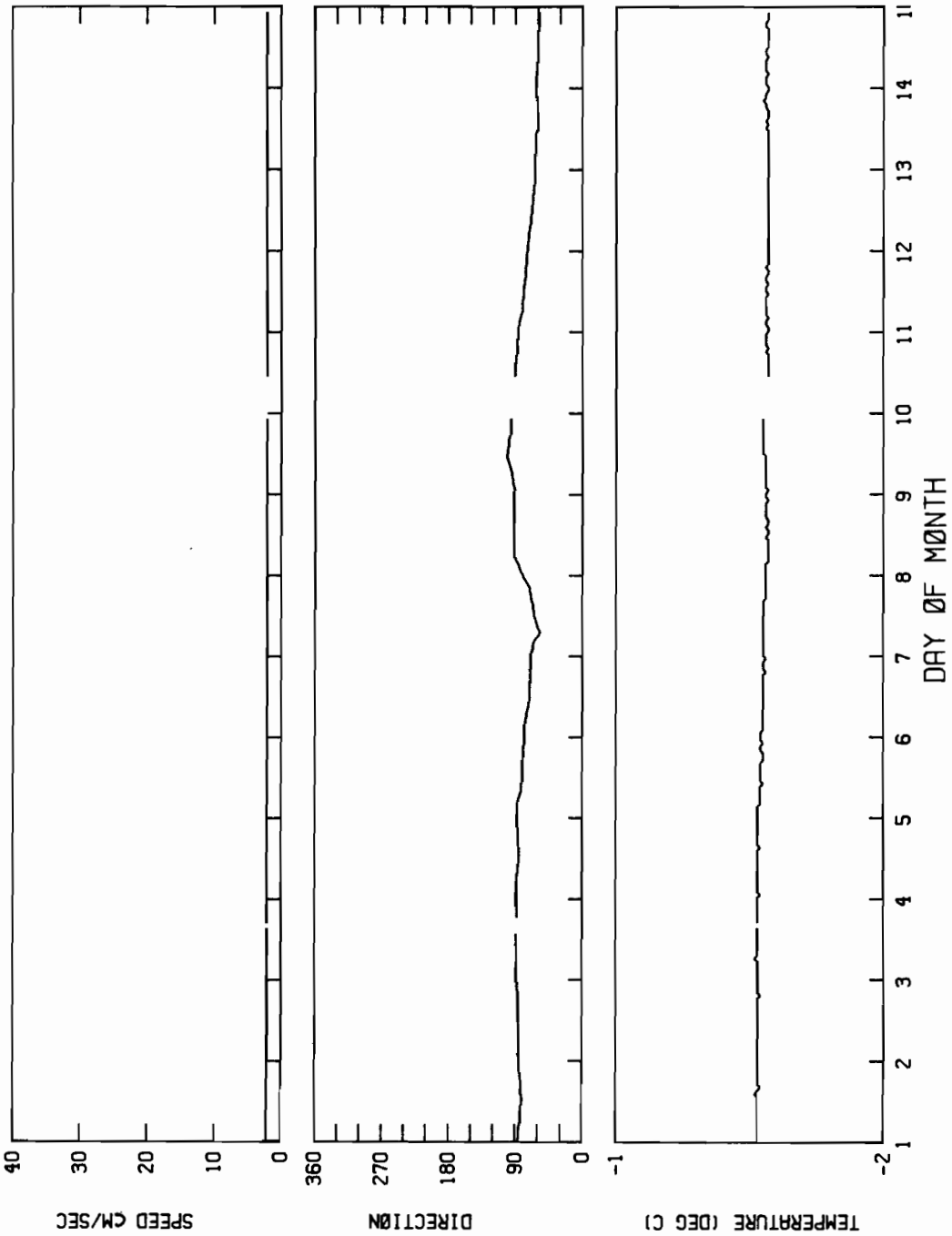


TIME SERIES PLOT FOR BERING 82 STA 5170
15 FEB 82 TO 1 MAR 82 INTERVAL= 60.0MINS

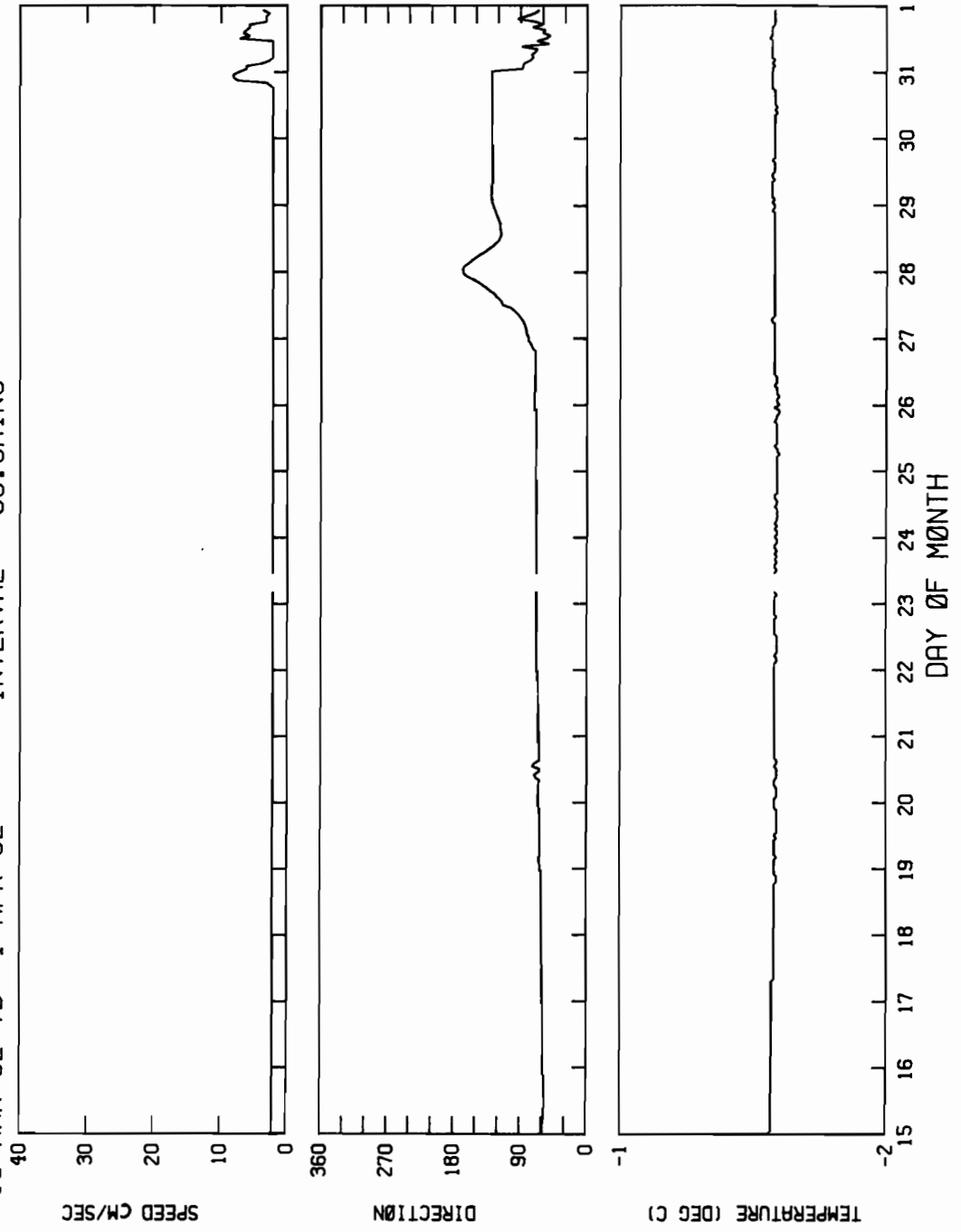


TIME SERIES PLOT FOR BERING 82 STA 5170

1 MAR 82 TO 15 MAR 82 INTERVAL= 60.0MINS

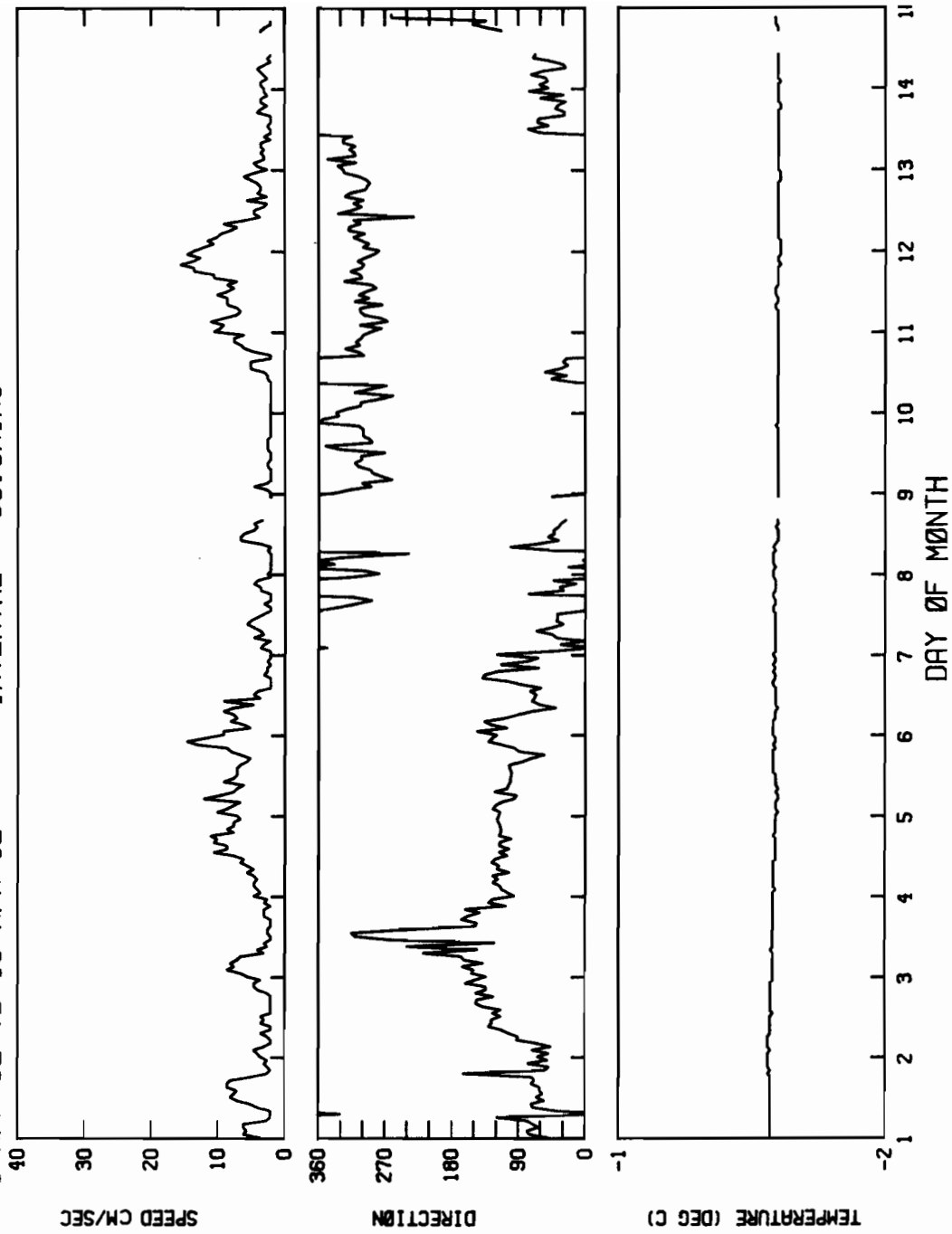


TIME SERIES PLOT FOR BERING 82 STA 5170
15 MAR 82 TO 1 APR 82 INTERVAL= 60.0MINS

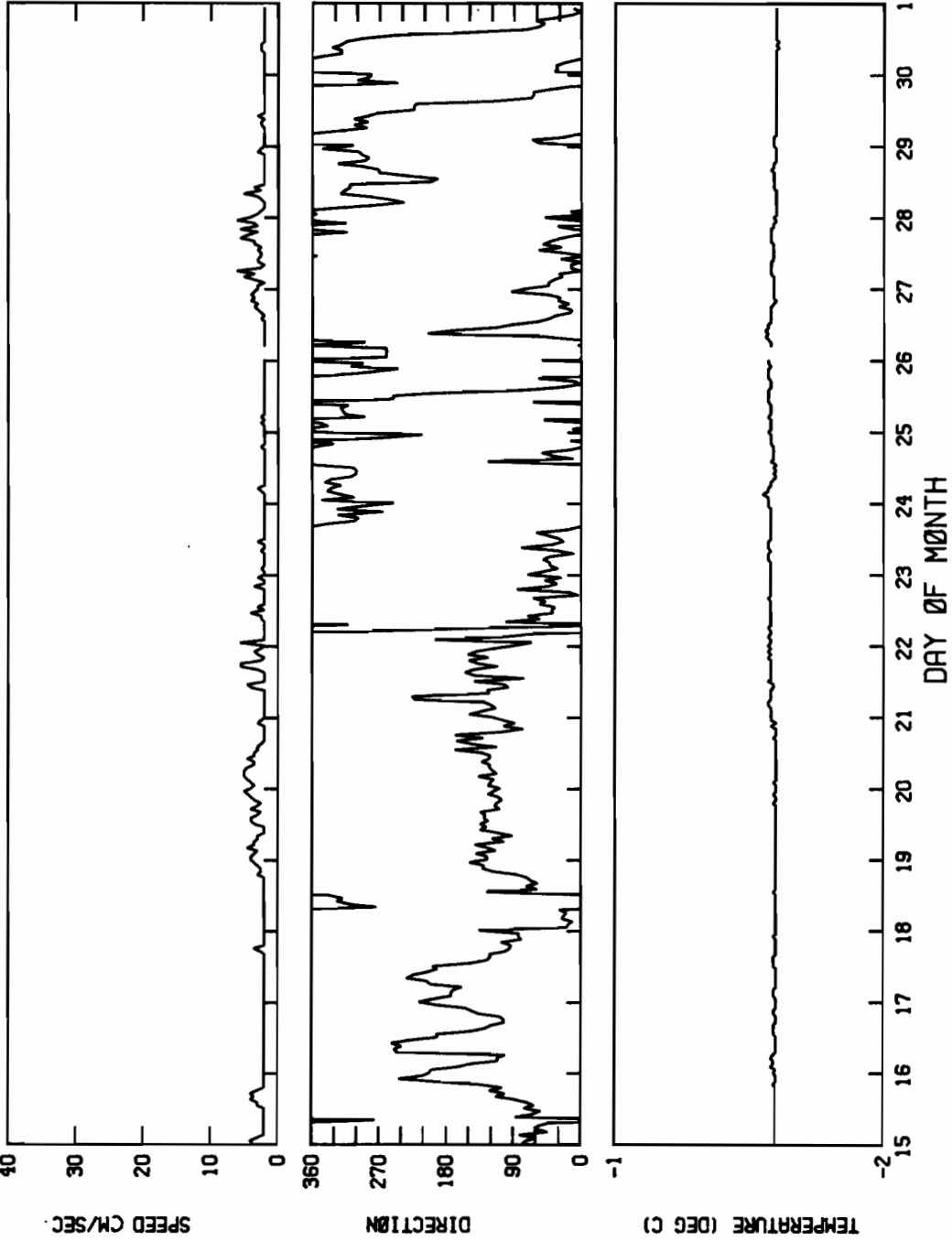


TIME SERIES PLOT FOR BERING 82 STA 5170

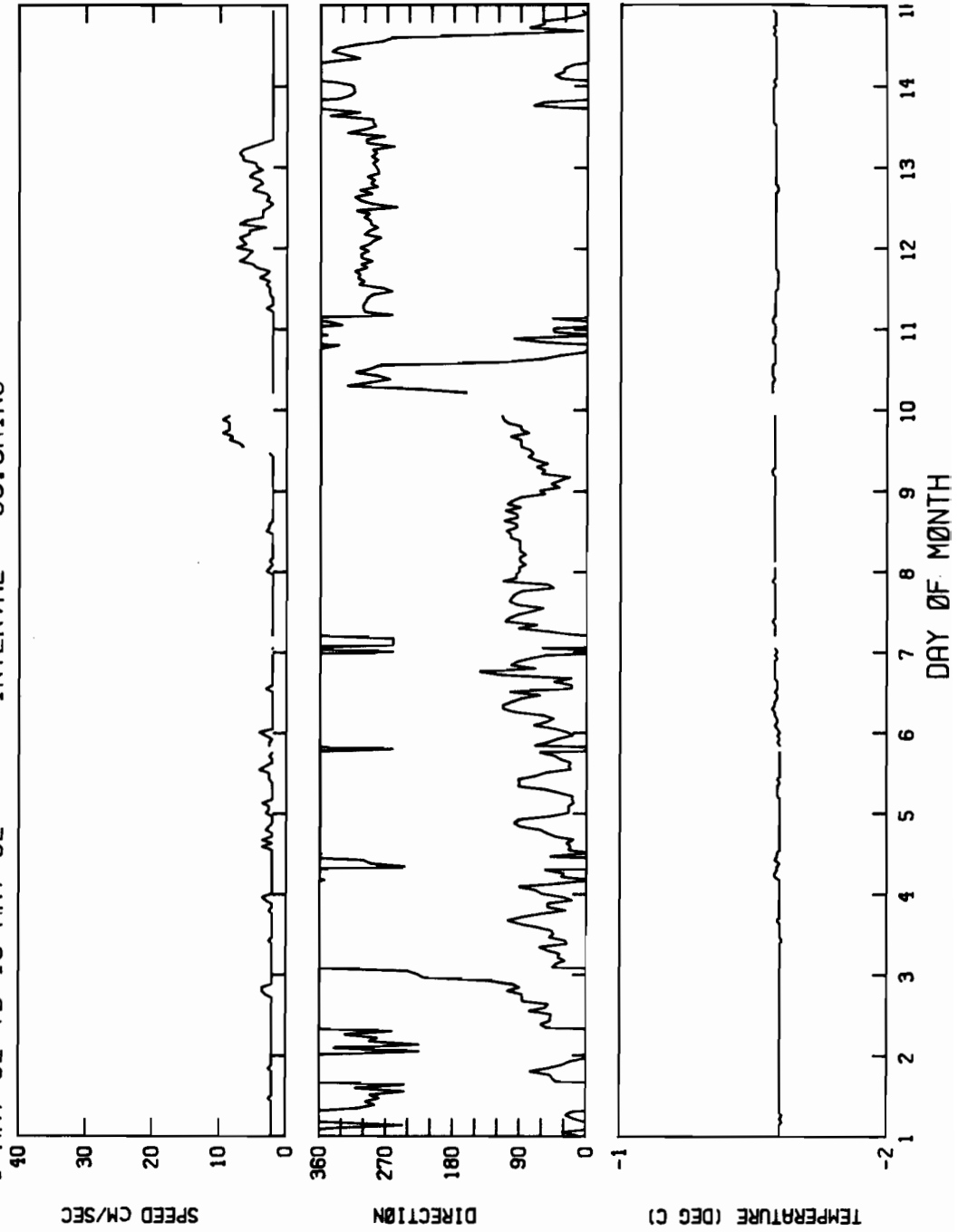
1 APR 82 T0 15 APR 82 INTERVAL= 60.0MINS



TIME SERIES PLOT FOR BERING 82 STA 5170
15 APR 82 TO 1 MAY 82 INTERVAL= 60.0MINS



TIME SERIES PLOT FOR BERING 82 STA 5170
1 MAY 82 TO 15 MAY 82 INTERVAL= 60.0MINS



TIME SERIES PLOT FOR BERING 82 STA 5170

15 MAY 82 TO 1 JUN 82 INTERVAL= 60.0MINS

